From Institute for Signal Processing

Director:

Prof. Dr. -Ing. Alfred Mertin

Monitoring of propofol in breath; pharmacokinetic modeling and design of a control system

Dissertation

for Fulfilment of requirements for

Doctoral Degree of the University of Luebeck

- from the Dept. of Informatics/Technology

Submitted by Balamurugan T Varadarajan

Born in Kumaralingam - TN, India

Luebeck, March 2011.

Erster Berichterstatter: Prof. Jörg -Uwe Meyer

Zweiter Berichterstatter: Prof. Hartmut Gehring

Tag der mündlichen Prüfung: 22.06.2011

Zum Druck genehmigt. Lübeck, den 23.03.2011

Balamurugan T Varadarajan
PhD Student
Institute for Signal Processing
University of Luebeck
Ratzeburger Allee 160,
23538, Luebeck
Germany

Acknowledgements

The hard work of so many people is involved in successful completion of this thesis, that a genuine list is virtually impossible.

I convey my thanks and gratitude to **Prof. Jörg -Uwe Meyer** for providing this opportunity to work in Dräger, Lübeck with this interesting topic and for his continued support throughout my Ph.D.

Thank you to **Dr. Andreas Hengstenberg** for being a trusted mentor and enlightening research partner. I specially thank for his constant source of inspiration and encouragement. I am very grateful to **Dr. Martin Grossherr, Prof. Hartmut Gehring and Dr. Kai Kueck** for their guidance and ideas, without their constant encouragement and support, it would have been impossible for me to complete this thesis.

I convey my gratitude to **Prof. Ulrich Hofmann** for offering supervision of the thesis despite his busy academic commitment. I offer my most profound thanks to **Prof. Claus-Peter Siegers** for broadening my research carrier.

I am very much thankful to my dear friend Krishna, for his help throughout the work and I also thank my friends Mr. Senthilkumar Murugesan and Mr. Ramasamy for their support and timely suggestions in LabVIEW programming. Special thanks go to the staff and technicians working in Dräger, Chemical and biochemical sensors department.

Last but not the least, I am extremely grateful to my parents and sister for their affection and constant encouragement without which I would not have come to this position in my life.

Abstract

The research work presented in this thesis discusses innovative strategies for breath propofol detection, monitoring and its pharmacokinetic modeling. Design of a breath based propofol control system is also presented. Propofol (2,6-diisopropylphenol) has become a commonly used hypnotic in total intravenous anesthesia. It has some volatility, so it can be detected in exhaled breath gas of individuals receiving intravenous propofol. Online detection and quantification of propofol bolus in breath reflect plasma propofol concentrations. The research work presented in this thesis focus on three main objectives

1. Monitoring and quantization of exhaled breath propofol using IMR-MS (Ion molecule reaction mass spectrometer) and electrochemical sensors that detects propofol from expired gas.
2. Design of a multi compartment pharmacokinetic model to describe the expired breath propofol concentrations.
3. Development of a breath based feedback control system which controls intravenous propofol application.

Proof-of-concept experiments were conducted to address the principles in monitoring of breath propofol and breath based feedback control system.

In the introduction Chapters 1 and 2, various principles of breath monitoring and methods used to detect propofol in breath are explained in detail. A brief introduction to the concepts of pharmacokinetic modeling (with emphasis on compartmental modeling) and anesthesia control are given. The goal is to acquaint the reader with the terminology and principles involved in breath monitoring and the mathematical model that has been proposed to describe it.

In Chapter 3, the experimental methods and procedures used in the study are elaborately explained. Details about the preclinical study protocols are also given.

Chapter 4 focuses on the detection of breath propofol by electrochemical sensor. The optimisation methods used in developing the sensor system are also briefly described in this chapter.

In Chapter 5, monitoring of exhaled propofol using ion molecule reaction mass spectrometry (IMR-MS) and electrochemical sensor after administering propofol boli with a continuous

infusion in pigs is well described. Also the characterization of breath propofol detected by both IMR-MS and electrochemical sensor is explained. Effects of changes in breath frequency, cardiac output and hemorrhagic shock on breath propofol pharmacokinetics are demonstrated.

Chapter 6 focuses on design of a multi compartment pharmacokinetic model to describe expired gas propofol concentrations. This model is used as a patient simulator for the design of the feedback control system. The performance of this model is presented.

Chapter 7 discusses the breath based control system design and its performance. Its performance in maintaining anesthesia is compared to results from previous studies using BIS (bi-spectral index) as the control variable.

Contents

1

Introduction

1.1 Anesthesia

Anesthesia refers to a condition of reduced sensibility in the body. The term comes from the Greek word aesthesia, which means “ability to sense”. The prefix a- (an-, in the presence of a vowel) is used for negation. Therefore anesthesia stands for “inability to sense” and it indicates a “condition of deprived sensibility”. Anesthesia is a reversible pharmacological state induced by the administration of anesthetic drugs. Delivery of adequate anesthesia during medical treatments ensures the patient hypnosis, analgesia and muscle relaxation [Morgan GE and Mikhail MS, 1996].

1.1.1 Hypnosis

Hypnosis describes a state of unconsciousness and the absence of post-operative recall. A patient undergoing a surgical procedure might feel pain and is generally in a position of great discomfort and anxiety. If the patient is not properly sedated, the awareness of the events taking place in the operating room can be a traumatic experience. It is therefore important to make sure that the patient is amnesic, i.e. that the patient will retain no explicit memory of the events occurring during the surgery [Durbin CG, 1999].

1.1.2 Analgesia

Analgesia is associated with the relief of painful stimuli. The stress produced by surgical pain triggers different autonomic responses that have an influence on metabolism, immune function and the cardiovascular system [Durbin CG, 1999]. Diverse reactions to surgical stimulation can be observed, from rapid hemodynamic changes to awakening. A stable analgesic state is necessary for the achievement of a steady level of hypnosis, and vice versa. However, difficulties in quantifying both painful stimulation and patient sensitivity make it troublesome to guarantee a

stable analgesic state. Analgesia is provided with the administration of analgesic drugs, such as opioids (fentanyl, alfentanil, sufentanil, and remifentanil, amongst others). At present there is no specific measure, parameter or sensor to evaluate analgesia intraoperatively. The concept of pain perception in the unconscious is actually still debated and questioned [Gentilini AL, 2001]. Another source of complexity results from the fact that clinical signs that could indicate the perception of pain by the patient, such as tearing, pupil reactivity, eye moving and grimacing, are partially suppressed by muscle relaxants, vasodilators and vasopressors.

1.1.3 Muscle relaxation

Skeletal muscle relaxation is induced to facilitate tracheal intubation and the access to internal organs. It also depresses movement responses to surgical stimulation that could represent a health threat for the patient. Relaxation is achieved via neuromuscular blocking agents and it can be assessed by the muscular response to electrical stimulation. For example, it can be evaluated by measuring the force of thumb adduction during ulnar nerve stimulation [Gentilini AL, 2001].

1.2 Types of anesthesia

There are several forms of anesthesia. Arguably the simplest classification is:

- general anesthesia
- local or regional anesthesia
- monitored anesthesia care (MAC), or (conscious) sedation.

1.2.1 General anesthesia

In modern clinical practice, general anesthesia is provided only when strictly necessary in order to reduce the invasiveness of the procedure. Hypnosis is delivered via the administration of a hypnotic, which can be a volatile (e.g. isoflurane) or an intravenous agent (e.g. propofol). When an intravenous agent like propofol is used as an hypnotic then the anesthesia is termed as the Total Intra Venous Anesthesia (TIVA). Propofol based TIVA represents the field of interest of the present work.

Propofol based total intravenous anesthesia (Propofol-TIVA)

Propofol is widely used short-acting, intravenously administered hypnotic agent. Propofol based total intravenous anesthesia (TIVA) has become popular in the past decades [Soliman HM, 2001]. Some advantages of propofol are its favorable pharmacodynamic and pharmacokinetic properties, such as high lipophilicity, which allows rapid penetration into the CNS, rapid onset of and emergence from sedation, short pharmacologic serum half-life, absence of pharmacologically active metabolites, and rapid metabolic clearance [Soliman HM, 2001]. Increased propofol administration was recently reported by 35% of intensive care physicians managing critically ill patients. But the manual control of propofol is not easy; the concept of target controlled infusion (TCI) was introduced by AstraZeneca as Diprifusor (Diprifusor manual Astrazeneca). The device is programmed to perform the pharmacokinetic calculations and infusion rate adjustments to achieve the given blood plasma or effect site propofol concentrations [Sheiner LB, et al., 1979]. TCI devices allow the anesthetist to provide anesthesia by controlling the theoretical (predicted) concentration of the drug in the central compartment. Rapid changes in the depth of anesthesia are therefore possible with similar ease to that achieved with inhalational anesthesia. But unlike inhalational anesthesia, where the end-tidal concentration of vapors can be monitored, on-line blood concentration monitoring is not practical at the present time. The analysis of propofol concentration in the expired alveolar gas may be a promising noninvasive method for monitoring plasma propofol concentrations.

1.2.2 Local or regional anesthesia

Most surgeries are performed with local/regional anesthesia or monitored anesthesia care. The former (spinal, lumbar epidural, caudal anesthesia are examples) requires small amounts of anesthetic and it is usually well tolerated by the body. Emergence of the anesthetized is often rapid and unproblematic. The latter entails the simultaneous practice of regional anesthesia and patient sedation, according to the American Society of Anesthesiologists (ASA) [Ghisi D, et al., 2005].

1.2.3 Conscious sedation

Conscious sedation is defined as a medically controlled state of depressed consciousness that allows protective reflexes to be maintained. The sedated patient retains the ability to breathe

autonomously and to protect the airways. Depending on the depth of sedation, the patient can respond to verbal commands and tactile stimulation with different degrees of purposefulness [Novak LC, 1998].

1.3 Motivation

The intravenous narcotic propofol (2,6-diisopropyl-phenol), is currently used in a wide range of anesthetic procedures. However, a noninvasive method for continuously monitoring plasma propofol concentrations is not yet available, and therefore, alternative procedures such as the technique of target-controlled infusion of propofol [Iwakiri H, et al., 2005; Pandin PC, et al., 2000; Egan TD and Shafer SL, 2003] or the control of propofol infusion by monitoring electroencephalographically derived indices (*e.g.*, Bispectral Index) [Struys, et al, 1998] have been developed.

The analysis of propofol concentration in the expired alveolar gas (C_pg_m) may be a promising noninvasive method for monitoring plasma propofol concentrations (C_ppl_m). However, several conditions must be fulfilled before introducing such a method into clinical routine: 1. an animal model has to be established in which the concentration of an anesthetic agent can be controlled and determined, and even minor changes in anesthetic concentration must be clearly registered in both breath and plasma samples; 2. as propofol is hardly volatile, its presence in exhaled air must be proven and quantified clearly; 3. the relation between breath and plasma concentrations of propofol must be characterized 4. taking into consideration that the lung may participate in the extrahepatic clearance or metabolism of propofol, the effects of pulmonary metabolism and distribution of propofol must be studied, e.g., by measuring its plasma concentrations in both the mixed venous and the arterial compartment of the vascular system; and 5. a reliable, simple and robust routine procedure must be developed to monitor propofol in breath gas [Grossherr M, et al., 2006].

Breath propofol is a best direct measure that reflects the plasma propofol concentrations. Hence this can applied in designing a automated closed loop propofol delivery system. To characterize and to design a closed loop system using breath propofol as the sensing parameter a pharmacokinetic model (which simulates breath propofol concentrations) may help in simulating the setup. Hence we designed a pharmacokinetic model from an existing three compartment model to simulate breath propofol concentrations.

The anesthetist's tasks are most of the time of routine nature. However, critical incidents occur in the operating theatre as in any other safety critical procedure. The anesthetist needs to be prepared for such critical incidents to minimize occurrence and subsequent negative effect for the patient. Moreover, recent developments of short acting drugs require persistent monitoring of the corresponding effect, which automatic control concepts are able to provide. The potential for automation is therefore in reducing the workload of the anesthetist's routine tasks such that increased supervision of the critical signs is possible. So far, the supervision of critical signs cannot be accomplished by a circuitry or a computer system [Linkens DA and Hacisalihzade SS, 1990]. Moreover, automated systems are not affected by distraction or to fatigue, thus they maintain the same vigilance level throughout the surgical procedure. Continuous supervision of certain patient parameters (generally, in clinical practice the term parameter (or patient parameter) is used for "time varying" measurements.) by a computer system in combination with increased possibilities of supervision by the anesthetist should obviously reduce critical incidents and therefore reduce patient risk. Other patient benefits are improved outcome (faster recovery, less side effects) due to improved stability of the controlled parameters.

Reducing costs by minimizing drug consumption is often discussed, but so far the impact is comparatively low. Such studies [Struys MM, et al., 2002a] show only a moderate potential to reduce cost compared to the general costs of a surgical procedure. The increasing number of open positions for anesthetists may require solutions along the line of an "autopilot" to free resources for tasks, which require an anesthetist. Many authors describe closed-loop control in anesthesia. Until now, most of the systems are still under development [Struys, et al MM, 2002b] and have not passed the testing phase. It should be remembered that it takes considerable time for a technique to mature into routine usage [Linkens DA and Hacisalihzade SS, 1990].Therefore, the development of closed-loop control systems for anesthesia needs also to focus on increasing the clinical applicability.

. The effectiveness of such controllers depends strongly on the reliability of the physiological signal to be controlled [Tucker GT, 1990] and on the optimisation of control algorithms. The controlled variable or variables must be measured reliably. An ideal sensor for control should reflect the dose-response relation of the drug, should also reflect the anesthetist’s observations, should not introduce non-linearities (especially discontinuities) and should not introduce (unknown or variable) additional delay. Some measured variables (e.g. blood pressure,

muscle activity, ventilatory parameters, inhaled drug concentration) are direct indicators of the controlled variable and have been applied to developing closed-loop systems [Gentilini A et al., 2001; Hoeksel SA et al., 2001].Other drug effects are not directly measurable. 'Depth of hypnosis' or 'level of analgesia' is not measurable, so surrogate measures (e.g. Bispectral index - BIS) have to be applied as the controlled variable. Most of the present day closed loop systems under research use BIS, blood pressure etc to control anesthesia. The breath propofol that is detected by IMR-MS or electrochemical sensor is a direct measure of the plasma propofol concentration.

1.4 Objectives

The main objectives for carrying out this work are described below

Breath propofol detection

Breath propofol monitored by IMR-MS and electrochemical sensors are compared to the plama propofol concentrations and standard techniques such as GC-MS (Gas chromatography-mass spectrometry) using Bland Altman's method [Bland JM and Altman DG, 1986] and Linear regression analysis. After characterizing the breath propofol data modeling was carried out.

Modeling

In pharmacokinetics different models are in common use [Gentilini AL, 2001] and a main objective was to develop a modeling framework, which could be applied to simulate expired gas propofol concentration. Automatic control concepts based on a mathematic model of the process show many advantages concerning robustness and possible artefact handling procedures.

Controller design

In general, the standard design technique of proportional-integral-derivative (PID) controller was used. Important features were added to meet the specification of the "imitated" anesthetist, safety strategies in case of measurement artefacts, failures or faults were also added.

Platform

The actual controllers were designed and implemented for the preclinical study after a detailed pharmacokinetic model analysis of exhaled propofol.

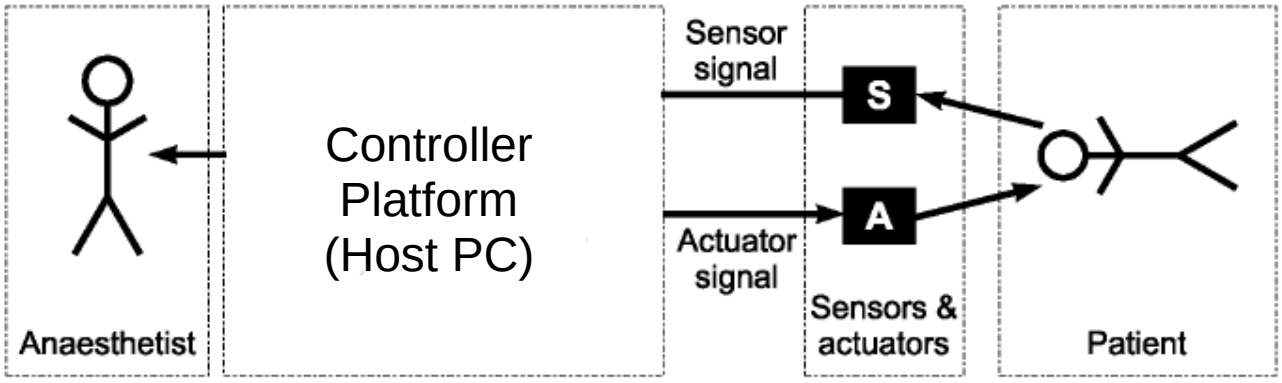

Figure 1.1 Schematic representation of the set-up used in the operating theatre, consisting of patient, sensors, actuators, the actual controller platform with the main components as well as the anesthetist who is operating the device.

In figure 1.1 the set-up of the controller platform in a clinical environment is represented. The host is a standard personal computer running under Windows XP. Many more sensors and actuators have been added to the system in recent years. In this thesis we have used output from ion molecule reaction mass spectrometer (IMR-MS) as the sensing signal and Fresenius base A (power supply) with Fresenius computer controlled infusion pump attached to it as the actuator to develop a breath based control system.

References

Apfel CC et al. A factorial trial of six interventions for the prevention of postoperative nausea and vomiting. N Engl J Med, 2004, 350,2441–51

Bland JM and Altman DG. Statistical methods for assessing agreement between two methods of clinical measurement. Lancet, 1986, 307-310

Charlton JE. (editor): Core Curriculum for Professional Education in Pain. IASP Press, Seattle,2005.

Durbin CG. Respiratory Therapists and Conscious Sedation. Respiratory Care, 44(8), 1999.

Dawidowicz A et al. The role of human lungs in the biotransformation of propofol. Anesthesiology, 2000, 93,992–7

Egan TD and Shafer SL. Target-controlled infusions of intravenous anesthetics: Surfing USA not! Anesthesiology, 2003, 99,1039–41

Gentilini A et al. Modeling and closed-loop control of hypnosis by means of bispectral index (BIS) with isoflurane. IEEE Transaction of Biomedical Engineering, 2001, 48, 874–889.

Gentilini AL. Feedback Control of Hypnosis and Analgesia in Humans. Dr. Tech. Sc. Thesis, Swiss Federal Institue of Technology (ETH), Zurich, Switzerland, 2001.

Ghisi D et al. Monitored anesthesia care. Minerva Anestesiology, 2005, 71(9),533–538.
Hoeksel SA et al. Computer control versus manual control of systemic hypertension during cardiac surgery. Acta Anesthesiologica Scandinavica, 2001, 45, 553–557.

Grossherr M et al. Discontinuous monitoring of propofol concentrations in expired alveolar gas and in arterial and venous plasma during artificial ventilation. Anesthesiology, 2006, 104, 786-90.

Hoymork SC et al. Bispectral index, serum drug concentrations and emergence associated with individually adjusted target-controlled infusions of remifentanil and propofol for laparoscopic surgery. Br J Anaesth, 2003, 91,773–80

Iwakiri H et al, Individual effect-site concentrations of propofol are similar at loss of consciousness and at awakening. Anesth Analg, 2005, 100,107–10

Linkens DA and Hacisalihzade SS. Computer control systems and pharmacological drug administration: a survey. Journal of Medical Engineering & Technology, 1990, 14, 41-51.

Morgan GE, and Mikhail MS. Clinical Anesthesiology, second ed. PrenticHall International, Inc., 1996.

Novak LC. ASA Updates its Position on Monitored Anesthesia Care. American Society of Anesthesiologists Newsletter, 62(12), 1998.

Pandin PC et al. Predictive accuracy of target-controlled propofol and sufentanil coinfusion in long-lasting surgery. Anesthesiology 2000, 93,653–61

Struys MMRF et al. Cost-reduction analysis of propofol versus sevoflurane: Manitenance of anesthesia for gynaecological surgery using the bispectral index. European Journal of Anesthesiology, 2002a, 19, 727-34.

Struys MMRF et al. Closed-loop control of anesthesia. Current Opinion in Anesthesiology,2002b,15, 421-425.

Soliman HM et al. Sedative and analgesic practice in the intensive are unit: the results of a European survey. Br J Anaesth, 2001, 87, 186-92.

Sheiner L.B et al. Simultaneous modeling of pharmacokinetics and pharmacodynamics: Application of d-tubocurarine. Clin. Pharmacol. Ther. 1979, 25,358-371.

Tucker GT. Pharmacokinetic and pharmacodynamic models. Advances in Pain Research and Therapy,1990, 14, 181-201.

2

Principles of breath analysis and exhaled propofol monitoring

2.1 Introduction

Breath analysis is a method to analyze exhaled gas from an animal or a human being. It is used for clinical diagnosis, detecting disease states and exposure to environmental conditions. The exhaled air contains volatile compounds which can be related to their blood concentrations. Nearly 200 compounds can be detected in human breath and they are correlated to various diseases. The actual breath contains mixture of oxygen, carbon dioxide, water vapour, nitrogen and inert gases. In addition it also contains various elements and more than 1000 trace volatile compounds with their concentrations ranging from parts per million to parts per trillion. The Volatile Organic Compounds (VOCs) commonly found in normal breath are acetone, ethane and isoprene [Manolis A, 1983; Cheng WH and Lee WJ, 1999]. This chapter explains the principles involved in breath analysis, diagnostic uses of clinical breath test and the instrumentation involved. Detailed explanations on detecting breath propofol concentrations (during TIVA using propofol infusion) by GC-MS (gas chromatography-mass spectrometry), IMR-MS (ion molecule reaction-mass spectrometry) and electrochemical sensors are also given here.

2.2 Principle involved in breath analysis

External chemicals enter the body by three ways namely ingestion, inhalation and topical contact. The chemicals absorbed into systemic circulation will distribute in the body or directly excreted into the faeces [Manolis A, 1983]. This absorbed chemicals are of two types,

volatile and non volatile. The volatile compounds get exchanged with alveolar air and are expired in the breath, known as VOCs. These VOCs can be detected through breath analysis. The breath analysis can be explained by pharmacokinetic models related to the VOCs.

Principle of breath analysis is based on the physiological basis gaseous exchange between air and blood. Gas exchange occurs at the surface of numerous tiny chambers known as alveoli, present at the tip of bronchial air passage (figure 2.1). Alveoli's are well adapted to their functions; they are lined with very thin membranes that are loaded with capillaries. A blood gas barrier is formed (shown by an arrow in figure 2.1) between a red blood cells moving through the capillaries and the air inside the alveoli. The large surface area and tiny distance associated with alveoli makes the VOC's to diffuse from the air into blood.

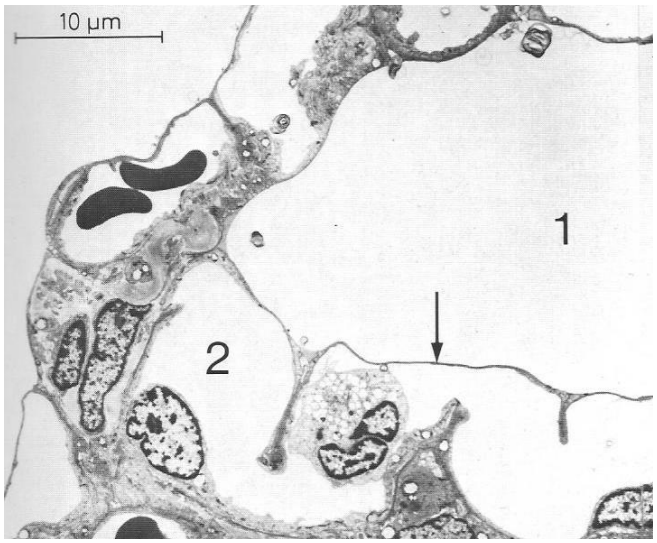

Figure 2.1 The blood gas barrier (arrow) has to be passed for substances which can be measured in breathing gas (1: alveoli) and which are distributed from the blood (2: capillary). The effect of this barrier on the distribution of substances between blood and breath gas is not yet known [Cheng WH, et al., 1999]

The key challenge in the analysis of breath is 'separating the alveolar breath', which contains analyte rich air delivered deep in the lungs from the 'dead space' air volume of breath contained in the upper airways namely mouth and pharynx which are not involved in gas exchange. Another challenge is separating and identifying the volatile breath components which are at just picomolar level concentrations [Wallace L et al., 1993; Phillips M et al., 1999].

2.3 Diagnostic uses of clinical breath test

The discovery of VOCs in breath, lead to its use in the diagnosis of diseases, disorder and metabolic studies. Phillips et al. [Phillips M et al., 1999] explained that breath can be analysed without analytical instruments, example in uncontrolled diabetic patients, breath smells like rotten apple due to the presence of acetone in their breath. Renal failure patients had urine like odor in their breath and a lung abscesses patient breath smell like sewer because of the proliferation of anaerobic bacteria [Phillips M et al., 1999;Schubert JK et al., 2004]. The techniques of breath test have progressed considerably in recent years. However, in order to introduce more breath tests into clinical practice, the test techniques/devices are expected to possess following characteristics: 1. high selectivity, high sensitivity, and fast response to test gas 2. immunity to the interference of water vapor in breath 3. size and ease of operation; and 4. low construction and maintenance cost. With these features, the breath test will make a very positive contribution to clinical practice.

New instrumentation for breath analysis was started in 1970, mainly by Gas Chromatography (GC), but the major challenge was correlation of physiological breath's VOCs and breath marker's with patient's clinical symptoms [Mukhopadhyay R, 2004; Phillips M, 1992]. Breath test studies have been conducted to detect lung diseases [Kharitonov SA et al., 1996], oxidative stress [Hansen TK et al., 2003; Izumi M et al., 2002; Phillips M et al., 2004] and gastrointestinal diseases [Perman JA,1991; Bauer TM, et al., 2000;Nieminen U et al., 2000]. A short explanation on lung disease diagnosis is given.

Lung diseases

Some common lung diseases are asthma, Chronic Obstructive Pulmonary Disease (COPD), Cystic Fibrosis(CF), bronchiectasis, interstitial lung disease etc. Elevated levels of hydrocarbons (pentane and ethane) in exhaled breath are used as biomarkers for detecting above mentioned diseases. Other than hydrocarbon markers, another notable marker is Nitric Oxide (NO). NO is used to detect different lung diseases such as Asthma, COPD and CF [Kharitonov SA et al., 1996].

Advantages of Breath Analysis

1. Breath analysis gives exact information of the blood constituent and many biomarkers found in the alveolar breath can be significantly detected in disease or disorders.
2. Breath analysis is non-invasive, easy process.
3. Breath analysis is correlated with arterial concentration of analytical constituents which is difficult to detect in blood samples.
4. Breath analysis is advantageous over blood and urine analysis with more number of sample collections.
5. Breath sample is less complicated mixture than blood and urine, therefore analysis of breath is easier and faster process.
6. Breath analysis gives information mostly related to respiratory system which is not given by other techniques.
7. Breath analysis shows status of decay of volatile toxic substances in the body.

Limitations in breath analysis

1. The major drawback of breath analysis is absence of standard analytical methods, therefore the are variation in results.
2. Breath analysis requires sample collection and pre-concentration because concentration of many substances ranges from nmol/L to pmol/L.
3. Pre-concentration can be performed by adsorption on sorbent traps, coated fibres or by direct cryofocusation. These types breath sample collection and pre-concentration methods are difficult to standardize compared to blood sampling techniques.
4. The exhaled breath contains more water content in pre-concentration sampling and detection of substances.
5. Breath analysis is more expensive than regular simple chemical tests which are used in blood and urine.
6. Another major problem is correlation between breath substances and disease.

2.4 Techniques for breath analysis

2.4.1 Gas chromatography techniques

There are various detection techniques by which breath can be analyzed using Gas chromatography (GC). Basically in GC, samples are injected into the headspace of the chromatographic column travels through it and gets separated in gaseous mobile phase. Separation efficiency depends on the type of GC column used.

The non-polar compound of the GC column such as silicone is separated on the basis of the boiling point and the separation of the polar component (analyte) depends on polarity of the substances [Giardina M and Olesik SV, 2003]. Various types of detection methods are employed together with GC for breath analysis. Some of them are explained in detail.

2.4.2 GC-MS (Gas chromatography – mass spectrometry)

In this technique MS detection is done on the basis of mass to charge ratio of ionized atoms or molecules of the analyte which quantitatively gives measures the compound. The compound can be identified by the fragmentation pattern and quantified by the formation of daughter ions [Pleil JD and Lindstrom AB, 1997], now GC-MS is a standard technique in the detection of VOCs in breath. Giardina el al. show that lung cancer is related compounds such as 2- methylheptane, styrene, propylbenzene, decane, and undecane [Giardina M and Olesik SV, 2003]. In breath these compounds can be detected with help of the low temperature glassy carbon (LTGC) and a macrofiber to be absorbed on. After desorption, the VOCs were analysed via GC-MS [Giardina M and Olesik SV, 2003]. Pleil and Lindstrom mentioned GC-MS breath test to assess exposure to halogenated VOCs [Pleil JD and Lindstrom AB, 1997]. Miekisch et al. applied headspace solid-phase microextraction coupled with gas chromatography–mass spectrometry (HS-SPME–GC–MS) to assess breath and blood concentrations of propofol in patients under sedation [Miekisch W et al., 2008].

Thermal desorption GC-MS

Thermal desorption GC-MS technique was used by our group to analyse propofol in breath (refer section 3.4). Thermal desorption is really a constellation of techniques that are used to extract and concentrate volatiles from a complex matrix prior to GC or GC/MS analysis. For gaseous samples such as air, one of the most convenient approaches is to draw a known volume through a

thermal desorption tube (eg. Tenax tube) that is packed with one or more adsorbents. When the thermal desorption tube is heated, volatiles are released from the trapping material or from the sample itself and are swept by a flow of inert gas into a secondary trap [Miekisch W et al., 2008]. Depending upon the instrumentation, the trap may be packed or unpacked and is often cooled below room temperature. Finally, the secondary trap is heated rapidly while a stream of carrier gas sweeps the desorbed volatiles into the GC for separation and analysis (refer Figure 2.2). From the secondary cold trap the gas to be analysed enters the GC-MS.

Grossherr et al discontinuously monitored propofol (after TIVA using propoofol) in expired alveolar gas with thermal desorption GC-MS which they correlated to the plasma propofol concentrations [Grossherr M et al., 2006]. In our study this method is used as the standard technique to correlate the exhaled breath propofol concentrations from IMR-MS and electrochemical sensor measurements.

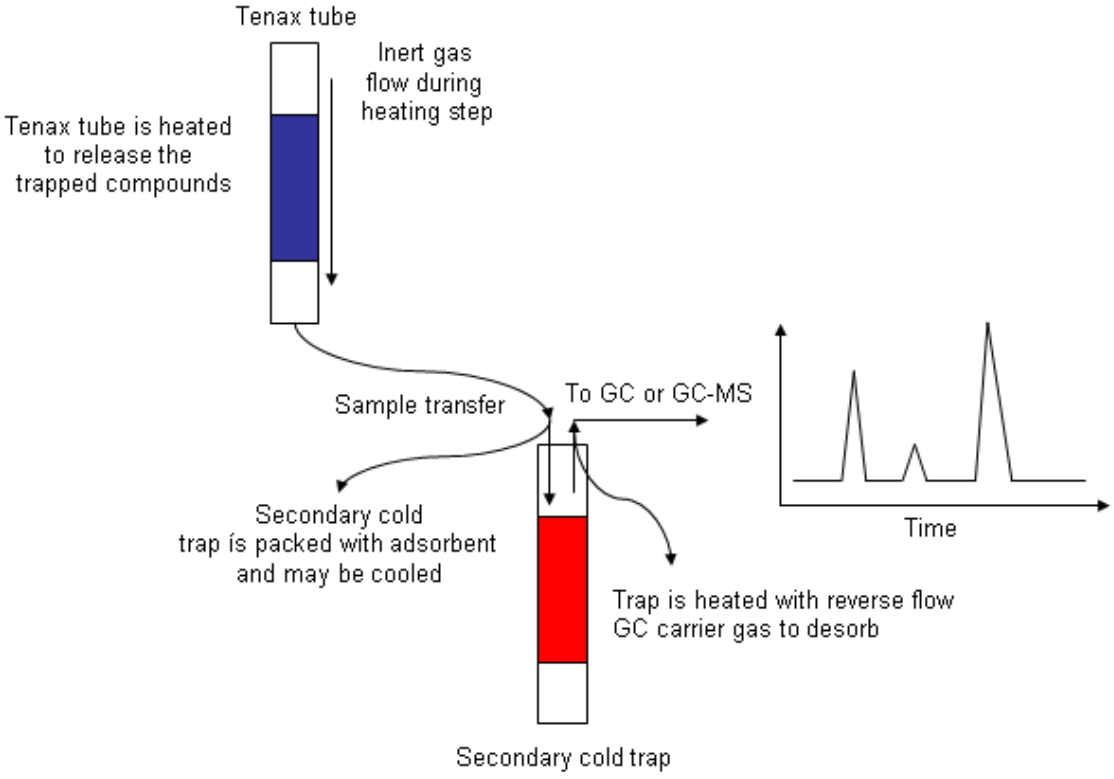

Figure 2.2 Schematic showing the Thermal Desorption Gas Chromatograph- Mass spectrometry process. [Grossherr M et al., 2006]

2.4.3 GC-FID (Gas chromatography-flame ionization detector)

In GC-FID effluent substances are mixed with hydrogen, air and ignited. Organic compounds burning in the flame produce ions and electrons that can conduct electric potential through the flame. High electrical potential is applied at the flame and a collector is located above the flame. The development of current from pyrolysis of organic compound is measured. FID's are more mass sensitive than concentration sensitive, this is an advantage, as for changes in mobile phase, flow rate do not affect the detector responses. FID is mostly used for organic compound detection, it highly sensitive with large response range and low noise. Therefore FID is used in GC for breath test [Kneepkens CME et al., 1994]. Sanchez et al. applied GC-FID for human breath analysis, in that they combined a nonpolar dimethyl polysiloxane column and trifluoropropylmethyl polysiloxane column for selectivity of the VOCs in breath. The detection level of their system is in low ppb range [Sanchez JM and Sacks RD,2003]. Phillips et al. assayed VOCs in breath using GC-FID. This method was sensitive, linear, accurate and reproducible for quantitative assay of endogenous isoprene in the breath [Phillips M and Greenberg J, 1991].

2.4.4 GC-IMS (Gas chromatography-ion mobility spectrometry)

Ion Mobility Spectrometry was discovered in the late 1960s. The principle method of IMS is to separate ions according to mobility as they travel through a purified gas in an electric field at atmospheric pressure. This ion travels with varying velocities through the purified gas. The total travel time depends on the drift length, electric field strength; drift gas as air or pure nitrogen, temperature and atmospheric pressure [Haley LV and Romeskie JM, 1998]. IMS is a selective detector capable of quantifying substances from mixtures and it is relatively portable and inexpensive. GC-IMS are two different technologies producing a new system that introduces the advantages of the individual technologies. Lord et al. investigated presence of ethanol and acetone as biological indicator of human health as well as exposure of VOC by GC-IMS [Lord H et al., 2002]. Ion mobility spectrometry is a method to characterize chemical substances using gas-phase mobility in a weak electrical field. The ion mobility alone might not be sufficient for a complete characterization of a sample. Therefore gas-chromatographic pre-separation techniques (e.g. Multi-Capillary Columns (MCC)) can be applied in addition.

Perl et al used MCC-IMS technique for detecting propofol in breath and compared it to serum propofol concentrations [Perl T et al., 2009].

2.4.5 Proton transfer reaction-Mass spectrometry (PTR-MS)

PTR-MS was discovered by A. Hansel and co-workers for online measurement of complex mixture of trace gas compounds in air with concentrations as low as one parts per billion [Tzanani N and Amirav A, 1997; Hansel A et al., 1995]. In PTR-MS, all VOCs had proton affinity than H_2O where proton transfer occurs in each collision .

Breath gas analysis by PTR-MS has more advantages for complex mixtures of gas because previous concentration of the compound to be measured and a separate separation procedure is not required. If compound is in higher concentration, like NO_2, CO_2,O_2 and H2O, it does not interfere with the measurement, here measurements upto part per billion and frequent/rapid measurements are possible. PTR-MS characterizes the substances individually according to their mass-to-charge ratio and chemical identification already proved using other techniques [Amann G, et al., 2004]. Karl et al used PTR-MS technique for measurement of breath isoprene, a correlation between breath isoprene and blood cholesterol levels was a shown [Karl T et al., 2001a;Amann G et al., 2004].Boschetti et al could monitor a large number of VOCs with in limited time period at high sensitivity upto parts per billion [Boschetti F et al., 1999]. Amann et al. mentioned results of three different studies of VOC emission using PTR –MS 1. analysis of VOC patterns in patients suffering from carbohydrate malabsorption 2. analysis of intra and intersubject variability of one particular mass 3. long-time, online monitoring of VOC profiles during sleep combined with polysomnography [Amann M et al., 2004]. This PTR-MS is related only to mass of the product ions but is not a unique technique to identify trace gases, because of overlap of mass spectra to different isomers which cannot be resolved [Gouw JD et al., 2003]. By coupling GC Column to PTR-MS, we can separate complex breath mixtures of different VOCs to single mass ions [Karl T et al., 2001b; Gouw JD, et al., 2003].

Propofol in breath was first measured in breath using PTR-MS by Harrison et al. [Harrison GR et al., 2003] they did a pilot study involving one patient, and the relation between the concentration of exhaled propofol and that of propofol in the blood was not evaluated. Following them Takita et al. characterised propofol in alveolar gas using PTR-MS with clear

statistical tests like Bland altman and linear regression analysis by comparing the plasma concentrations with alveolar gas propofol concentrations [Takita A et al., 2007]. In the study by Takita et al. a propofol bolus was also detected. But the bolus was not characterised.

2.4.6 Selected ion flow tube-Mass spectrometry (SIFT-MS)

SIFT-MS is constructed to allow on-line analyses of the exhaled breath, headspace of aqueous liquid and polluted air. SIFT-MS combines fast flow tube technique with quantitative mass spectrometry. The exhaled breath sample is taken into fast flowing inert gas e.g. helium carrier gas, present as trace gas in the sample and reacts with reagent ions (H_3O+, $NO+$ or O_2+) to form specific product ions that identify the compound and is quantified from knowledge of the kinetics of the ion. SIFT allows the direct analysis of single exhalations of breath and provides the clinician with immediate results [Smith D and Spanel P, 2005]. Spanel et al used SIFT-MS to detect isoprene from breath of 29 healthy volunteers for a period of 6 month during variable time periods of the day [Spanel P et al., 1999]. By using SIFT-MS technology, we can detect acetonitrile both in the exhaled breath and the headspace of urine from cigarette smokers and non-smokers [Smith D and Spanel P, 2005]. This study showed that detected quantity of acetonitrile depends on the cigarette consumption as compared to the absences in non smokers. Smith and Spanel presented, quantitative study of increasing ammonia from breath of patients after known to be infected with Helicobacter pyroli [Smith D and Spanel P, 2005].

2.4.7 Other detection methods

Chemiluminescence analyser

It is a more advantageous technique because breath is analyzed directly online to a analyzer or indirectly by sampling of breath in balloon which is analyzed later. This method specially is for asthmatic patients to detect nitric oxide level in breath. Nitric oxide level in breath is measured in parts per billion (ppb) [Abbott SN, et al., 2003].

Colorimetric sensor arrays

Colorimetric sensor arrays can be used in the exhaled breath analysis for detection of compounds. It is specially for the lung cancer patient. Mazzone et al showed that the

colorimetric sensor array has 36 spots which contain chemically sensitive compound on disposable cartridges. The changes in colour of spots occur due to its contact with volatile active compound which are present in exhaled breath [Mazzone PJ et al., 2007].

Flowing afterglow Mass Spectrometry (FA-MS)

FA-MS technique have same principle of SIFT-MS in that it exploits ion chemistry coupled with fast flow tube techniques and quantitative mass spectrometry. Mostly FA-MS is specifically used for the on-line determination of the deuterium content of water vapour in exhaled breath and the vapour above aqueous liquids [Lundberg J et al., 1994].

Differential mobility spectrometer (DMS)

It is micromachined Differential mobility spectroscopy used in breath analysis for identification of many chemicals on low level concentration as parts per billion and diagnosis of many diseases. It is a very sophisticated instrument as compared to traditional GC-MS in all its function [Sankan S et al., 2007].

2.5 Ion Molecule Reaction - Mass Spectrometry (IMR-MS)

The IMR-MS system used in this study was originally designed to measure trace gas components in industrial fields such as fuel cell or reformer gas development, work space control, and environmental measurements (Airsense Mass Spectrometry Systems; V&F Medical Development, Absam, Austria). The system is based on the use of ion–molecule reactions coupled with quadrupole mass spectrometry and provides a highly sensitive method for on-line and off-line sampling of organic and inorganic compounds in exhaled breath. A schematic diagram of the IMR-MS is shown in figure 2.2.

In the IMR-MS analyzers, the principle of ion–molecule reactions is applied as the interaction of positively charged atomic ions with neutral sample gas molecules in two body collision processes. This results in the formation of product ions whenever the ionization potential of the sample molecule is less than the potential energy of the incoming primary ion and hence the entropy of the process becomes positive. The excess energy of the binary reaction is first stored in the product ion as transition state and either is statistically distributed in internal degrees of freedoms (electron vibration, bond oscillations) or is used up to break the weakest bond of the ionized molecule leaving a lower molecular weight ion. Differences in ionization

potentials between primary and product ions may result in a bond rupture and hence a lower molecular weight fragment ion. The IMR-MS uses krypton, xenon, or mercury atomic gas to form the primary ion beam *via* electron impact ionization (section 1, figure. 2.2). In our experiments, mercury ions were used. They were generated out of mercury vapor by electron impact ionization. The patented IMR ionization method can use the atomic mass scale to detect different molecules with the same molecular weight. As an example, acetaldehyde and carbon dioxide have the same mass [Hornuss C et al., 2007]. The mercury beam with an ionization potential of 10.4 eV does not ionize carbon dioxide (13.8 eV), but it ionizes acetaldehyde (10.2 eV). Switching different ion beams and hence energy levels is fast and takes 400 ms. Krypton ions (14.0 eV) do well separate nitrogen (15.6 eV—not ionized) against carbon monoxide (13.7 eV) on mass 28 [Hornuss C et al., 2007]

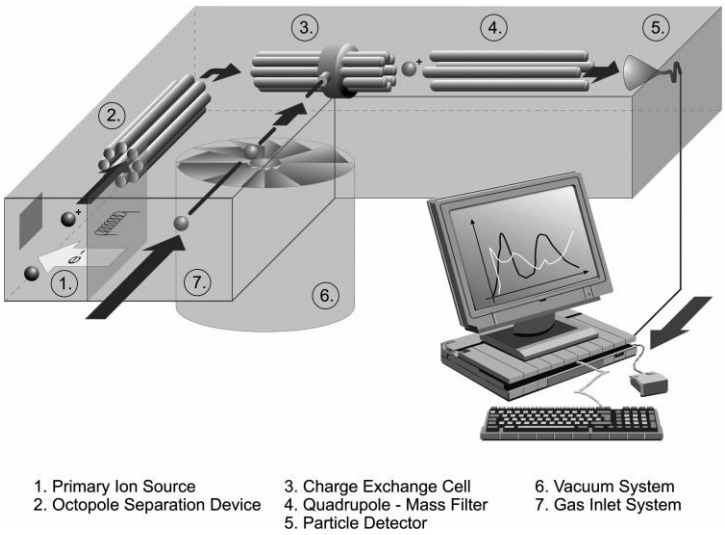

Figure 2.2. Schematic drawing of the ion–molecule reaction mass spectrometry system used in the study (57).

The instrument uses two octopole systems (section 2 and 3, figure 2.2) operated at high frequencies to store primary as well as product ions in a confined volume against their coulomb repulsion and transmit ions to the quadrupole mass analyzing section. The quadrupole mass separator (section 4, fig. 1), driven by direct current and alternating current, operates as an electromagnetic filter according to a parametric resonance to a specific mass over charge ratio.

At a given alternating to direct current ratio, only one specific mass of ions experiences a stabile trajectory through the quadrupole. A secondary electron multiplier (section 5, figure. 1) may generate as much as 108 electrons for each incoming ion. This allows the generation of an electrical pulse strong enough to be accepted by a computer counting system. The pulse rate represents the concentration of the molecular species in the gas sample brought to the instrument. The sample gas (section 7, figure. 2.2) is transferred in a 2.5-m-long heated capillary system (Silcosteel®; Restek,Bellefonte, PA) at a flow rate of 50 ml/min to the instrument. A constant pressure controller feeds *via* a second capillary a stable amount of 1.5 ml/min into the high vacuum ionization section. Gas response times to concentration changes are 50 ms, and gas dead times depending on the duration of the transfer capillary range between 2 and 4 s [Hornuss C et al., 2007]

2.5.1 Monitoring of Propofol using IMR-MS

In our study we monitored both the intact propofol molecule of 178 Da (propofols molecular weight) and also the fragment with the mol mass of 163 Da. Propofol 163 appears because during the ionization of propofol, one methyl group of the two isopropyl groups of the molecule is removed, thus resulting in a fragment of 163 Da. Early experiments (55) did show, however, that propofol 178 interacted during the ionization process with trace amounts of residual sevoflurane, which are usually present in the anesthesia circuit. This was caused by an interaction of the $C_4H_2OF_6$ fragment of sevoflurane that influenced mass 178, which was adjusted to a soft mass separation to gain signal strength. This resulted in a false-positive increase in propofol 178 signaling. This interaction was not seen when measuring a propofol fragment with a molecular mass of 163 Da.

Hornuss et al [Hornuss C et al., 2007] used IMR-MS to characterise the exhaled breath propofol concentrations for the first time. In this work, we monitored the expired gas breath propofol concentrations after propofol boli administration using IMR-MS (refer chapter 5 for details) [Varadarajan B et al., 2011].

2.6 Electrochemical sensor

2.6.1 Principle of Operation

Electrochemical sensors operate by reacting with the gas of interest and producing an electrical signal proportional to the gas concentration [Wang J, 2006]. A typical electrochemical sensor

consists of a sensing electrode (or working electrode), and a counter electrode separated by a thin layer of electrolyte. Gas that comes in contact with the sensor first passes through a small capillary-type opening and then diffuses through a hydrophobic barrier, and eventually reaches the electrode surface figure 2.3. This approach is adopted to allow the proper amount of gas to react at the sensing electrode to produce a sufficient electrical signal while preventing the electrolyte from leaking out of the sensor. The gas that diffuses through the barrier reacts at the surface of the sensing electrode involving either an oxidation or reduction mechanism. These reactions are catalyzed by the electrode materials specifically developed for the gas of interest. With a resistor connected across the electrodes, a current proportional to the gas concentration flows between the anode and the cathode. The current can be measured to determine the gas concentration. As current is generated in this process, this type of a sensor is often described as an amperometric gas sensor or a micro fuel cell.

2.6.2 Importance of a Reference Electrode

For a sensor requiring an external driving voltage, it is important to have a stable and constant potential at the sensing electrode. In reality, the sensing electrode potential does not remain constant due to the continuous electrochemical reaction taking place on the surface of the electrode. It causes deterioration of the performance of the sensor over extended periods of time.

To improve the performance of the sensor, a reference electrode is introduced. This reference electrode is placed within the electrolyte in close proximity to the sensing electrode. A constant potential is applied to the sensing or working electrode. The reference electrode maintains the value of this fixed voltage at the working electrode. No current flows to or from the reference electrode. The gas molecules react at the working electrode and the current flow between the sensing and the counter electrode is measured and directly proportional to the gas concentration. The value of the voltage applied to the sensing electrode makes the sensor specific to the target gas. The micro fuel cell-type electrochemical sensors do not require an external driving voltage. For example, an electrochemical sensor specific to oxygen has an anode, either Pb or Cd that supplies electrons for the reduction of oxygen at the cathode. During the oxidation of the anode, the electrons are released which then travel via an external circuit to the cathode where oxygen molecules consume the electrons as follows:

In acidic electrolyte

Oxidation at the anode: 2Pb + 2H2O → 2PbO + 4H+ + 4e-

Reduction at the cathode: O2 + 4H+ + 4e- → 2H2O

In basic electrolyte

Oxidation at the anode: 2Pb + 4OH- → 2PbO + 2H2O + 4e-

Reduction at the cathode: O2 + 2H2O + 4e- → 4OH

The overall reaction in both cases is: 2Pb + O2 → 2PbO.

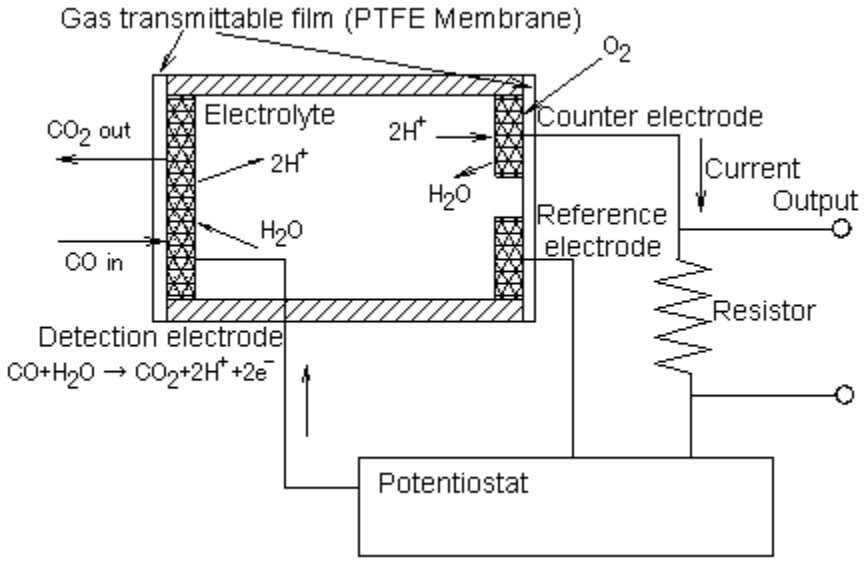

Figure 2.3 Cross sectional view of an amperometric gas sensor (carbon mono-oxide detection) [Wang, 2006]

2.6.3 Major Components

An electrochemical sensor (figure 2.3) consists of the following major components:

A. **Gas Permeable Membrane** (hydrophobic membrane): This is used to cover the sensor's sensing (catalyst) electrode and, in some instances, to control the amount of gas molecules reaching the electrode surface. Such barriers are typically made of thin, low-porosity Teflon membranes. Such sensors are called membrane clad sensors. Alternatively, the sensing electrode is covered with a high-porosity teflon and the amount of gas molecules reaching the electrode surface is controlled by a capillary. Such sensors are referred to as capillary-type sensors.

Besides offering a mechanical protection to the sensor, the membrane performs the additional function of filtering out unwanted particulates. Selecting the correct pore size of the membrane and capillary is necessary to transfer the proper amount of gas molecules. The pore size should be such as to allow enough gas molecules to reach the sensing electrode. The pore size should also prevent liquid electrolyte from leaking out or drying out the sensor too quickly.

B. **Electrode:** The selection of the electrode material is very important. It is a catalyzed material which performs the half cell reaction over a long period of time. Typically, the electrode is made from a noble metal, such as platinum or gold, and catalyzed for an effective reaction with gas molecules. Depending on the design of the sensor, all three electrodes can be made of different materials to complete the cell reaction.

C. **Electrolyte:** The electrolyte must facilitate the cell reaction and carry the ionic charge across the electrodes efficiently. It must also form a stable reference potential with the reference electrode and be compatible with materials used within the sensor. If the electrolyte evaporates too quickly, the sensor's signal will deteriorate.

D. **Filter:** Mostly a filter is fixed in front of the sensor to seperate unwanted gases. There is a limited selection of filters, each with different degrees of effectiveness. By properly selecting the filter medium, an electrochemical sensor can be made more selective to its target gases.

Choosing the suitable materials for the above components, and arranging the geometry of all these components to determine the optimum operating performance presents a challenge to scientists. Minor variations in the details of the sensor design can have a profound influence on the sensor's accuracy, response time, sensitivity, selectivity, and life expectancy. A more detailed explanation about the electrochemical propofol sensing is given in Chapters 3 and 4.

References

Abbott SM et al. Quantification of acetonitrile in exhaled breath and urinary headspace using selected ion flow tube mass spectrometry. I Int J Mass Spect, 2003, 228(2-3), 655-665.

Amann G et al. Applications of breath gas analysis in medicine. Int J Mass Spect, 2004, 239(2-3, 227-233.

Bauer TM, et al. Diagnosis of small intestinal bacterial overgrowth in patients with cirrhosis of the liver: poor performance of the glucose breath hydrogen test J Hepatol, 2000, 33, 382–386.

Boschetti F et al. PTR-MS real time monitoring of the emission of volatile organic compounds during postharvest aging of berryfruit. Postharvest Biology And Technology, 1999, 17(3), 143-151

.

Cheng WH and Lee WJ. Technology development in breath microanalysis for clinical diagnosis. J Lab Clin Med, 1999,133: 218-228.

Giardina M and Olesik SV. Application of low-temperature glassy carbon-coated macrofibers for solid-phase microextraction analysis of simulated breath volatiles. Ana Chem, 2003, 75(7), 1604-1614.

Ghoos Y et al. open-tubular gas chromatography in combination with an ion trap detector to assess volatile metabolites in human breath Biomedical and Environmental Mass Spectrometry 1989, 18(8), 613- 616.

Grossherr M et al. Discontinuous monitoring of propofol concentrations in expired alveolar gas and in arterial and venous plasma during artificial ventilation. Anesthesiology, 2006, 104, 786-90.

Gouw JD et al. Sensitivity and specificity of atmospheric trace gas detection by \proton-transfer-reaction mass spectrometry. Int J Mass Spect, 2003, 223-224,365-382.

Harrison GR et al. Real-time breath monitoring of propofol and its volatile metabolites during surgery using a novel mass spectrometric technique: A feasibility study. Br J Anesth, 2003, 91,797-9.

Hansel A et al. Proton-transfer reaction mass spectrometry-Online trace gas analysis at the ppb level. J Mass Spect Ion Proc, 1995, 150, 609-619.

Haley LV and Romeskie JM. Development of an explosives detection system using fast GC-IMS technology. IEEE 32nd Annual 1998 International Carnahan Conference on Security Technology, 12-14 Oct, Alexandria, VA, USA 1998, 59-64.

Hansen TK et al. Intensive insulin therapy exerts antiinflammatory effects in critically ill patients and counteracts the adverse effect of low mannose-binding lectin levels. J Clin Endocrinol Metab, 2003, 88, 1082–1088.

Hornuss C et al. Real-time monitoring of propofol in expired air in humans undergoing total intravenous anesthesia. Anesthesiology, 2007, 106, 665-74

Izumi M et al. Superoxide dismutase mimetics with catalase activity reduce the organ injury in hemorrhagic shock. Shock, 2002, 18, 230–235

Joseph Wang. Analytical electrochemistry, 3rd ed; John Wiley and sons,2006

Karl T et al. Human breath isoprene and its relation to blood cholesterol levels: new measurements and modeling. J App Physiol, 2001a, 91(2), 762-770.

Karl T et al. High concentrations of reactive biogenic VOCs at a high altitude site in late autumn. Geophysical Research Letters, 2001b, 28(3), 507-510.

Kharitonov SA et al. The elevated level of exhaled nitric oxide in asthmatic patients is mainly derived from the lower respiratory tract. Am J Respir Crit Care Med, 1996, 153, 1773–1780

Kneepkens CME et al. The potential of the hydrocarbon breath test as a measure of lipid peroxidation. Free Radic Biol Med, 1994, 17, 127-160.

Lindinger and Hansel A. Analysis of trace gases at ppb levels by proton transfer reaction mass spectrometry (PTR-MS). Plasma Sources, Science and Technology 1997, 6(2), 111-117.

Lindinger A et al. Online monitoring of volatile organic compounds at pptv levels by means of proton- transfer-reaction mass spectrometry (PTR-MS) medical applications, food control and environmental research. J Mass Spect Ion Proc, 1998, 173(3), 191-241.

Lord H et al. Breath analysis and monitoring by membrane extraction with sorbent interface. J. Ana Chem, 2002, 74(21), 5650-5657.

Lundberg J et al. Nasally exhaled nitric oxide in humans originates mainly in the paranasal sinuses. Acta Physiol Scand, 1994, 152, 431-432.

Manolis A. The diagnostic potential of breath analysis. Clin Chem, 1983, 29, 5-15.

Mayr D et al. Applications of breath gas analysis in medicine. Int J Mass Spect, 2003, 223-224, 743-756.

Mazzone PJ et al. Diagnosis of lung cancer by the analysis of exhaled breath with a colorimetric sensor array. Thorax, 2007, 62, 565-568.

Miekisch W et al. Assessment of propofol concentrations in human breath and blood by means of HS-SPME-GC-MS. 2008, Clin Chim Acta, 395,32–3

Mukhopadhyay R. Don't waste your breath. Anal Chem, 2004, 76, 273-276.

Nieminen U et al. Lactose malabsorption: use of breath hydrogen test and serum glucose analyses in diagnostics. Gastroenterology, 2000,118, 1132.

Perman JA. Clinical application of breath hydrogen measurements. Can J Physiol Pharmacol 1991, 69, 111–115.

Perl T et al. Determination of serum propofol concentrations by breath analysis using ion mobility spectrometry. Br J Anesth, 2009, 103,822-7.

Pleil JD and Lindstrom AB. Exhaled human breath measurement method for assessing exposure to halogenated volatile organic compounds. Cli Chem, 1997, 43, 723-730

Phillips M et al. Variation in volatile organic compounds in the breath of normal humans. J Chromatogr B Biomed Appl, 1999, 729, 75–88

Phillips M. Breath tests in medicine. Sci Am, 1992, 267, 74-79

Phillips M et al. Increased breath biomarkers of oxidative stress in diabetes mellitus. J. Clin Chim Acta, 2004, 344, 189–194.

Phillips M and Greenberg J. Ion-trap detection of volatile organic compounds in alveolar breath J Chrom Biomed Appl, 1991, 564(1), 242-249.

Sankaran S et al. Microfabricated differential mobility spectrometers for breath analysis. Sensors, 2007, 28-31, 16 – 19.

Sanchez JM and Sacks RD. GC analysis of human breath with a series-coupled column ensemble and a multibed sorption trap. Ana Chem, 2003, 75, 2231-2236.

Scholpp J et al. Breath markers and soluble lipid peroxidation markers in critically ill patients. Clin Chem Lab Med, 2002, 40, 587–594.

Schubert JK et al. Breath analysis in critically ill patients: Potential and limitations. Expert Review of Molecular Diagnostics, 2004, 4, 619-629

Smith D and Spanel P. The novel selected ion flow tube approach trace gas analysis of air and breath. Rapid Comm Mass Spect, 1996,10, 1183-1198.

Smith D and Spanel P. Selected ion flow tube mass spectrometry (SIFT-MS) for online trace gas analysis. Mass Spectrometry Reviews, 2005, 24, 661- 700.

Spanel P et al. Quantification of breath isoprene using the selected ion flow tube mass spectrometric analytical method. Rapid Comm Mass Spect, 1999, 13(17), 1733-1738.

Spanel P, Smith D. Selected ion flow tube mass spectrometry (SIFT-MS) and flowing afterglow mass spectrometry (FA-MS) for the determination of the deuterium abundance in water vapour.in Pier A. de Groot (ed.) Handbook of Stable Isotope Analytical Techniques, Elsevier. 2004, 88-102 .

Taucher J et al. Analysis of compounds in human breath after ingestion of garlic using protontransfer-reaction mass spectrometry. J Agr Food Chemy, 1996, 44(12), 3778-3782.

Takita A et al. On-line monitoring of end-tidal propofol concentration in anesthetized patients. Anesthesiology, 2007, 106,659-64.

Tzanani N and Amirav A. Flame-Based Method and Apparatus for Analyzing a Sample. Ana Chem, 1997, 69, 1248-1255

Varadarajan B et al. Monitoring of propofol boli in blood and breath described with a pharmacokinetic model.2011 (Under review)

Wallace L, et al. A linear model relating breath concentrations to environmental exposures: application to a chamber study of four volunteers exposed to volatile organic chemicals. J Expo Anal Environ Epidemiol, 1993, 3, 75–102.

Williams J et al. An atmospheric chemistry interpretation of mass scans obtained from a proton transfer mass spectrometer flown over the tropical rainforest of Surinam. J Atm Chem, 2001, 38(2), 133-166.

3

Procedures and methods

3.1 Introduction

This chapter explains about the standard experimental procedures involved in gas sampling, quantifying propofol concentrations in plasma and alveolar gas. Also detailed explanations on the performance indices used in predictive performance analysis of pharmacokinetic models and control system are included.

3.2 Anesthesia protocol

After approval from the regional authorities for animal research twelve (preclinical study I) and eight (preclinical study II) pigs (n=12 and 8, weight – 29 - 42 kg) were included in this study. After premedication and obtaining intravenous access, anesthesia was induced with etomidate and ketamine. Pancuronium was given to facilitate endotracheal intubation.

3.2.1 Preclinical study I

After collecting blank blood samples, propofol was applied as a bolus (4 mg/ kg bodyweight) at 0, 30, 60 min along with continuous infusion (9.6 mg/ kg body weight x h). This standard dosage profile was maintained for all twelve pigs. The IMR-MS and the electrochemical sensor lines (two sensors were used) were directly connected to T-pieces in fixed to the endotracheal tube. The sensor 2 had an nafion tubing attached in the sample line. Samples of arterial blood were obtained at 2, 5, 10, and 20 min after each bolus injection. The samples were analysed for propofol content using reversed-phase high-performance liquid chromatography (HPLC)

3.2.2 Preclinical study II

After collecting blank blood samples, propofol was applied as a bolus (4 mg/ kg bodyweight) along with continuous infusion. The controller was started with the steady state breath

concentrations as the set point. The set point was decreased to half the value after 60 minutes and then back to the initial value. Blood samples were taken before and after change of set point (six samples (two at each set point change) were collected after 3 hours).

3.3 Gas sampling procedure for GC-MS

Samples of exhaled breath from mechanically ventilated animals were collected using a method essentially described by Schubert et al [Schubert JK et al., 2001]. Alveolar gas was detected using a mainstream carbon dioxide sensor connected to the endotracheal tube. From the gas mainstream samples were drawn through a T-piece by a pump (figure. 3.1), which was automatically activated and deactivated when a preset carbon dioxide concentration of 25 mmHg was passed. End-tidal gas, 7–10 ml, was obtained from several breaths, revealing a total gas volume of 100 ml for pigs drawn through the adsorption tubes [Grossherr M et al., 2006].

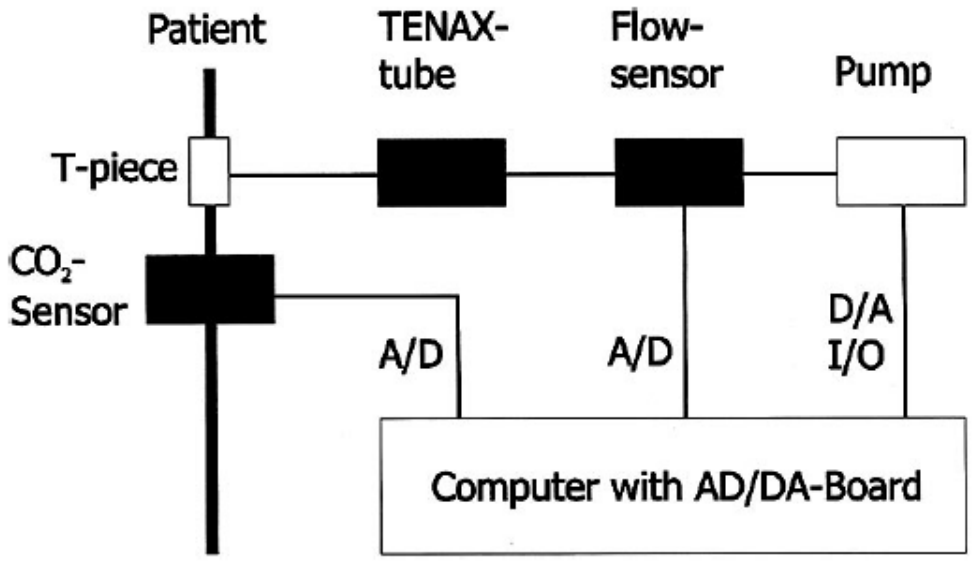

Figure 3.1 Schematic setup for the gas sampling system: A mainstream carbon dioxide sensor triggered the pump, which was automatically activated and deactivated when a preset carbon dioxide (CO2) concentration of 25 mmHg was passed. Gas samples were drawn through a T-piece into a Tenax TA tube. The setup was computer controlled with analog to- digital (A/D) and digital-to-analog (D/A) converters and input/ output (I/O) lines. Gas flow and volume of the

samples were automatically recorded using the computer-controlled sampling system [Grossherr M et al., 2006].

3.4 Analysis of propofol concentrations through GC-MS

Alveolar breath samples were adsorbed in duplicates onto Tenax TA tubes (Supelco, Bellefonte, PA), which were thermally desorbed and transferred using a cryotrap (Thermodesorption system; Gerstel, Muelheim, Germany) to a gas chromatograph–mass spectrometer (6890 Plus and 5973; Hewlett-Packard Co., Waldbronn, Germany). The chromatography conditions were as follows: carrier gas: 1 ml/min helium; column: Optima 5 MS, 60m-0.25mm-0.25m (Macherey & Nagel, Dueren, Germany); temperature injection/thermo desorption: 260°C; temperature detection: 260°C; temperature oven: 40°- 290°C. The retention time for propofol was 22.6 min. For the calibration procedure, known amounts of 2,6-diisopropylphenol (0.096 –19.2 ng/tube in six levels; Acros Organics, Geel, Belgium) dissolved in cyclohexane were applied onto the Tenax TA polymer of the adsorption tubes and analyzed in the same way as described above. Repeated measurements (n- 21) throughout the study period with the same amount of 2,6-diisopropylphenol (1.92 ng/tube) yielded an interassay coefficient of variation of 12.1%. The mean recovery of the propofol added onto the Tenax polymer for these repeated measurements was 106% (range, 84 - 136%) [Grossherr M et al., 2006].

3.5 Analysis of plasma propofol concentrations C_pl_m

The C_pl_m samples were measured in triplicate by reversed phase high-performance liquid chromatography with fluorometric detection essentially according to Kita et al. [Kita F et al., 2002] The measurable range of this method extended from 0.001 to 6.0 g/ml; samples with higher propofol concentrations were appropriately diluted with physiologic saline before analysis. Pooled plasma samples repeatedly tested for propofol yielded intraassay coefficients of variation of 2.6, 0.5, and 0.7% at mean concentrations of 0.04, 0.49, and 2.85 -g/ml, respectively. Interassay coefficients of variation of 8.7 and 4.5% were obtained by analyzing blank plasma spiked with propofol to concentrations of 0.05 and 1.00 -g/ml (n -14); the mean recovery of added propofol was 103 and 100%, respectively (range, 91–115% and 94–111%). Coefficients of variation derived from triplicate determinations of C_pl_m in individual samples was (1.7 - 2.0%; range, 0.2–13.0%) in pigs [Grossherr M et al., 2006].

3.6 Averaging of C_pg_m value

C_pl_m value was interpolated with the C_pg_m data. Window of 20 seconds (10 seconds in ascending and 10 seconds in descending time course) was extracted and values were averaged (figure 3.2).

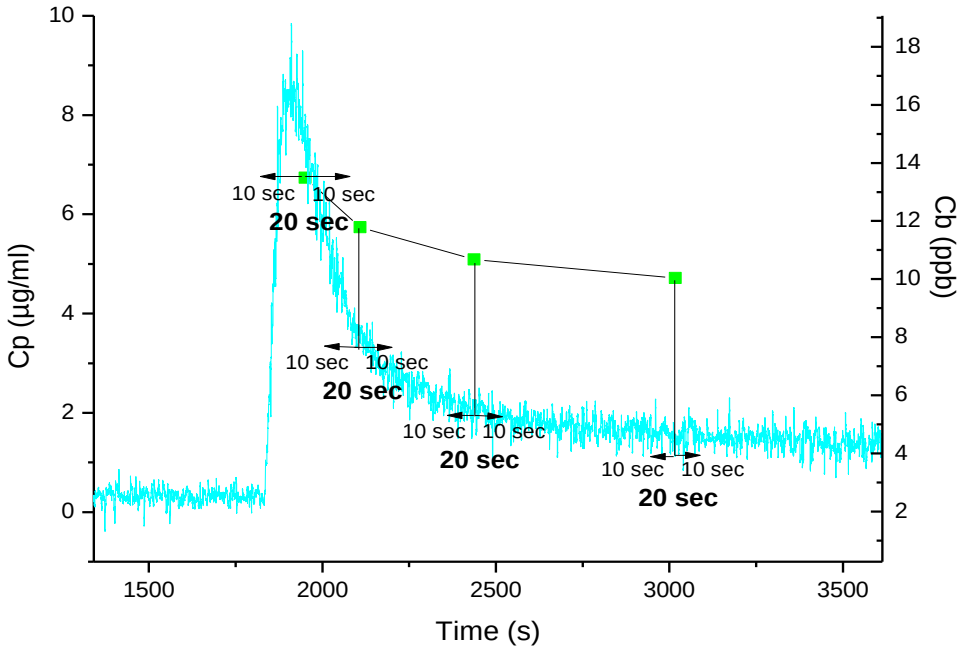

Figure 3.2 Averaging of C_pg_m data using C_pl_m values. Window of 20s was taken with 10 s in both ascending and descending time course.

This technique derives out 4 values (same number as of C_pl_m values) of C_pg_m data for each bolus and hence the interpolated curves as in figure 3.3 were plotted. Hence we will get 12 values for the three boli (each bolus have 4 values – 2,5,10 and 20 minutes).

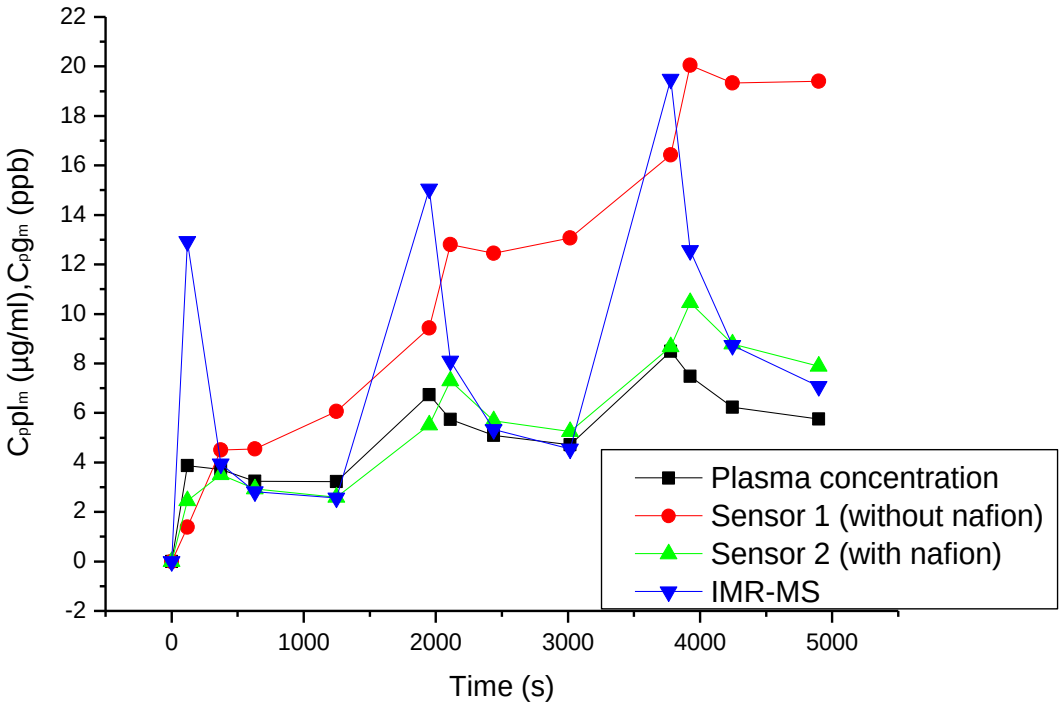

Figure 3.3 Plasma propofol concentrations for first three boli and corresponding averaged breath propofol concentrations from sensor 1, sensor 2 and IMR-MS are shown in the figure for an individual pig.

3.7 Predictive performance analysis

Intra subject data analysis (both in pharmacokinetic modeling and control system) was performed according to Varvel et al., based on the four indicators (MDPE, MDAPE, wobble, divergence) of predictive performance [Varvel JR et al., 1992].

The percentage performance error, PE is calculated by $PE_{ij} = (C_pg_{mij} - C_pg_{sij})/ C_pg_{sij} \times 100$,

where PE_{ij} is the performance error for the j^{th} prediction of the i^{th} pig, C_pg_{mij} is the j^{th} prediction of the measured expired propofol concentration and C_pg_{sij} is the j^{th} prediction of the simulated propofol concentration from the pk-model.

Median prediction error (MDPE) indicates the bias for the i^{th} pig.

$MDPE_i$ = median $\{PE_{ij}, j = 1,\ldots, N_i\}$where N_i is the number of PE values incurred for the i^{th} pig.

Median absolute performance error (MDAPE) reflects the inaccuracy of each measurement $MDAPE_i$ = median {| PE_{ij} |, j = 1,..., N_i}where N_i is the number of PE values incurred for the i^{th} pig.

Wobble is the parameter that measures intra-subject variability of the PE_{ij}

$Wobble_i$ = median {| PE_{ij} - $MDPE_i$|, j = 1,…, N_i}where $MDPE_i$ is the median performance error in the i^{th} pig.

Divergence is calculated for the i^{th} pig as the slope obtained from linear regression of that pig's | PE_{ij} |s against time (minutes). A negative value indicates a convergence of the measured towards the predicted values and a positive value shows an increase in error between simulated and measured propofol breath gas concentrations [Coetzee JF et al., 1995].

3.8 Statistical analysis

Correlation of C_ppl_m, C_pg_m (sensor and IMR-MS) and C_pg_s (simulated breath propofol concentrations from PK-model) were examined using least square linear regression analysis.

Bland altman method was used to compare electrochemical sensor measurements with the standard mass spectrometric techniques (GC-MS and IMR-MS) [Bland JM and Altman DG., 1986]. Data is expressed as mean values ± SD.

3.9 Modeling and simulation tools

LabVIEW® was used in our project for the pharmacokinetic model simulation and the control system design. LabVIEW is a short form of "Laboratory Virtual Instrumentation Engineering Workbench" and a platform and development environment for a visual programming language from National Instruments. The graphical language is named "G". Originally released for the Apple Macintosh in 1986, LabVIEW is commonly used for data acquisition, instrument control, and industrial automation on a variety of platforms including Microsoft Windows, various flavours of UNIX, Linux, and Mac OS. It is also used for analysis & signal processing, automated test, embedded designing and measurement. As here, it is used to desigh the pharmacokinetic model and simulate it by differing various parameters. It is also used to simulate and realize in real time the breath propofol based PID (proportional integral derivative) controller. Origin 7.0® was used for data analysis and to visualize the same as graphs.

References

Bland JM and Altman DG. Statistical methods for assessing agreement between two methods of clinical measurement. Lancet, 1986, 307-310.

Coetzee JF et al. Pharmacokinetic model selection for target controlled infusions of propofol. Anesthesiology 1995; 82: 1328-45

Grossherr M et al. Discontinuous monitoring of propofol concentrations in expired alveolar gas and in arterial and venous plasma during artificial ventilation. Anesthesiology, 2006, 104, 786-90.

Kita F et al. Determination of propofol in blood by high performance liquid chromatography. Okayama Shigakkai Zasshi, 2002, 21, 191-4

Schubert JK et al. CO2-controlled sampling of alveolar gas in mechanically ventilated patients. J Appl Physiol, 2001, 90,486–92.

Varvel JR et al. Measuring the predictive performance of computer-controlled infusion pumps. J Pharmacokinet Biopharm, 1992, 20, 63-94

4

Electrochemical sensor characteristics optimisation

4.1 Electrochemical propofol sensing

Due to the low concentrations of propofol in breathing gas, complex analysis equipments such as gas chromatography-mass spectrometry (GC-MS) and specialized mass spectrometers have been used (chapter 2). However, a continuous real-time monitoring of propofol in breathing gas in the clinical setting requires suitable detection technologies that are robust, easy to use, and economically feasible. [Hengstenberg A et al., 2006].The first results on the detection of propofol in breathing gas employing electrochemical gas sensor technology was presented by Hengstenberg et al. [Hengstenberg A et al., 2006].

The basic construction of the propofol sensor is similar to the amperometric gas sensor explained in the chapter 2 (refer section 2.4.2). For this sensor, propofol is oxidised (an electron is removed) at the working electrode-electrolyte junction (figure 4.1a and 4.1b). This gives the signal proportional to the concentration of propofol entering the sensor [www.permapure.com].

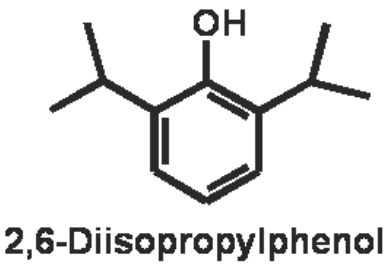

Figure 4.1a Chemical structure of propofol

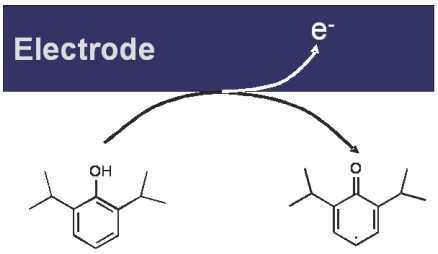

Figure 4.1b Electrochemical oxidation of Propofol[Hengstenberg A et al., 2006].

The electrochemical sensor adequately responded to the changes in propofol concentrations in exhaled breath gas. The breath gas concentrations measured by electrochemical sensor was in agreement with the concentrations obtained using GC/MS-method [Hengstenberg A et al., 2006].

4.2 Factors associated with breath propofol sensing

The electrochemical sensor optimisation was done in different stages. There are several factors that influence the propofol detection by the sensor and also the pathway (setup in which propofol is handled) in which propofol enters the sensor.

4.2.1 Factors influencing the electrochemical sensor detection

Two parameters are optimized for electrochemical sensor detection. They are i. potential applied to the working electrode and ii. influence of humidity on the sensor in propofol detection. The techniques used to optimize both the parameters are explained below.

Potential for the working electrode

In the lab different potentials were applied to working electrode with the protocol of 5 minutes synthetic lab air, 45 minutes propofol (5.73 ppb) and 30 minutes lab air.

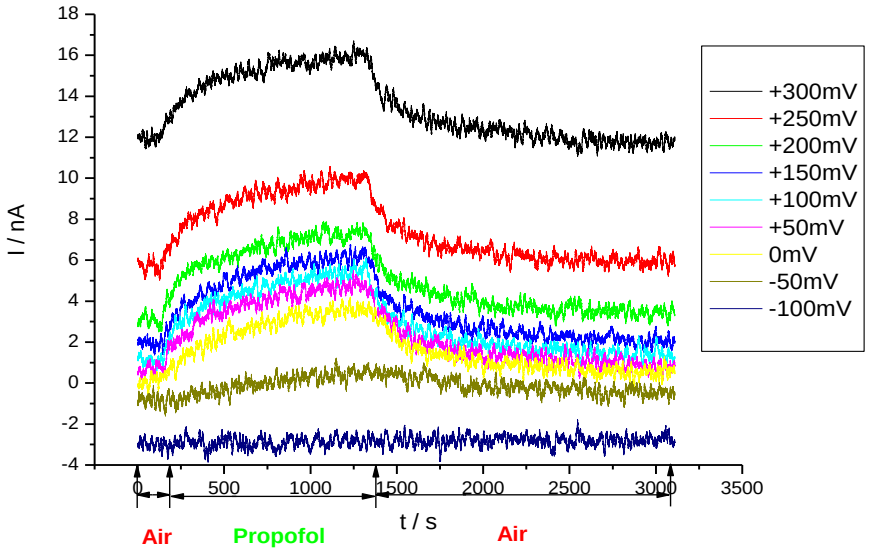

Figure 4.2 Electrochemica propofol sensor response at different potentials (-100mV to +300mV) applied at the working electrode.

The same protocol was repeated with the potential range of -100 mV to 300 mV, with increments of 50 mV. Show the responses of a sensor working at different potentials. Response time (Start of propofol (T_0) to 90% of the peak signal (T_{90}) and peak signal current were calculated from the graphs. figure 4.2. The range of response time and signal current are displayed in the figure 4.3.

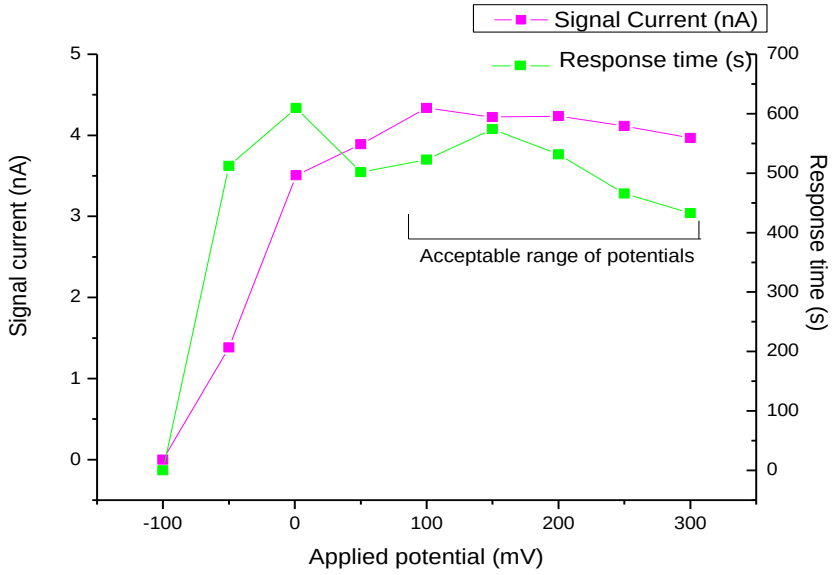

Figure 4.3 Signal current and response time at different operating potentials are shown in the plot the operating range is in the range of 100 to 300 mV.

The graphs in figure 4.3 shows that response time and signal current were maintained constant in a specific potential range (figure 4.2 and figure 4.3) it is in the range of 100 mV to 300 mV. The working electrode potential was chosen as 220 mV for future experiments.

Influence of humidity on propofol sensing

The humidity in breath is one of the major cause for an erroneous signal from the sensor. As the electrolyte used in sensor is hygroscopic it absorbs water from the breath gas and increases the volume of the electrolyte. The error can be reduced by introducing a nafion tubing in the sample line which exchanges the humidity present in the breath sample to the air surrounding the tubing. The plots (figures 4.4a) below show the effect of humidity on sensor response (humidity induced error shown as green line sensor 1) and the error caused by humidity is reduced by introducing a

nafion tubing in the sample line (red line sensor 2 with nafion tubing – figure 4.4a). (Nafion is very selective and highly permeable to water and have a very high water-of-hydration, so it efficiently absorb water. It is used to continuously dry gas streams removing only water vapour. [Wang J, 2006]

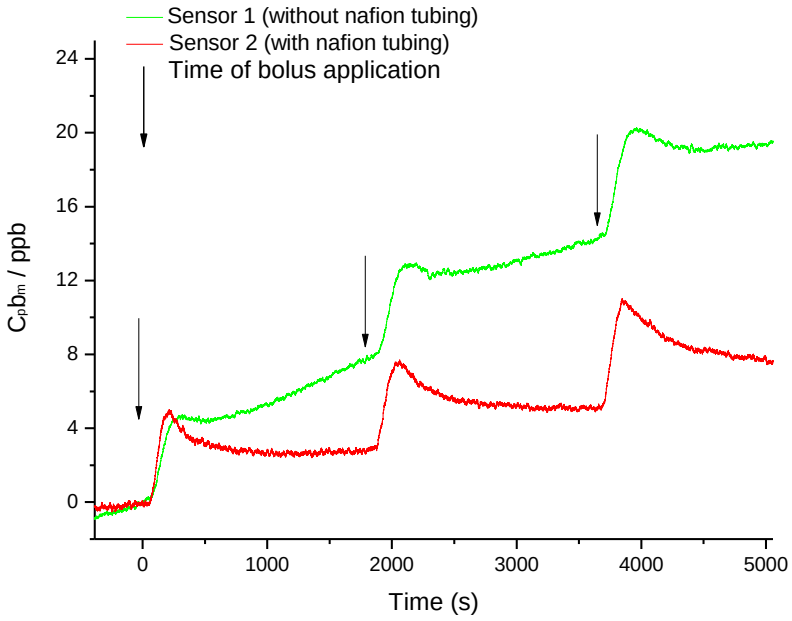

Figure 4.4a Response from two sensors (sensor1 without nafion tubing in sampling line and sensor 2 with nafion in sampling line) of same construction.(Data was taken from an animal study after injection of three boli) A deviation in signal with time can be clearly noted in sensor 1 which wass without nafion tubing.

Figure 4.4b Figure showing nafion tubing used in this study

As the error induced by humidity depends also on the electrolyte volume (electrolyte is hygroscopic the volume of electrolyte was reduced to half (0.5 ml) of the default volume (1 ml). The sensor with half of the electrolyte gave a good response compared to the sensor (with 1 ml electrolyte) without nafion tubing. Figure 4.5 show the comparison between two types of sensors, a normal sensor with default amount of electrolyte (1 ml) and the other sensor with 0.5 ml of electrolyte. Both respond in a similar manner with same signal peaks for all three boli.

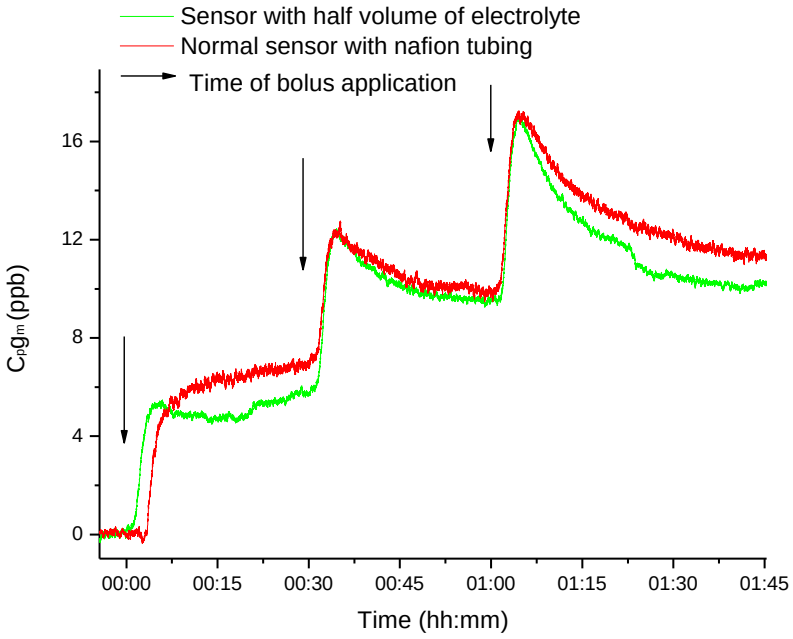

Figure 4.5 Response from sensors with 1ml (red line) and 0.5 ml (green line) of electrolyte. Reduction in error (as observed in figure 3a) is noted in sensor with reduced volume even without nafion tubing in the sample line.

4.2.2 Factors influencing the propofol pathway in sensing module

The major factor influencing the propofol path (from the endotracheal tube to sensor) was the adsorptive nature of the compound. It was necessary to find the adsorptive nature of each component in the path (tubing materials, water trap, adapter and T-pieces) separately. All components were individually analysed for the adsorption by comparing the response from the components to the standard response from IMR-MS. The figure 4.6 displays the adsorptive nature of different components. The water trap and metal adapter were found to adsorb much of

propofol exhaled. The metal adapter (standard adapter) was replaced with a PEEK (Polyethelene ether ketone) adapter and plastic T pieces were used instead of metal T pieces.

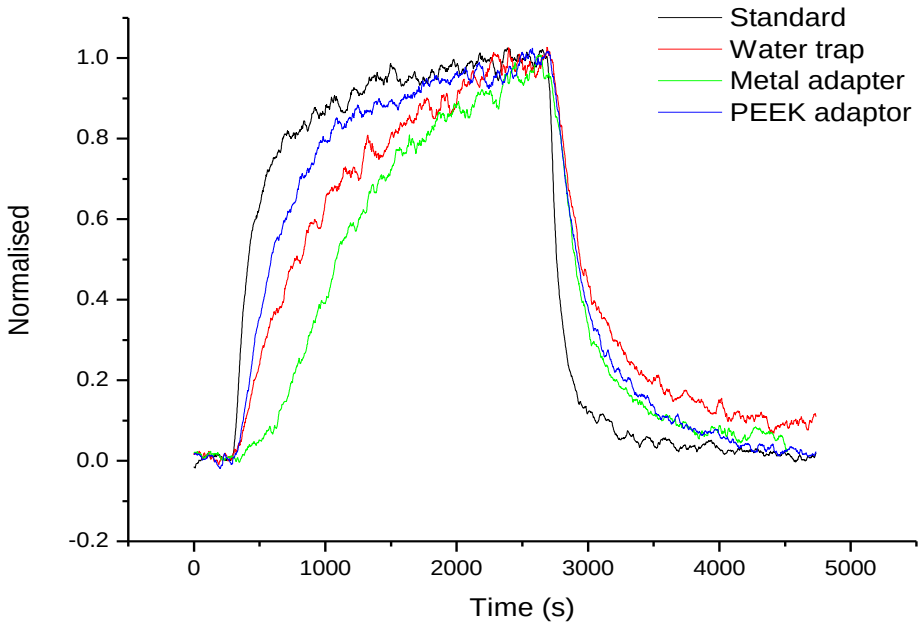

Figure 4.6 The adsorbtive nature of different components (water trap, PEEK (Polyethelene ether ketone) adapter and metal adapter) compared with the standard measurement.

Figure 4.7 Different T-pieces used in the sensor optimisation study are shown. Metal T-pieces adsorbed more propofol compared to the plastic T-Piece which was then selected as the standard T-piece in future experiments. Water traps used in the study are also shown.

Different types of T-pieces and water traps (metal adapters and the standard adapter) used in the optimisation procedure are shown in figure 4.7. Metal T-pieces adsorbed more propofol compared to the plastic T-Piece which was then selected as the standard T-piece for future experiments.

References

Hengstenberg A et al. Continuous Real-Time Monitoring of Propofol in Breathing Gas during Anesthesia. Anesthesiology, 2006, 105, A557

Joseph Wang. Analytical electrochemistry, 3rd ed; John Wiley and sons.

5

Monitoring of propofol sedation with IMR-MS, electrochemical sensor

5.1 Pre-clinical study design

The preclinical study was designed with five phases. The first phase had the 6 boli (B1 – B5 for propofol except E1), the E1 is an ethanol bolus and B4 a combined propofol ethanol boli. Phase 2 includes the measurements done to check the effect of breath frequency change in expired propofol. Phase 3 (dobutamine infusion) and 4 (metaprolol infusion) to check the effect of cardiac output change on expired breath concentration. The final phase 5 was designed to check the effect of haemorrhagic shock on breath propofol concentration (refer figure 5.1).

After approval from the local authorities for animal research, twelve pigs (n=12) were included in the study. After premedication and obtaining intravenous access, anesthesia was induced with etomidate. The airway was secured by means of endotracheal intubation or tracheotomy together with standard endotracheal tubes. After collecting blank blood samples, propofol was applied as a bolus (4 mg/ kg bodyweight) with continuous infusion (9.6 mg/ kg body weight x h) at 0, 30, 60 minutes. Ethanol bolus (16µg/kg) was also injected individually and as a combined bolus. The dosage profile was maintained same for all twelve pigs. The preclinical study was designed with five distinct phases.

Phase I

The first phase had the 6 boli (B1 – B6 for propofol except B4), The E1 was a pure ethanol bolus. B5 was a combined bolus of ethanol and propofol. B6 was a propofol boli with half the standard quantity (4 mg/ kg bodyweight) of drug used. The bolus was given at thirty minute intervals.

Phase II

Pigs were mechanically ventilated at 18 cycles/minute. Breath cycles were altered from 18 cycles/minute to 10 cycles/minute, increased to 25 cycles/minute, reduced to 10 cycles/minute and finally increased to 18 cycles/minute.

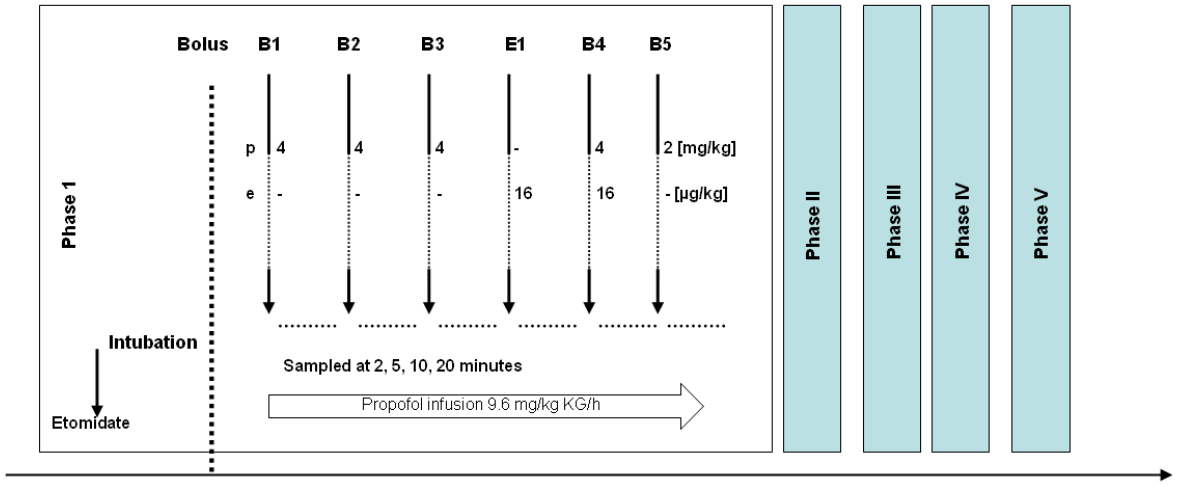

Figure 5.1 Schematic diagram showing the dosage profile followed for 12 pigs. The first phase had 6 boli (B1 – B5 for propofol except E1), the E1 is an ethanol bolus and B4 a combined propofol ethanol boli. Phase 2 includes measurements done to check the effect of breath frequency change in expired propofol. Phase 3 (dobutamine infusion) and 4 (metaprolol infusion) to check the effect of cardiac output change on expired breath concentration. Final phase 5 was designed to check the effect of haemorrhagic shock on breath propofol concentration.

Phase III

We examined the exhaled propofol concentrations and plasma propofol concentrations in anesthetized pigs when cardiac output (CO) (cardiac output is the volume of blood being pumped by the heart in particular by a ventricle in a minute) was altered. To increase the CO dobutamine was infused for 10 minutes and then the infusion was stopped.

Phase IV

The CO was allowed to return to baseline. CO was decreased with the administration of three metaprolol boli.

Phase V

Finally blood was removed (750 ml) to induce haemorrhagic shock and was resuscitated with saline (750 ml).

The plasma and breath propofol concentrations were recorded through out the study. A detailed explanation on phase II to V are given in the sub-section 5.3. Section 5.2 give an insight to the phase I.

5.2 Time course analysis after propofol boli injection

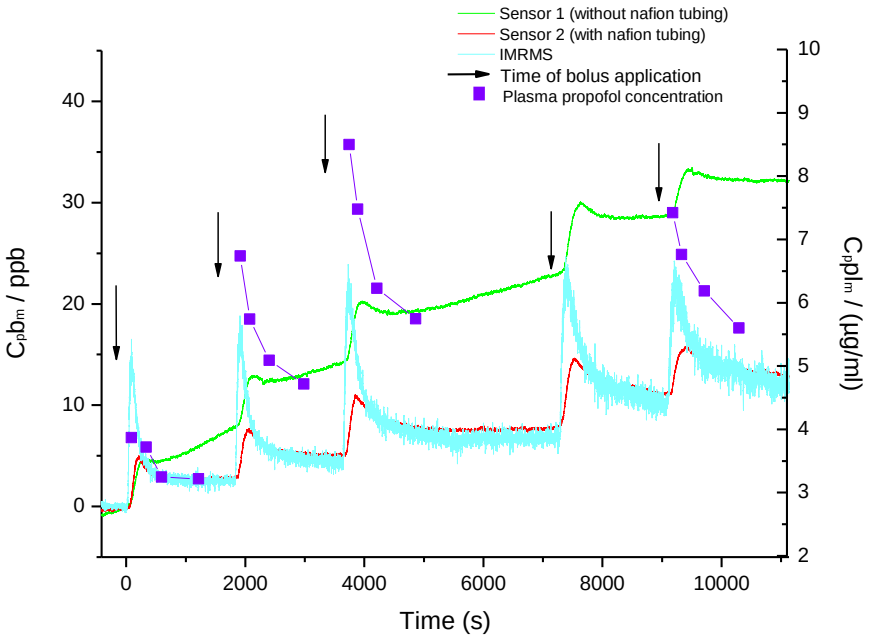

Figure 5.2 The response of the electrochemical sensor (sensor 1 - with nafion tubing attached and sensor 2 - without nafion tubing attached to it), Ion molecule reaction mass spectrometer after application of five propofol boli with a time interval of 30 min in-between the bolus. The violet dots indicate the plasma concentrations. (Pig no 4)

According to the protocol five propofol boli were injected with a time interval of 30 min. All boli were well detected by sensors 1 and 2 figure 5.2 clearly shows the response of electrochemical sensors and the IMR-MS along with blood plasma propofol concentrations.

The acquired data reflects the time course of changing propofol concentrations in blood that were induced by the application of three propofol boli along with a continuous infusion. After each bolus application a sudden increase in breath and blood propofol concentration was observed which gradually decreased over time.

Concentration ranges observed in different methods

Concentration ranges varied in different measurement techniques (Sensor 1, Sensor 2, IMR-MS and GC-MS) and inter-individual variability in C_pg_m among the animals was observed.

The concentration ranges detected in different methods are given below

Sensor 1 – 0 to 40 ppb

Sensor 2 – 0 to 30 ppb

IMR-MS – 0 to 50 ppb

GC-MS – 0 to 36 ppb

Plasma propofol concentrations by HPLC – 0 to 10 µg/ml

The interindividual variability found among the animals can be seen in C_pg_m graphs (IMR-MS) shown in figure 5.3.

Discussion

Grossherr et al. [Grossherr M et al., 2006] reported inter-individual differences in propofol levels (range, 0–1.4 ppb) in alveolar gas samples within the same species by measuring different alveolar propofol concentrations at the same plasma propofol concentration. There exist several possibilities that could explain these findings. The permeability of the alveolocapillary membrane could significantly influence the amount of propofol in exhaled breath. The function of this diffusion barrier can be altered in disease state such as pulmonary edema or emphysema, which could affect alveolar propofol concentrations. Possible other effects may include an influence of tidal volume and ventilation/perfusion mismatches as a consequence of decreased functional residual capacity due to general anesthesia. To be able to characterize these different effects on exhaled propofol with the IMR-MS, a good calibration procedure is prerequisite

[Hornuss C et al., 2007]. In this preclinical study we used tedlar bags filled with known concentration of propofol (5.73 ppb) for the calibrating the IMR-MS.

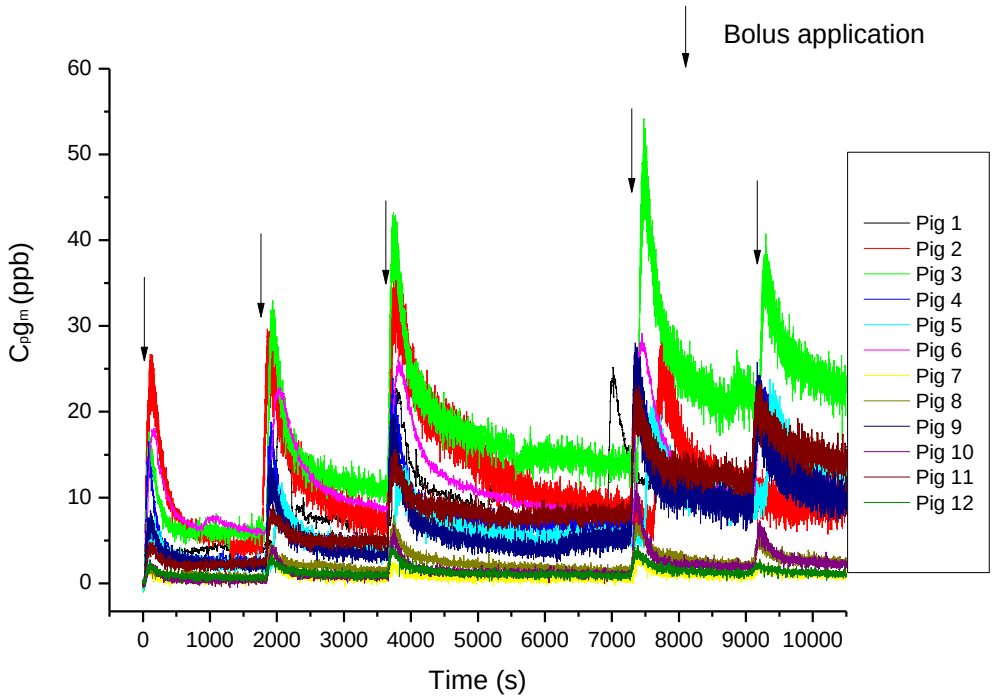

Figure 5.3 Expired gas propofol concentrations (C_pg_m) from 12 pigs. Pigs received three propofol boli (4mg/kg) at 30 minute intervals. Inter-individual variability in expired gas propofol concentrations was observed between the animals.

5.2.1 Data analysis

The breath gas signals were analysed for time based and signal based parameters after each propofol dosing.

Time based parameters

The following time based parameters were determined

Detection time is defined as the interval between the time of bolus injection to the time of breath propofol concentration change detection by IMR-MS.

Delay time is the time interval between T_0 and T_{10}. Hence it's the time after a jump in gas concentration to 10 % of the final measured value.

Time to peak is the interval between the time of bolus infusion and the time when the maximum concentration is reached.

Response time is the time after a jump in gas concentration to 90% of the final measured value (T_0 to T_{90})

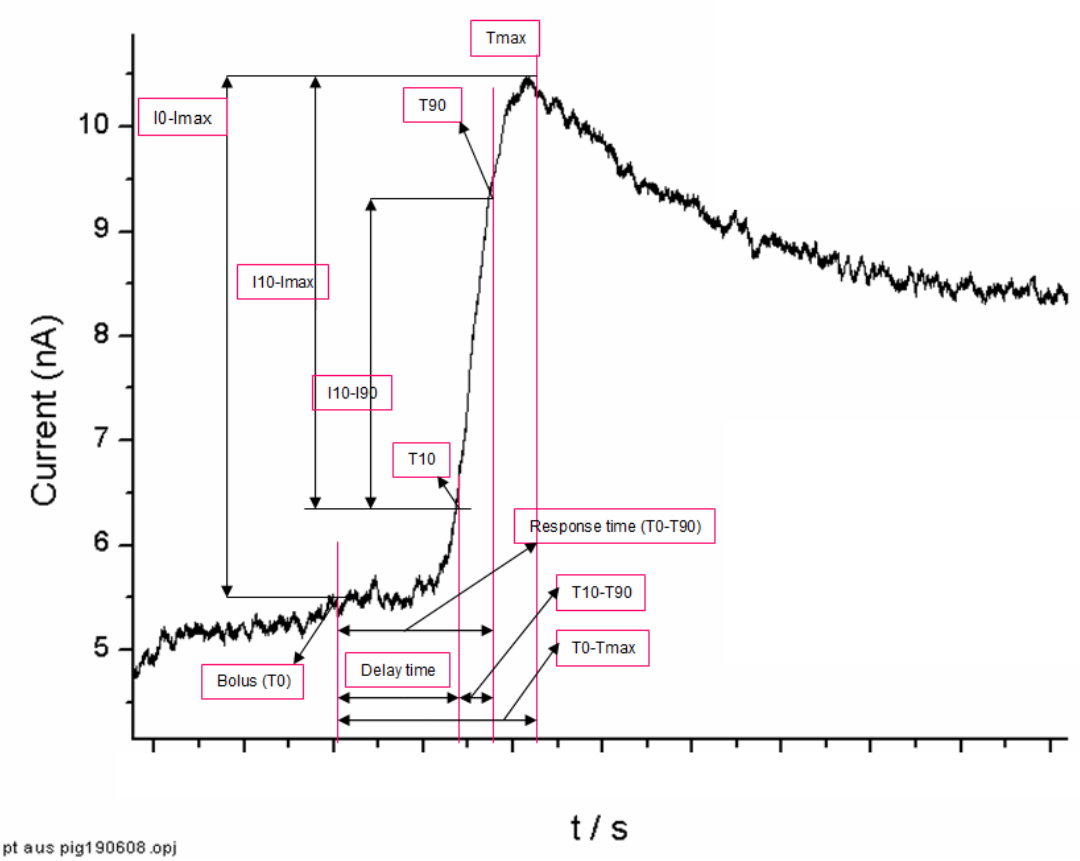

Figure 5.4 Both time based and signal based parameters extracted from the bolus curve are shown.

T10 to T90 - Time during a jump in gas concentration from 10% to 90% of the measured value.

Here T_0 - the time of injecting the bolus. T_{10} – time taken to reach 10 % of entire amplitude (I_0 - current at that time point). T_{90} - time taken to reach 90 % of maximum amplitude (I_{90}). T max – time taken to reach the maximum amplitude (I_{max}), jump - refers to the sudden increase in propofol concentration after bolus application (figure 5.4).

Signal amplitude based parameters:

1. Peak concentration - Difference in signal before and after a jump in gas concentration

To have a clear idea about the time course of sensor 1, 2 and IMR-MS the box plots for both the time based (figures 5.5 and figure 5.6) and signal amplitude based parameter (figure 5.7) are explained in detail.

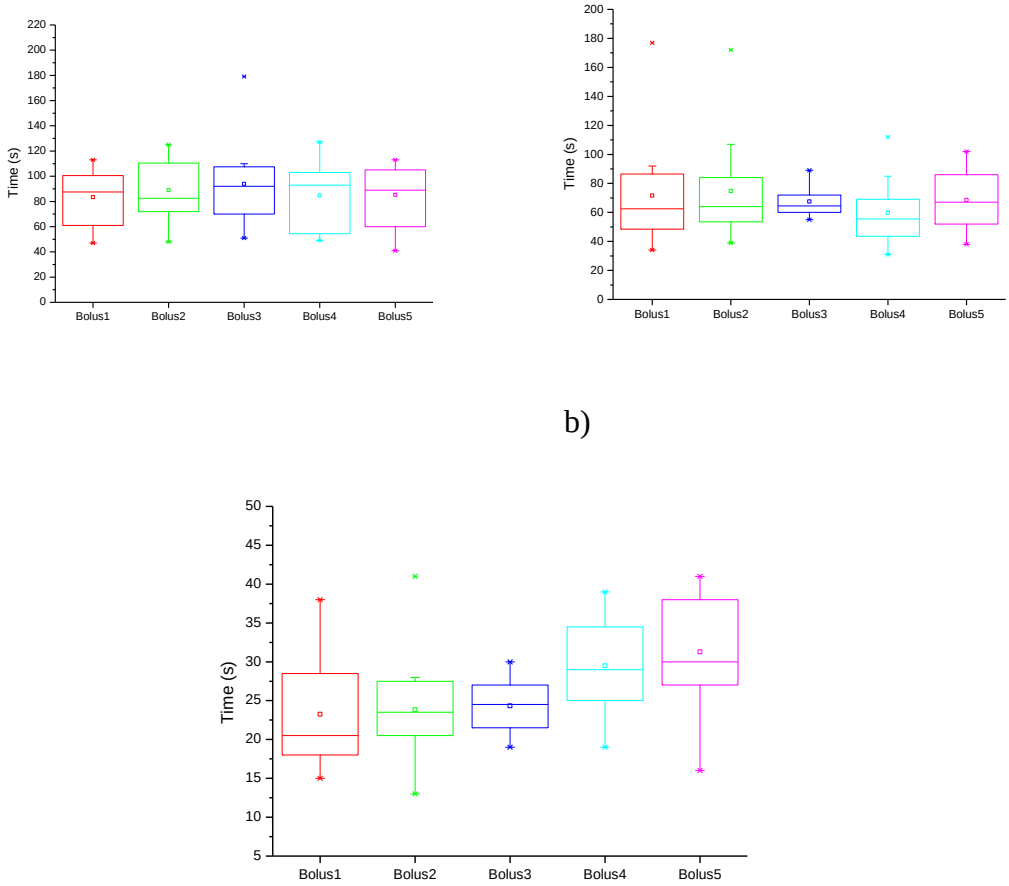

a) b)

c)

Figure 5.5 Detection time values from sensors 1 (a), sensor 2 (b) and IMR-MS (c) described as box plots.

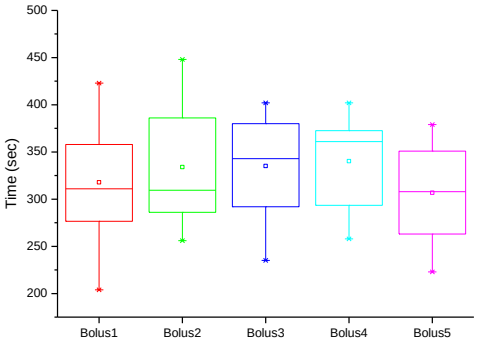

a)

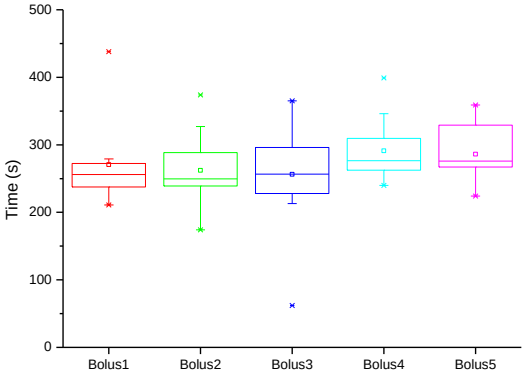

b)

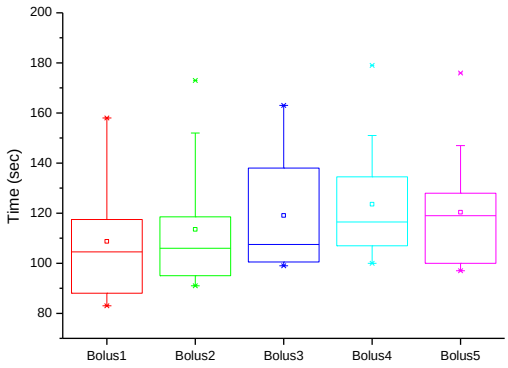

c)

Figure 5.6 Time to peak (TTP) values from sensors 1 (a), sensor 2 (b) and IMR-MS (c) described as box plots.

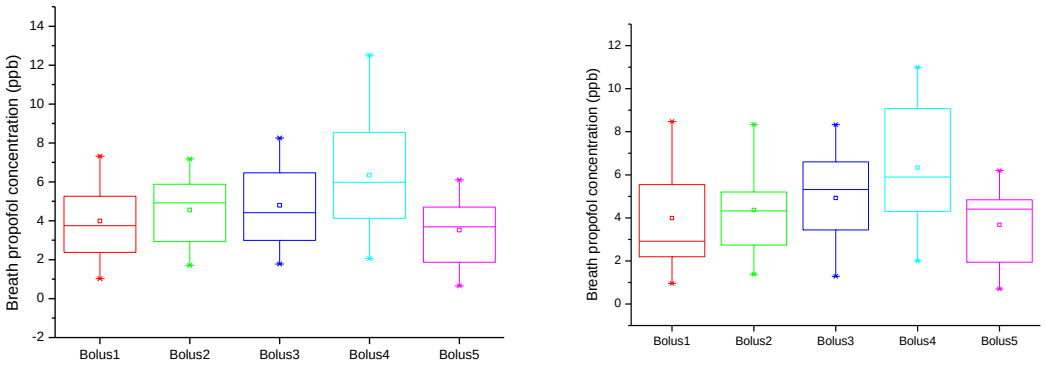

a)

b)

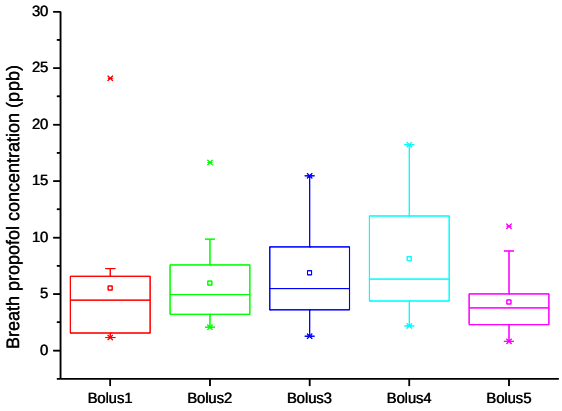

c)

Figure 5.7 Peak concentrations values from sensors 1(a), sensor 2 (b) and IMR-MS (c) described as box plots.

Figure 5.5 shows that the bolus 1 values are lower compared to other boli values and the values increase with time (see IMR-MS (figure 5.5 c)). A similar effect is seen in other parameters too (delay time, response time, T10 to T90 and peak concentrations).

The peak breath propofol concentrations obtained from sensor 1, sensor 2 and IMR-MS can be compared to the peak plasma propofol concentrations (2 minute values). The 2 minute

values from C_pl_m for all boli are shown in the figure 5.8. Among the 2, 5, 10, 20 minute values the 2 minute values were be considered as the peak values in plasma propofol concentrations.

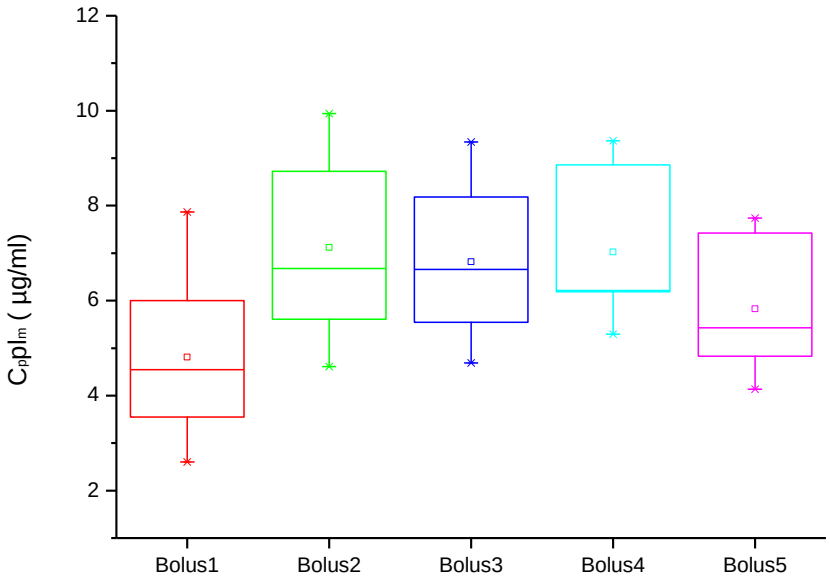

Figure 5.8 Plasma propofol concentrations at 2 minutes after bolus application. Bolus 1 values were much lower compared to other boli.

Discussion

From the figure 5.8 it can be inferred that peak propofol concentrations (PC) at bolus 1 (5.53 ± 6.29) was low compared to the PC at bolus 2 (5.96 ± 4.10), bolus 3 (6.87 ± 4.56), bolus 4 (8.12 ± 5.24), and bolus 5 (4.28 ± 3.09). We observed the same effect in the plasma propofol concentrations also (bolus 1 - 4.81 ± 1.69, bolus 2 - 7.12 ± 1.83, bolus 3 - 6.82 ± 1.49, bolus 4 - 7.02 ± 1.66 and bolus 5 - 5.82± 1.35), as shown in figure 5.9. This effect of low PC at bolus 1 can be well explained with the"first pass lung up take"("Propofol undergoes extensive uptake and first - pass elimination in the lungs" as described by Kuipers et al.) [Kuipers JA et al, 1999]. The PC values gradually increased at bolus 2, 3, 4, 5 in Sensor 2 and IMR-MS only, this is not noticed in C_pl_m concentrations. This may be due to the humidity in breath (section 4.3).

In previous studies Takita et al. and Hornuss et al. reported that in humans a bolus peak can be detected using proton transfer mass spectrometry and IMR-MS respectively [Takita A et

al., 2007;Hornuss C et al., 2009]. They have observed the maximal peak concentrations of exhaled propofol after bolus application at 333.8 ± 70 s (Takita et al.) and 190 ± 24 s [Takita A et al., 2007;Hornuss C et al., 2009].

Table 5.1 Time to peak concentration ($TTPC_m$) and detection time (DT) in measured expired gas propofol concentrations (C_pg_m). The values are shown for the initial bolus along with infusion (bolus 1), 2nd bolus at 30 min (bolus 2) and the 3rd bolus at 60 minutes (bolus 3). Data expressed as mean ± SD.

Bolus	DT in s C_pg_m (mean ± SD)	$TTPC_m$ in s C_pg_m (mean ± SD)
1	23 ± 7	108 ± 25
2	23 ± 7	113 ± 25
3	24 ± 3	119 ± 24
Mean	23 ± 6	113 ± 24

In our study, peak concentrations of exhaled propofol were detected earlier using IMR-MS system (see Table 5.1). The peak concentrations for all boli (time to peak) were reached in the range of 113.51 ± 24.4s. Propofol was detected earlier [23.82 ± 6.09s] in our study compared to results from Takita et al. [41.8 ± 8s] and Hornuss et al. [41 ± 21s] [Takita A et al., 2007;Hornuss C et al., 2009]. We assume that propofol appeared earlier in our study due to the weight of the animals, the animals included in the study were of 25 to 42 kg, which is low in comparison to the weight of patients involved in studies by Hornuss et al. [63 – 90 kg] and Takita et al [Takita A et al., 2007;Hornuss C et al., 2009].

5.2.2 Statistical analysis

Relation of breath propofol concentrations with blood propofol concentrations, C_pg_m from electrochemical sensors [sensor 1 and 2], IMR-MS, and GC-MS were examined using linear regression analysis (simple least square method).The agreement between standard mass spectrometric method (IMR-MS and GC-MS) data with sensor's data was evaluated using the Bland Altman method [Grossherr M et al., 2006].

As the response from sensor 1 without nafion tubing was not significant (noise introduced due to humidity in breath) the results from sensor 2 and IMR-MS were considered for statistical analysis. First to check the relation of breath propofol and plasma propofol concentrations C_pg_m (from both Sensor 2 and IMR-MS) and C_ppl_m were compared. The results shown are from an individual pig in figure 5.9 (pig 4).

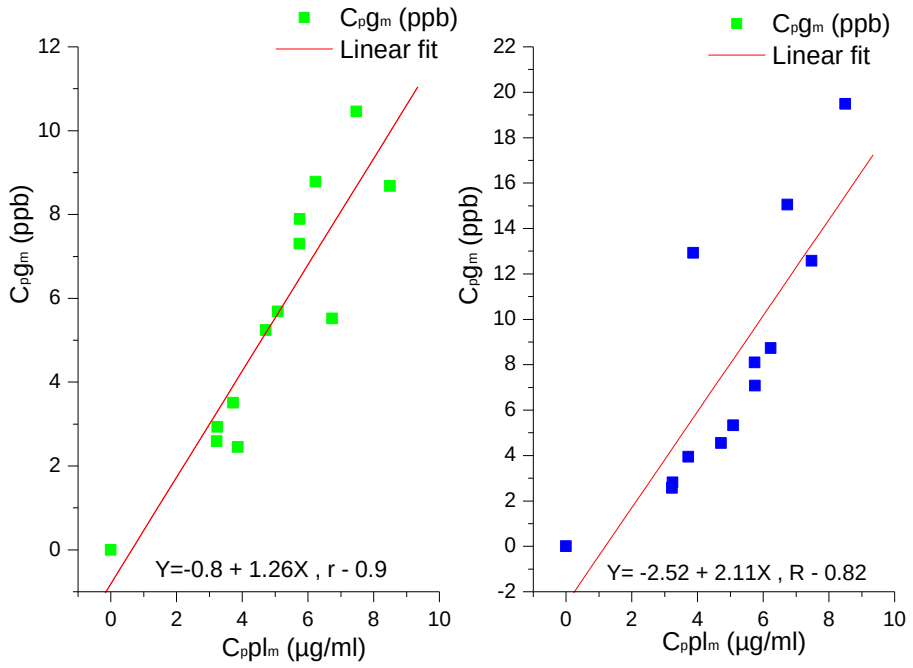

a) b)

Figure 5.9 Linear regression plots for plasma concentrations and exhaled propofol concentrations. Plasma propofol concentrations (C_pl_m) vs expired breath propofol concentrations (C_pg_m) – a) for Sensor and b) for IMR-MS

The sensor C_ppl_m vs C_pg_m plot with all values (2, 5, 10, 20 minute values) yielded a r value of 0.59 ± 0.21 and IMR-MS - 0.79 ± 0.06 . The r values increased to 0.85 ± 0.05 (sensor) and 0.86 ± 0.07 (IMR-MS). A detailed explanation about this effect is described.

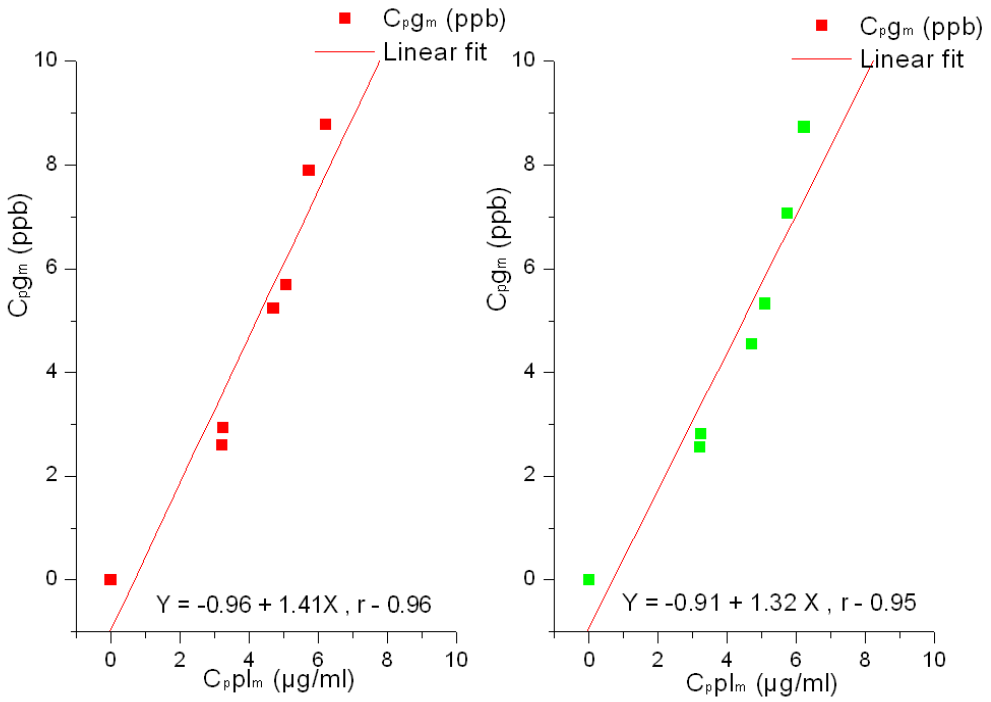

Figure 5.10 Linear regression plots for plasma concentrations and exhaled propofol concentrations with the 2 and 5 minute values removed. Plasma propofol concentrations (C_pPl_m) vs expired breath propofol concentrations (C_pG_m) – a) for sensor and b) for IMR-MS

Correlation of breath and blood propofol in steady and non-steady state conditions

Previous studies [Grossherr M et al., 2006; Perl T et al., 2009; Miekisch W et al., 2008] have focussed on the correlation between C_ppl and C_pg_m during steady state conditions. Here we examined the correlation during both steady state (where equilibrium between C_ppl_m and C_pg_m is reached as well as non-steady state conditions (immediately after bolus application) [Grossherr M et al., 2006;Takita A et al., 2007].

. We hypothesize that a decrease of correlation will be observed when data from non-steady state phase is included along with data from the steady state.

The correlation between C_pg_m with C_ppl_m were examined at 2,5,10 and 20 minute values

after bolus injection using linear regression analysis (range of correlation coefficient r C_pg_m vs $C_p$pl: 0.68 - 0.88; p <0.01 for individual animals). The results of the linear regression analysis are shown in figure 5.11. Figure 5.11 depicts the C_pg_m vs $C_p$pl plot for a single pig with only the data in steady state phase (initial 10 and 20 minute values). All 2 minute values and two 5 minute values (represented as large and small circles) located outside the 95% confidence interval are shown.

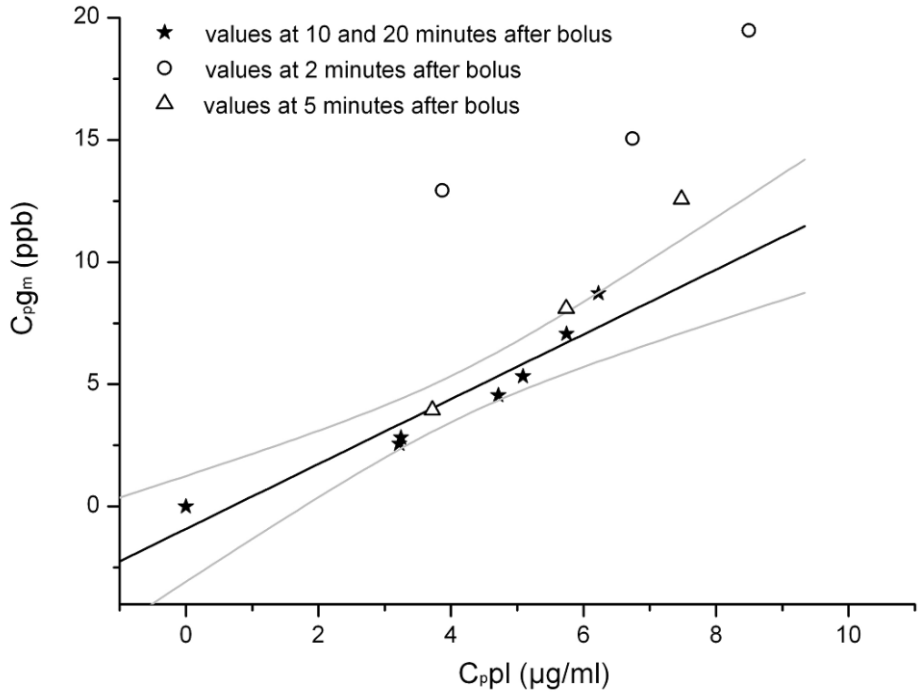

Figure 5.11 Linear regression plot plasma propofol concentrations ($C_p$pl) vs exhaled breath propofol concentrations (C_pg_m) (excluding 2, 5 minute values that were not steady-state).

Figure 5.9b shows the C_pg_m vs $C_p$pl regression plot including all steady and non-steady state values. Hence if 2, 5 minute values of induction phase are included correlation coefficient decreases from 0.95 to 0.82. Correlation coefficients for C_pg_m vs $C_p$pl with non-steady state phase points (2, 5 minutes) included (range – 0.68 to 0.88, p <0.01) and excluded (range – 0.74 to 0.93, p <0.01) are shown in Table 5.2.

The breath propofol concentrations are linearly related to the respective plasma concentrations during steady state phase conditions. A noteworthy correlation between $C_p$pl and

C_pg_m at steady state conditions was shown in animals by Grossherr et al. [Grossherr M et al., 2006].

. In this previous study only propofol infusion (without bolus) was given to the animals (goats and pigs) and the breath propofol concentrations were discontinuously measured using thermal desorption GC-MS. Samples were collected at 10 minutes after infusion change. In our present study three propofol boli were injected along with propofol infusion and the breath gas propofol concentrations were continuously monitored using IMR-MS. Then the recorded data was analyzed together with blood samples obtained at 2,5,10 and 20 minutes after bolus injection.

Table 5.2 Intercept A, Slope B and Correlation coefficient r for twelve pigs obtained from linear regression plots between plasma concentrations and exhaled propofol concentrations. Plasma propofol concentrations (C_pg_m) vs expired breath propofol concentrations (C_pg_m) with non-steady state phase values included, plasma propofol concentrations (C_pg_m) vs expired breath propofol concentrations (C_pg_m) with non-steady state phase values excluded. Y = A + BX. Data expressed as mean ± SD.

Parameter	$C_p$pl (µg/ml) Vs C_pg_m (ppb) non-steady state phase values included	$C_p$pl (µg/ml) Vs C_pg_m (ppb) non-steady state phase values excluded
Intercept	-1.94 ± 2.22	-0.43 ± 0.96
Slope	1.96 ± 1.46	1.34 ± 1.01
Correlation coefficient(r)	0.79 ± 0.06	0.86 ± 0.07

In this study we have measured in both the non-steady state phase (initial 10 minutes) and steady state phase (10 – 30 minutes) conditions after each bolus. From the results it can be inferred that immediately after bolus application the deviation between plasma and breath

concentrations is high. This deviation from the regression line gradually decreases over time. Our results indicate that the non-steady state phase lasts for a time period of approximately 10 minutes, hence we notice the 2 minute and 5 minute values (both within the non-steady state phase) are located outside the 95% confidence interval in the C_ppl_m vs C_pg_m plot (figure 5.11). All the 2 minute values are positioned outside the confidence interval and the number of values outside confidence interval decrease in the 5 minute values. Therefore we can conclude that the non-steady state extends at least for 10 minutes after which the breath concentrations reach the equilibrium with plasma propofol concentrations. To our knowledge for the first time we have characterised the propofol bolus (pharmacokinetics of propofol) with IMR-MS and defined the non-steady state phase (initial 10 minutes after bolus application).

Linear regression analysis for GC-MS C_pg_m compared with C_pg_m from sensor and IMR-MS

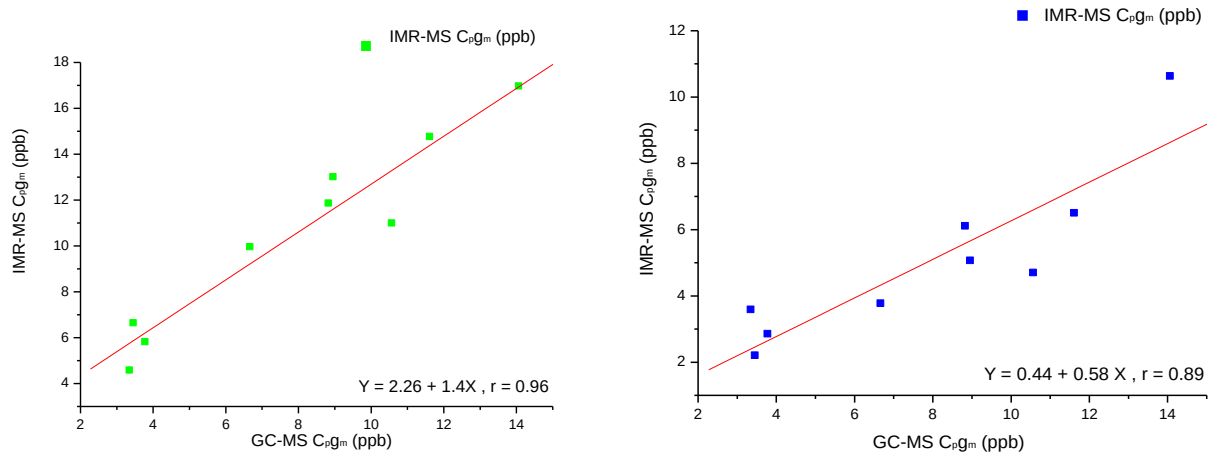

Figure 5.12 Linear regression plots between breath propofol concentrations from GC-MS C_pg_m compared with sensor C_pg_m and IMR-MS C_pg_m . A close relation was observed in both the cases.

When propofol concentrations obtained from GC-MS were compared with sensor and IMR-MS C_pg_m . There was a good agreement between IMR-Ms concentrations and C_pg_m from

sensor and IMR-MS. The r value ranges from 0.55 ± 0.16 – Sensor and 0.62 ± 0.15 – IMR-MS (figure 5.12).

Bland Altman method

Bland Altman method was used to check the agreement of the sensor and IMR-MS with GC-MS [Takita A et al., 2007]. Here the GC-MS measurement is taken as the reference standard method.

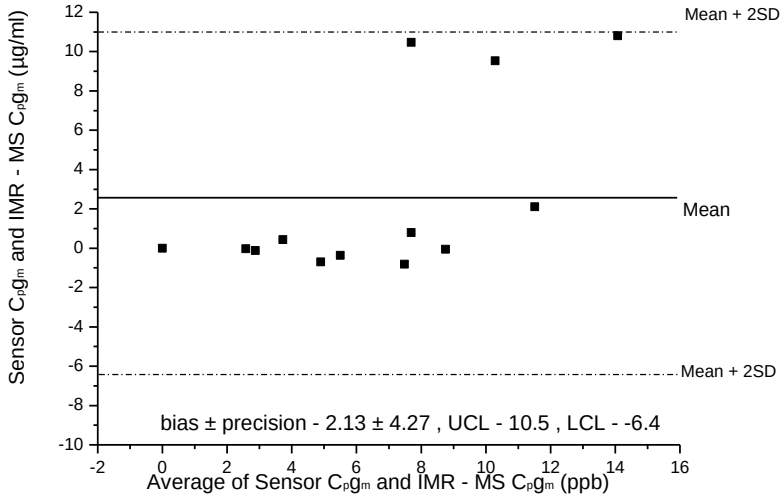

Figure 5.13 Bland Altman plot for IMR-MS data and sensor. The bias and precision was 2.13 ± 4.27. The upper confidence level (UCL) and lower confidence interval (LCL) are also given in the figure.

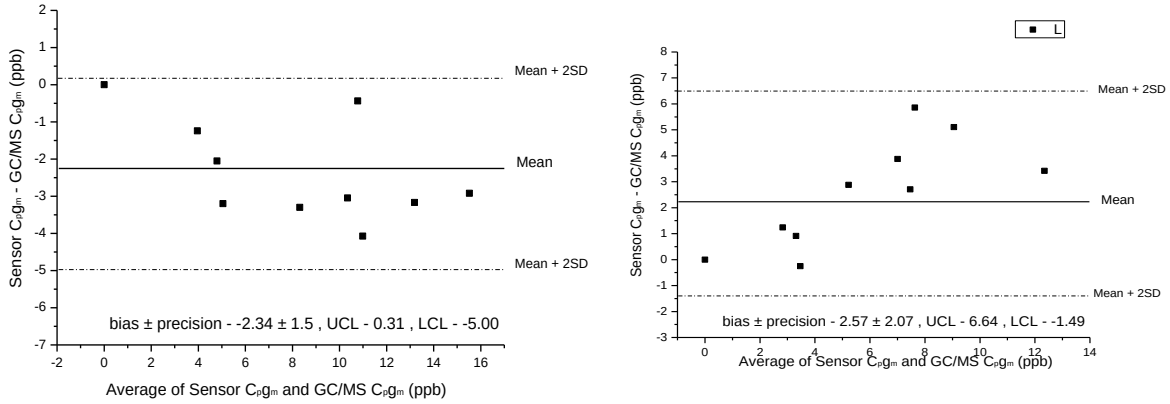

a) b)

Figure 5.14 Bland Altman plot between GC-MS data and sensor – figure a, IMR-MS – figure b.

The Bland Altman method signifies, that in both cases of having IMR-MS and GC-MS as the standard or reference measurement for the comparison with the sensors, the sensors shows us an acceptable agreement (as most of the values lies inside 95% confidence interval) with gold standards. To conclude, the electrochemical sensors may be substituted instead of the IMR-MS or GC-MS for the measurement of propofol.

5.3 Factors influencing propofol exhalation

5.3.1 Preclinical study design

The study to check the factors influencing the propofol exhalation consisted of four phases (phase II to V).

Phase II

Breath frequency was altered to check the effect on plasma propofol concentration. Pigs were mechanically ventilated at 18cycles/minute. Breath cycles were altered from 18 cycles/minute (tidal volume) to 10 cycles/minute, increased to 25 cycles/minute, and reduced to 10 cycles/minute and finally increased to 18 cycles/minute. Commutation of breath cycles were carried out to evaluate how much plasma and breath propofol concentrations were affected when breath cycle is altered. Plasma samples were collected 10 min after each breath change.

Phase III

We examined the exhaled propofol concentrations and blood plasma propofol concentrations in anesthetized pigs when cardiac output (CO) (cardiac output is the volume of blood being pumped by the heart in particular by a ventricle in a minute) was altered. A continuous infusion (10 min) of dobutamine was administered to increase the cardiac output the infusion was then stopped and cardiac output was returned to baseline.

Phase IV

The cardiac output was allowed to decrease with the administration of three metaprolol (β1-Adrenoreceptor blocker) boli.

Phase V

Finally blood was shed (750 ml) to induce haemorrhagic shock. 750 ml of saline was used for resuscitation.

5.3.2 Altered breath frequency

Changes observed in C_pPl_m

Commutation of breath cycles were carried out to evaluate how much plasma and breath propofol concentrations were affected when breath cycle was altered. Plasma samples were collected 10 min after each breath change. Measured plasma concentrations (C_pPl_m) are plotted in figure 5.14. Plasma concentration measured before the start of breath change events is also shown in figure 5.14.

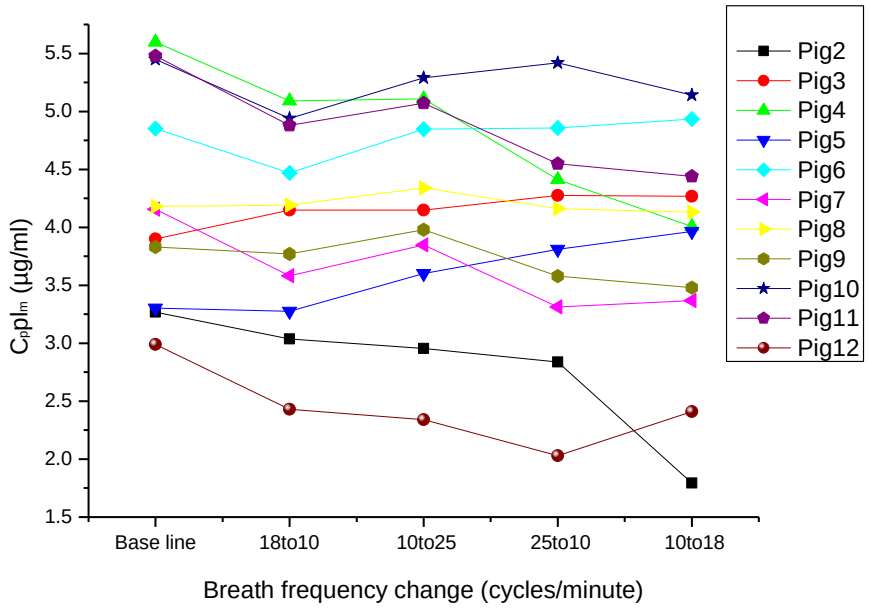

Figure 5.15 Changes in blood plasma propofol concentration when the breath frequency was changed. X-axis of the plot has five parts first being the plasma values measured before breath change events were started, followed by C_pPl_m values measured after 10 minutes of each breath cycle change

Changes in breath frequency have a significant effect on blood propofol concentration (Figures 5.15, 5.16). When breath cycle was reduced from the normal rate of 18 cycles/minute to 10 cycles/minute C_pg_m values show a drop from zero (first box of figure 5.15) and increases when the breath frequency is altered to 25 cycles/minute (second box in figure 5.15). Again C_pg_m values drop down when the breath frequency is decreased to 10 cycles/minute and finally C_pg_m steps up with the change to 18cycles/minute

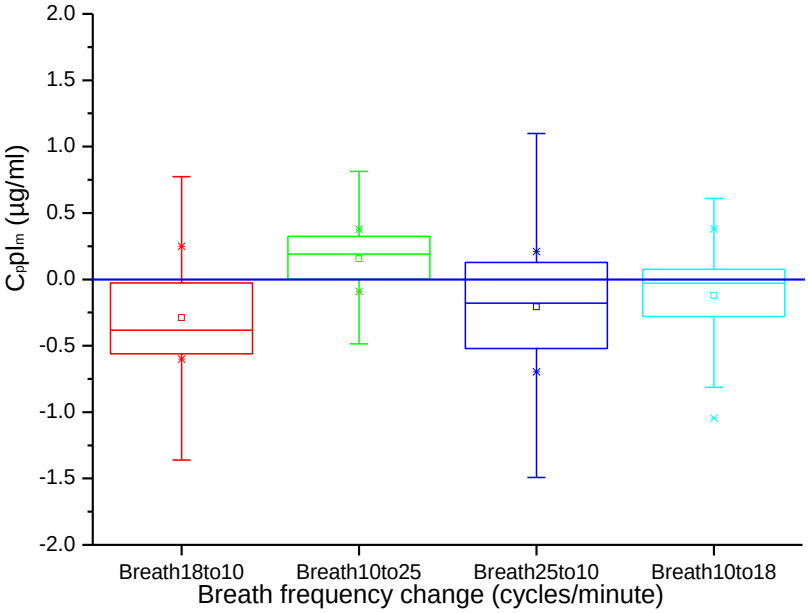

Figure 5.16 Difference between plasma propofol concentrations after each breath cycle change and previous event is displayed as box plots. Effect of each breath cycle on C_pl_m change can be observed. C_pl_m values increases with an increment in breath frequency.

Changes observed in C_pg_m

Breath propofol concentrations (C_pg_m) reflect a similar trend as noted in plasma propofol concentration (C_pg_m). The figure 5.16 below shows the changes in sensor and IMR-MS signal when the breath frequency was altered. Magenta coloured straight lines in figure 5.16 note the time when breath frequency was altered and the 10 minutes time interval after breath frequency change. Corresponding C_pg_m values were derived from sensors and IMR-MS curves. Difference between breath propofol concentrations (C_pg_m) after each breath cycle change (10 min interval)

and previous event's C_pg_m value is displayed as box plots. The figure 5.18a, b show this in box plots for the sensors and IMR-MS.

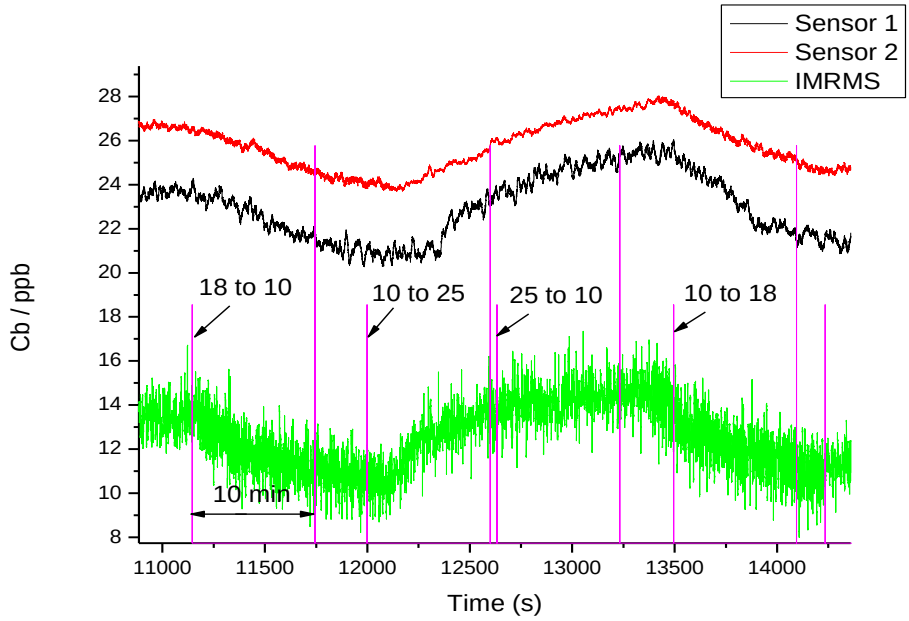

Figure5.17 Changes in the sensor and IMR-MS signal when the breath frequency is altered (pig 11). The signal rise and fall can be well noted in the figure.

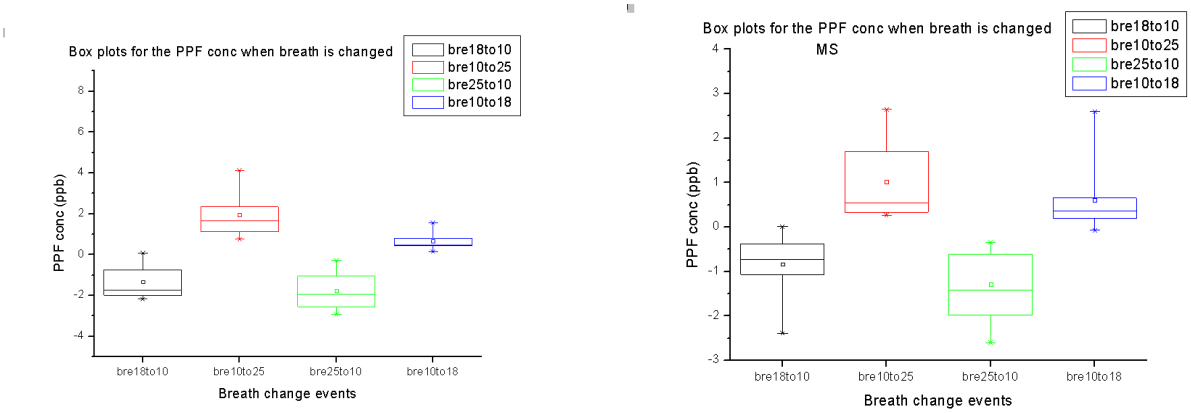

a) *b)*

Figure 5.18 – C_pg_m response to breath frequency change in Sensor (a) and IMR-MS (b). Alterations observed in C_pl_m is observed in C_pg_m

Discussion

Alveolar propofol concentrations (C_pg_m) depict a similar pattern as shown by C_ppl_m values (figure 5.18 and 5.17). Reasons for change in propofol concentrations, both in plasma and breath are unknown. The oscillations in breath frequency may alter the acid base balance in blood which in turn disturbs the ph balance of blood. The propofol binding to proteins in blood gets altered when breath frequency is changed (as acid base balance is disturbed).

5.3.3 Altered cardiac output – dobutamine and metaprolol infusion

During anesthesia with propofol infusion (9.6 mg/kg bodyweight * h) CO was determined by means of the thermo dilution method (using a swan ganz catheter- Monitor: Sirecust 1260, Munich, Germany). When C_pg_m reached steady state (maintained for at least 20 minutes after infusion start), dobutamine (50µg/kg/hr) was infused for 10 minutes. CO was determined (each value was measured five times and the mean of final three values were recorded) and arterial blood samples were collected at 10 minutes before infusion start, 10 minutes after infusion start and 10 minutes after stop of dobutamine infusion

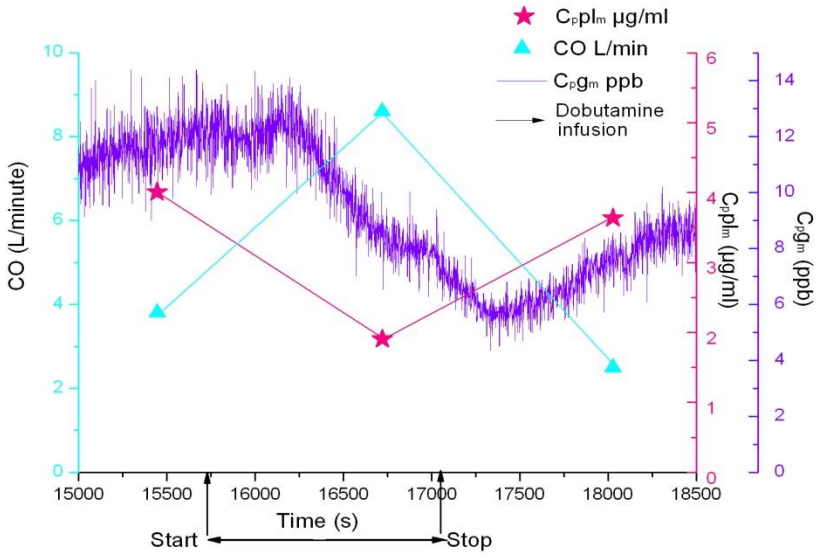

Figure 5.18 The plasma and breath propofol concentration decreases with start of dobutamine infusion and increase in the propofol concentrations after the stop of infusion is also well noted.

Variations observed in C_pPl_m values after dobutamine infusion is shown in figure 5.18. We notice an inverse relation between CO and propofol concentrations after short infusion (10 minutes here) of dobutamine. The effect observed in C_pPl_m is well reflected in C_pg_m values extracted from sensors and IMR-MS data (table 5.3).

Table 5.3 The changes observed in cardiac output (CO), plasma propofol concentrations C_pPl_m and expired gas propofol concentrations C_pg_m (IMR-MS) during dobutamine infusion.

	Difference in CO L/min (mean ± SD)	Difference in C_pP_m µg/ml (mean ± SD)	Difference in C_pgm ppb (mean ± SD)
After start of dobutamine infusion	4.74 ± 2.38	-1.69 ± 0.51	-2.69 ± 1.93
After stop of dobutamine infusion	-4.04 ± 2.42	0.78 ± 0.62	0.39 ± 0.82

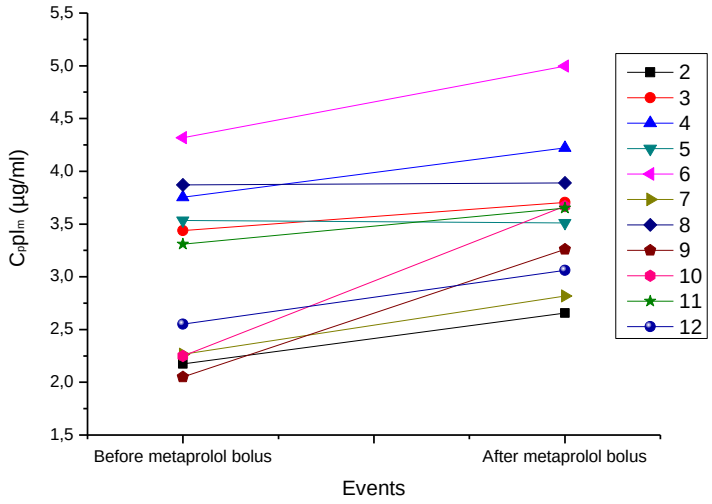

Figure 5.19 The plasma propofol concentrations increases with the metaprolol injection.

After the three metaprolol injections CO decreased from 5.41 ± 2.57 to 3.9 ± 1.46. An inverse effect can be noted in the $C_p pl_m$ and $C_p g_m$ concentrations. The $C_p pl_m$ increased from 3.04 ± 0.08 to 3.58 ± 0.68.

Difference between $C_p g_m$ values after metaprolol boli application and before the application was 0.61 ± 0.7 [sensor], 0.74 ± 0.74 [IMR-MS].

There was a marked increase in $C_p pl_m$ after the injection of metaprolol injection but the same is not well reflected in the $C_p g_m$ concentrations. But an inverse effect can be noted.

5.3.4 Haemorrhagic shock

Previous work has demonstrated that ongoing hemorrhagic shock dramatically alters the distribution, clearance and potency of propofol Johnson et.al. [Johnson KB et.al., 2003]. In our study Pigs (n=8) were allowed to bleed until 750 ml of blood had been removed. Subsequently, animals were resuscitated with saline. Plasma samples were collected at an interval of 10 minutes before and after shock and resuscitation.

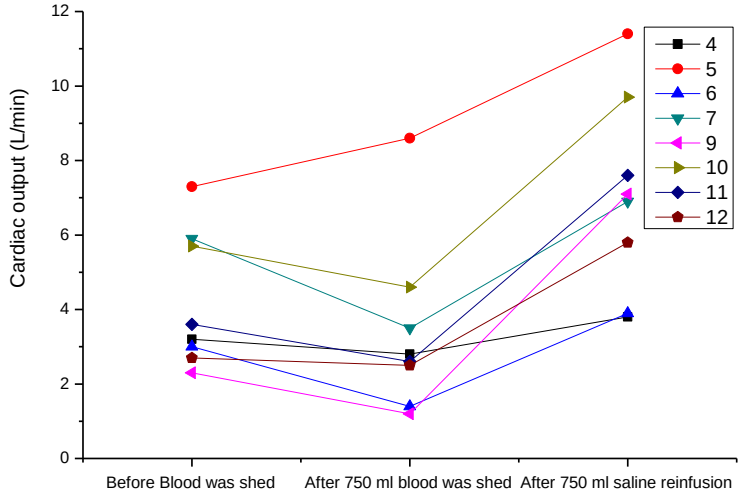

Figure 5.20 Hemorrhagic shock was induced to the pigs, 750 ml of blood was shed then saline was re-infused; cardiac output was recorded after each event. We can notice a decrease in cardiac output when blood was shed and an increase when the blood was re-infused.

CO decreased during blood shed and increased when saline was re-infused (figure 5.20). Cp values responded opposite to CO (figure 5.21). The effect observed in C_pPl_m is well reflected in C_pg_m values extracted from sensor and IMR-MS data also.

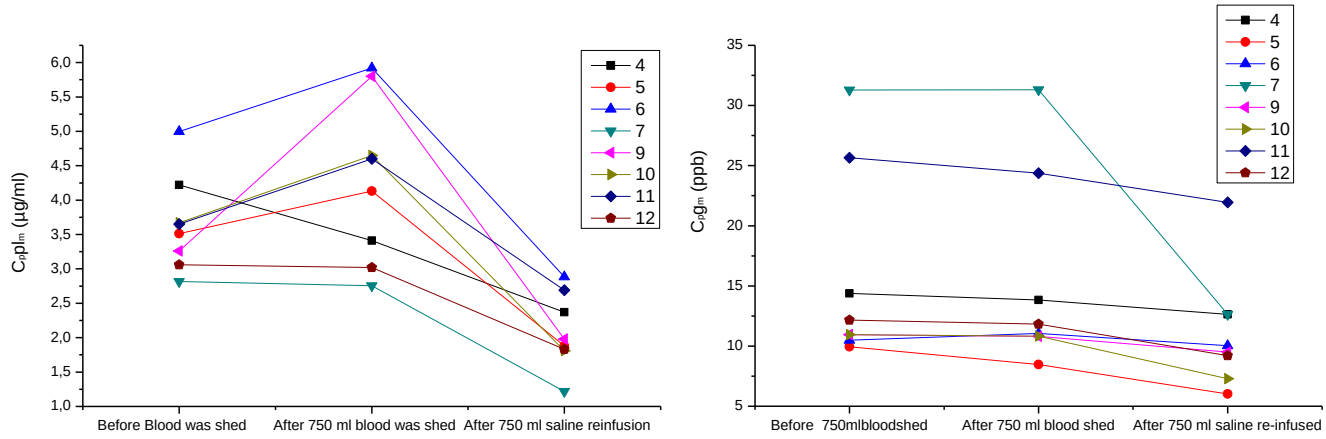

a)

b)

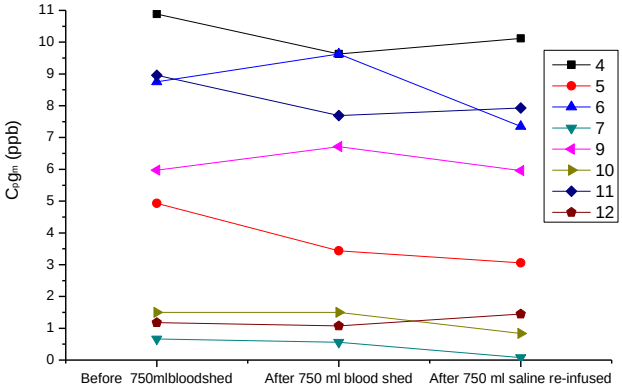

c)

Figure 5.21 An increase in both C_pPl_m (a) and C_pg_m (fig 5.21b – sensor, fig 5.21 c – IMR-MS) is observed when blood was removed and an decrease when the blood was re-infused.

Conclusion

To summarize the IMR-MS which was able to detect expired gas propofol concentrations was used to quantify propofol boli. The results from both IMR-MS and electrochemical sensors were in agreement with GC-MS and blood propofol concentrations. The small differences induced by cardiac output and breath cycle alterations were detected by IMR-MS and the changes noted in blood propofol concentrations were well reflected in expired propofol concentrations.

References

Grossherr M et al. Discontinuous monitoring of propofol concentrations in expired alveolar gas and in arterial and venous plasma during artificial ventilation. Anesthesiology, 2006, 104, 786-90

Hornuss C et al. Real-time monitoring of propofol in expired air in humans undergoing total intravenous anesthesia. Anesthesiology, 2007, 106, 665-74

Hornuss C et al. The Relationship between Expiratory Propofol Concentrations and Changes in the Bispectral Index, Annual Meeting of the American Society Anesthesiologists,2009, A461

Johnson KB et al.: The influence of haemorragic shock on propofol: a pharmacokinetic and pharmacodynamic analysis. Anesthesiology, 2003,99,409-20

Kuipers JA et al.First-pass lung uptake and pulmonary clearance of propofol. Anesthesiology, 1999, 91, 1780-7

Miekisch W et al. Assessment of propofol concentrations in human breath and blood by means of HS-SPME-GC-MS. Clin ChimActa, 2008, 395(1-2),32-37

Perl T et al. Determination of serum propofol concentrations by breath analysis using ion mobility spectrometry. Br J Anesth, 2009, 103,822-7

Takita A et al. On-line monitoring of end-tidal propofol concentration in anesthetized patients. Anesthesiology, 2007, 106,659-64

6

Pharmacokinetic modeling of breath propofol

6.1 Introduction

The aim of this chapter is to acquaint the reader with the terminology and basic concepts of pharmacokinetics that will be used in this thesis. An overview of the most widespread modeling methodologies for drug distribution and action is provided. Pharmacokinetics characterizes the distribution and elimination of drugs by the body, in particular the relationship between drug concentration and time [Gibaldi M and Prescott L, 1983]. Pharmacokinetics is a fundamental scientific discipline that underpins applied therapeutics. Pharmacokinetics includes the study of the mechanisms of absorption and distribution of an administered drug, the rate at which a drug action begins and the duration of the effect, the chemical changes of the substance in the body (e.g. by enzymes) and the effects and routes of excretion of the metabolites of the drug [Caruso A, 2009].

6.2 Pharmacokinetic analysis

Pharmacokinetics (PK) are identified on the basis of observed input-output data sequences. A drug bolus is administered and the concentration time course is measured by blood sampling. The infusion time of the bolus is usually neglected; therefore the response of the physiological system can be regarded as an approximation of the system impulse response [Stadler K.S, 2003]. The time course of drug disposition in the body can be described through a number of approaches.

6.2.1 Compartmental pharmacokinetic analysis

Pharmacokinetic analysis is performed by non-compartmental (model independent) or compartmental methods. Non-compartmental methods estimate the exposure to a drug by estimating the area under the curve of a concentration-time graph. Compartmental methods estimate the concentration-time graph using kinetic models. Compartment-free methods are often

more versatile in that they do not assume any specific compartmental model and produce accurate results also acceptable for bioequivalence studies [Gibaldi M and Prescott L, 1983]. Three widespread approaches characterize drug distribution and elimination via:

- empirical models;
- compartmental mammillary models;
- physiologically based models;
- catenary models.

Empirical models are black box models relating input and output by means of an analytical expression, such as the n-exponential function. Compartmental models are formulated on the basis of the minimum number of compartments that adequately fits the observed data. Physiologically based models are the most realistic representation of drug kinetics, because the parameters relate directly to physiology, to anatomy and to biochemistry [Stadler K.S, 2003]. In the mammillary models peripheral compartments are arranged around a central compartment. All peripheral compartments are only linked via micro rate constants to the central compartment. The compartments of the catenary model are on the other hand arranged in a chain. The most common structure is the mammillary model [Gibaldi M and Prescott L, 1983].

Non-compartmental analysis

Non-compartmental PK analysis is highly dependent on estimation of total drug exposure. Total drug exposure is most often estimated by area under the curve (AUC) methods, with the trapezoidal rule (numerical differential equations) the most common area estimation method.

Compartmental analysis

Compartmental models represent a customary solution for pharmacokinetic modeling. They are based on the assumption that different regions of the body can be represented by virtual compartments disregarding the physical properties of the described tissues. This may lead to one compartment, two compartment and multi compartment pharmacokinetic models. The pharmacokinetics problem then commonly reduces to finding the constants of the exponentials with a curve-fitting procedure. Pharmacokinetic models are hypothetical structures that are used to describe the fate of a drug in a biological system following its administration. Mammillary and

physiologically based models are further discussed in the following [Dhillon S, Kostrzewski A, 2006].

Pharmacokinetic parameters

Some basic pharmacokinetic parameters are explained below:

Elimination rate constant

Consider a single IV bolus injection of drug X (see Figure 6.1). As time proceeds, the amount of drug in the body is eliminated. Thus the rate of elimination can be described (assuming first-order elimination) as:

$X = X0 \exp(\ \ kt)$

where X = amount of drug X, X0 = dose and k = first-order elimination rate constant.

Volume of distribution

The volume of distribution (V_d) has no direct physiological meaning; it is not a 'real' volume and is usually referred to as the apparent volume of distribution. It is defined as that volume of plasma in which the total amount of drug in the body would be required to be dissolved in order to reflect the drug concentration attained in plasma. The body is not a homogeneous unit, even though a one-compartment model can be used to describe the plasma concentration–time profile of a number of drugs. It is important to realise that the concentration of the drug (C_p) in plasma is not necessarily the same in the liver, kidneys or other tissues.

Thus C_p in plasma does not equal C_p or amount of drug (X) in the kidney or C_p or amount of drug (X) in the liver or C_p or amount of drug (X) in tissues. However, changes in the drug concentration in plasma (C_p) are proportional to changes in the amount of drug (X) in the tissues. Then

C_p (plasma) = V_d • X (tissues)

where V_d is the constant of proportionality and is referred to as the volume of distribution, which thus relates the total amount of drug in the body at any time to the corresponding plasma concentration [Dhillon S and Kostrzewski A, 2006].

Clearance

Drug clearance (CL) is defined as the volume of plasma in the vascular compartment cleared of drug per unit time by the processes of metabolism and excretion. Clearance for a drug is constant if the drug is eliminated by first-order kinetics. Drug can be cleared by renal excretion

or by metabolism or both. With respect to the kidney and liver, etc., clearances are additive, that is:

$CL_{total} = CL_{renal} + CL_{nonrenal}$

Mathematically, clearance is the product of the first-order elimination rate constant (k) and the apparent volume of distribution (V_d). Thus

$CL_{total} = k \text{ X } V_d$

Hence the clearance is the elimination rate constant – i.e. the fractional

rate of drug loss – from the volume of distribution [Dhillon S, Kostrzewski A, 2006]..

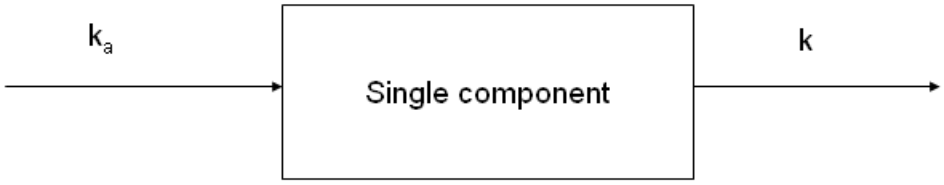

a)

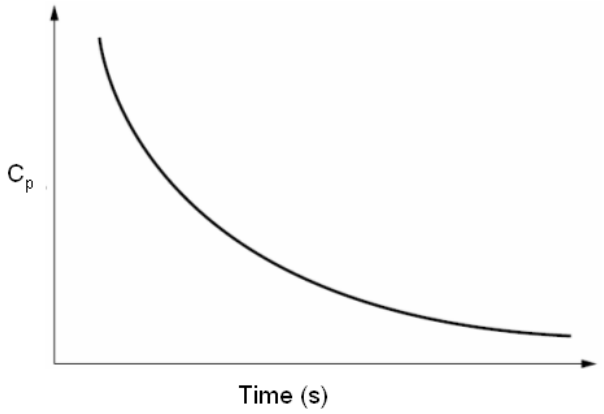

b)

Figure 6.1 a) One-compartment model. k_a = absorption rate constant (h^{-1}), k = elimination rate constant (h^{-1}). b) Plasma concentration (C_p) versus time profile of a drug showing a one-compartment model[Dhillion S and Kostrzewski A, 2006].

One-compartment model

Following drug administration, the body is depicted as a kinetically homogeneousunit (see Figure 6.1). This assumes that the drug achieves instantaneous distribution throughout the body and that the drug equilibrates instantaneously between tissues. Thus the drug concentration–time profile shows a monophasic response (i.e. it is monoexponential; Figure 6.1b). It is important to note that this does not imply that the drug concentration in plasma (C_p) is equal to the drug concentration in the tissues. However, changes in the plasma concentration quantitatively reflect changes in the tissues. This represents a one-compartment model.

Two-compartment model

The two-compartment model resolves the body into a central compartment and a peripheral compartment (figure 6.2a). Although these compartments have no physiological or anatomical meaning, it is assumed that the central compartment comprises tissues that are highly perfused such as heart, lungs, kidneys, liver and brain. The peripheral compartment comprises less well-perfused tissues such as muscle, fat and skin. A two-compartment model assumes that,

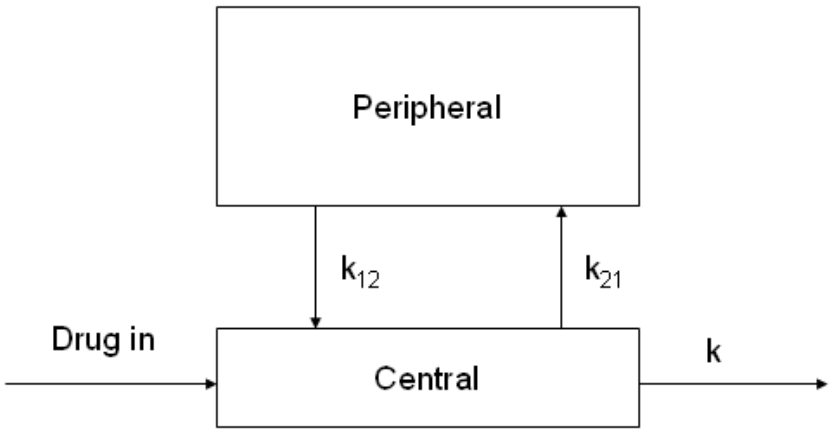

a)

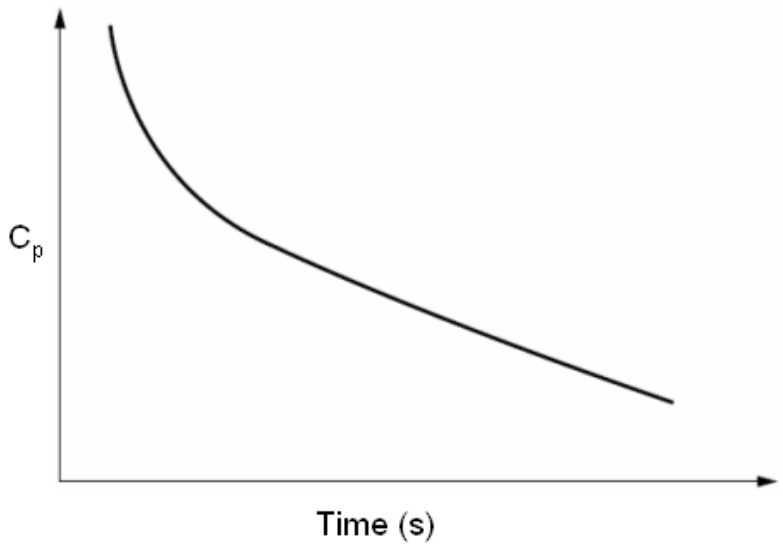

b)

*Figure 6.2 a) Two-compartment model. k_{12}, k_{21} and k are first-order rate constants:k_{12} = rate of transfer from central to peripheral compartment; k_{21} = rate of transfer from peripheral to central compartment; k = rate of elimination from central compartment.b) Plasma concentration versus time profile of a drug showing a two compartment model[*Dhillion S and Kostrzewski A, 2006*]*.

following drug administration into the central compartment, the drug distributes between that compartment and the peripheral compartment. However, the drug does not achieve instantaneous distribution, i.e. equilibration, between the two compartments. The drug concentration–time profile shows a curve (figure 6.2b).

Multi compartment model

A hypothetical three-compartment mammillary model is shown in Figure 6.3a, where a central compartment is connected to two peripheral compartments. As mentioned above, the plasma concentration time course following a drug bolus can be fitted by a n-exponential function. The pharmacokinetics problem then commonly reduces to finding the constants of the exponentials with a curve-fitting procedure. In this model the drug distributes into more than one compartment and the concentration–time profile shows more than one exponential (figure 6.3b). Each exponential on the concentration–time profile describes a compartment. In the case of

mammillary models, drug distribution to and from each PK model compartment is usually considered a first order process [Sheiner LB et al., 1979]. Therefore, the solution consists in the identification of compartmental volumes and first order rate constants.

Estimating the parameters of a sufficient number of compartments allows for the fitting of experimental data. The major advantage of mammillary models is that an adequate description of the concentration time course can be achieved with a low level of complexity [Stadler KS, 2003]. Strictly speaking, the compartments have no physiological meaning [Stadler KS, 2003]. In clinical literature the central compartment is often identified as the "plasma" compartment, given that the compartmental concentration is the plasma concentration, C_p. However, the exponential equation should be regarded as the solution of the differential equation describing the central compartment drug concentration that results from a bolus injection into the n-compartment model. The central compartment concentration is calculated from the intake rate, the elimination rate, the inflow and outflow compartmental rates, which are assigned to fit experimental observations.

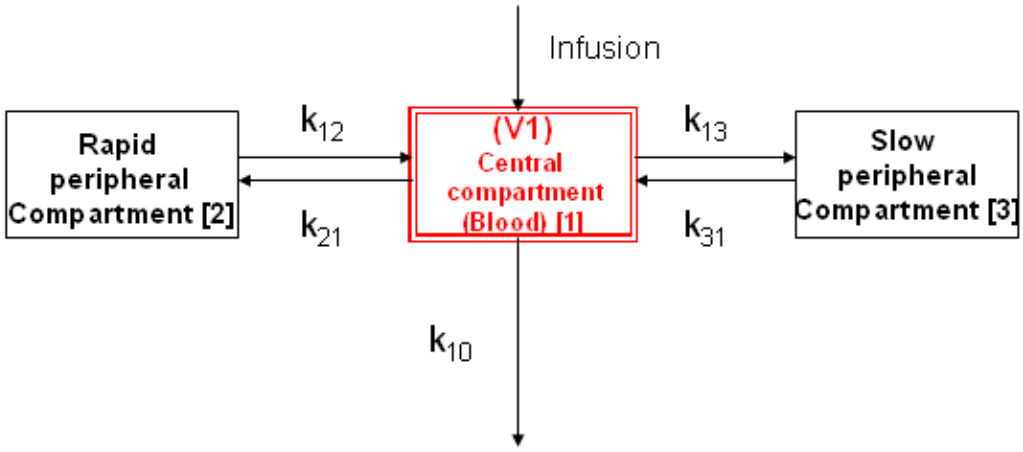

a)

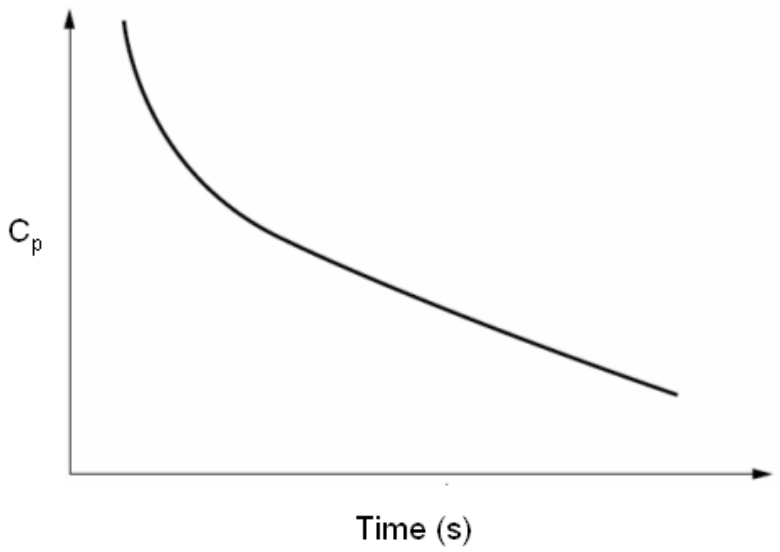

b)

*Figure 6.3 a) Diagram of a 3-compartment mammillary model with 1 being the central compartment and 2,3 being the peripheral compartments. V_i is the volume of the i-th compartment (i = 1, 2, 3); k_{ij} the drug distribution rate from compartment i to compartment j (i, j = 1, 2, 3); k_{10} the drug elimination rate from the central compartment.b) Plasma concentration versus time profile of a drug showing multi compartment model[*Dhillion S and Kostrzewski A, 2006*]*.

Physiology based models

Physiology based pharmacokinetic models use actual physiological parameters such as breathing rates, blood flow rates and tissue volumes to describe the pharmacokinetic process. These parameters are coupled with chemical-specific parameters like blood/gas partition coefficients, tissue/blood partition coefficients and metabolic constants to predict the dynamics of compound distribution in the physiological system. An advantage of such models is that by simply using appropriate physiological and biochemical parameters, the same model can be employed to describe the dynamics of different drugs in different species [Hetrick DM et al., 1991].

The greatest potential of physiology based modeling is that it offers the possibility of predicting physiological phenomena. A suitable pharmacodynamic model can be coupled to the

physiologically based pharmacokinetic model. The modeled pharmacological effect can then influence drug pharmacokinetics via physiological homeostatic mechanisms. This would be particularly useful for drugs that influence cardiac output and regional blood flows, which in turn can affect drug distribution and elimination [Ludden TM et al., 1995].

Another advantage of physiology based over mammillary models is that elimination can be modeled as occurring in the tissue where it actually takes place in the body [Stadler KS, 2003]. Given that a mammillary model compartment does not represent a clearly defined physiological region, for example it is not possible to model explicitly the renal or hepatic clearance.

On the other hand, a serious disadvantage of whole-body physiology based PK models is their extensive dimensionality and complexity. Such drawbacks have limited their use to date. Compromising between model descriptive properties and computational complexity is a critical issue in physiologically based model development. This approach should only be applied to cases where the potential benefits justify the time and cost associated with its implementation [Charnick SB et al., 1995].

A common approach to decrease the complexity of physiologically based pharmacokinetics is *lumping* suitable tissues within the structure of the model. Lumping can be defined as a structural transformation of a complex physiological model to obtain a simpler model with identical kinetic behavior. Proper lumping should guarantee that no useful information about the kinetics of the underlying process are lost [Nestorov et al., 1998].

6.3 Breath based pk-model analysis

A mamillary three compartment pharmacokinetic (pk) model for propofol was first described by Gepts et al [Gepts et al., 1987]. A computerised drug delivery system with an incorporated mathematical model was used by White et al. to maintain target plasma concentrations of propofol [Kenny GNC and White MA, 1987]. The rate constants which described the elimination and distribution of propofol during anesthesia was described using the same three compartment model (study conducted in children) by Marsh et al. [Marsh B et al. 1991]. The model was described solely based on the body weight. Schnider et al. included factor of age in deriving the rate constants to describing pharmacokinetics of propofol [Schnider TW et al., 1999].

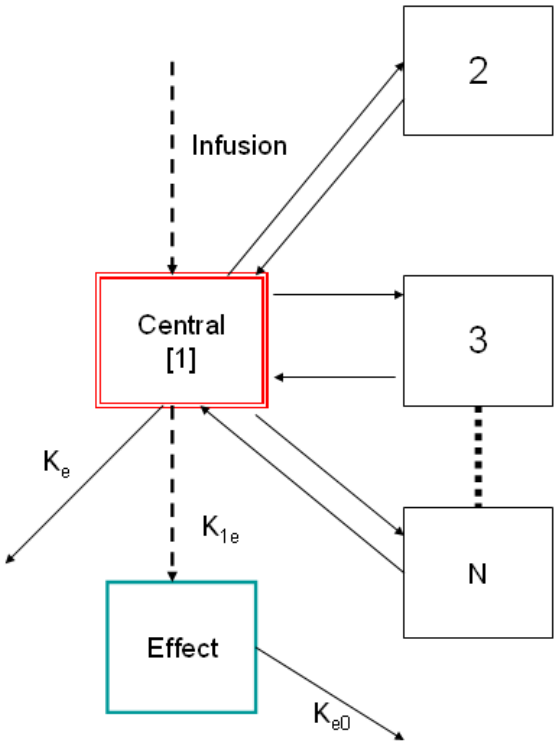

Figure 6.4 A N-compartment mammilary model with an effect compartment attached to it. The central compartment is represented as 1 and the peripheral compartments attached to the central compartment are given with 2,3….N. K_e – the equilibration rate constant.[Schnider LB et al., 1979]

A pk-model for breath formed by a simple modification of the existing Marsh model is proposed. We linked a breath compartment to the Marsh et al. [Marsh B et al., 1991] model's central plasma compartment similar to Sheiner et al. [Sheiner LB et al., 1979] hypothetical effect site compartment connected to the N-compartment mammillary model (figure 6.4). The predictive performance for breath gas concentrations was evaluated.

The Marsh model with its pharmacokinetic variables was modified with an additional expired gas compartment to simulate expired gas propofol concentrations. This approach is similar to the multi-compartment pharmacokinetic effect site model as proposed by Sheiner et al. [Sheiner LB et al., 1999] (figure 6.4). A simulated gas phase equilibrium rate constant (K_{LS} – similar to the effect site equilibrium rate constant Ke0 given for brain-effect site), and a simulated blood gas coefficient (BGC_s) are two model parameters included for the pk-model

adaptation (figure 6.5).

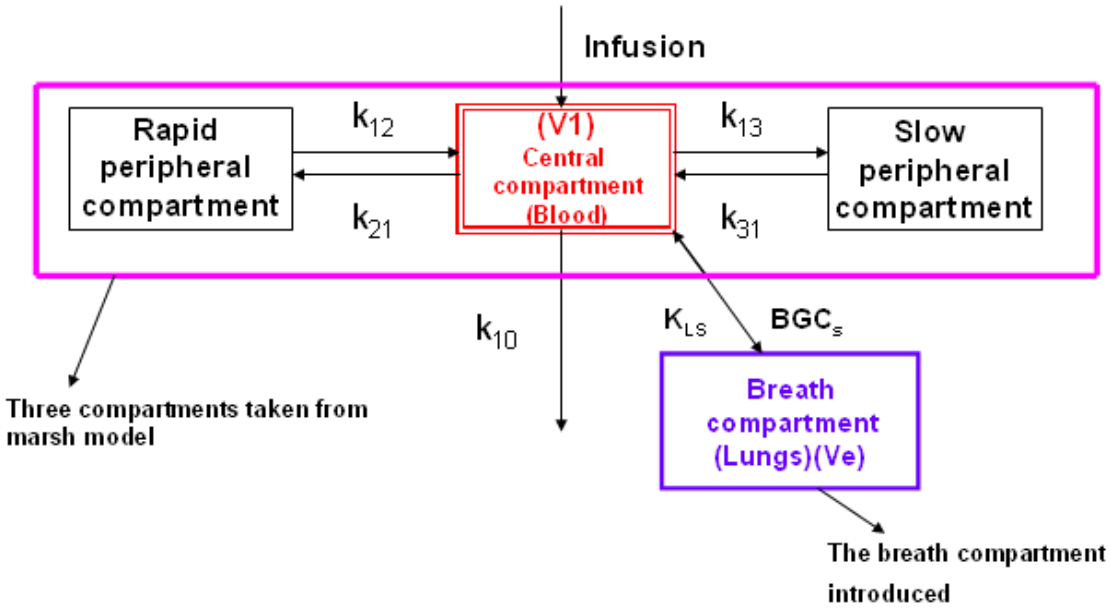

Figure 6.5 The three compartment breath based pharmacokinetic model derived from the Marsh model modified with an additional expired gas compartment to simulate expired gas propofol concentrations. K_{10} – elimination rate constant, K_{12}, K_{21}, K_{31} and K_{13} – distribution rate constants. K_{LS} – simulated gas phase equilibrium rate constant and a simulated blood gas coefficient (BGC_s) are two model parameters included for the pk-model adaptation.

Equations governing the pk-model

$$X_n = (1-(k_{10}+k_{12}+k_{13})\,\Delta t)\,X_n\text{-}1+k_{21}\Delta t Y_n\text{-}1+k_{31}\Delta t Z_n\text{-}1+U_n\text{-}1\Delta t \qquad (6.1)$$

$$Y_n = k_{12}\Delta t X_n\text{-}1 + (1-k_{21}\Delta t)\,Y_n\text{-}1 \qquad (6.2)$$

$$Z_n = k_{13}\Delta t X_n\text{-}1 + (1-k_{31}\Delta t)\,Z_n\text{-}1 \qquad (6.3)$$

The equations 6.1, 6.2, 6.3 are the basic equations taken from the three compartment pk model. Using these equations the propofol concentrations in central (X_n) and the peripheral compartments (fast - Y_n and slow - Z_n) can be calculated.

$$C_n = K_{LS}\left(\left(\frac{X_{n-1}}{V}\right)\left(\frac{1}{BGC_s}\right)\text{-}C_n\text{-}1\right) + C_n\text{-}1 \quad (6.4)$$

The amount of expired gas propofol (C_n) can be calculated using the equation 6.4.

$$C_e = Ke0\ (C_1\text{-}C_{en}\text{-}1) + C_{en}\text{-}1 \quad (6.5)$$

The effect site concentrations (C_e) can be calculated from equation 6.5.

Here K_{LS} – Respiratory rate constant, BGC_s – Simulated blood gas coefficient

The Marsh model rate constants used in our model are given below.

k_{10} – 0.119
k_{12} – 0.112
k_{13} – 0.0419
k_{21} – 0.055
k_{31} – 0.0033
Ke0 – 0.021

Here K_{10} – elimination rate constant, K_{12}, K_{21}, K_{31}, K_{13} – distribution rate constants
The central compartment volume (V) can be calculated by V = 0.228 * Weight of patient.

6.4 Model parameters adaptation

The two parameters K_{LS} and BGC_s were varied to allow fitting of the recorded expired gas concentration to yield a maximal correlation coefficient as well as a low MDAPE. The fitting was carried out over the entire experiment (all three boluses over 90 minutes).

Steps for optimizing K_{LS} and BGC_s values:

A range of K_{LS} (0.001 to 0.05) and BGC_s (10000 to 500,000) values was chosen according to Grossherr et al. [Grossherr M et al., 2009] and Marsh et al. [Marsh B et al., 1991] for selecting the BGC_s and K_{LS} ranges.

Determination of K_{LS}: The BGC_s is fixed at a mid-value (BGC_s does not influence r value) and K_{LS} is iteratively varied (step size ΔK_{LS} of 0.0001) until a maximum r value is reached.

Determination of BGC_s: the K_{LS} value is fixed at the point where the maximum r value was reached then BGC_s was iteratively varied (step size ΔBGC_s of 100) until MDAPE reaches a minimal value.

The two modified pk-model parameters (K_{LS}, BGC_s) were varied to fit the measured level of expired gas concentration with a maximal correlation coefficient and a low MDAPE within a range from 0.015 – 0.034 min^{-1} for K_{LS} and 39500 – 473500 for BGC_s.

6.4.1 Time course analysis of the simulated data

The time courses of plasma and expired gas propofol concentrations simulated with the three compartment pk-model linked with a breath compartment are shown in figure 6.6.

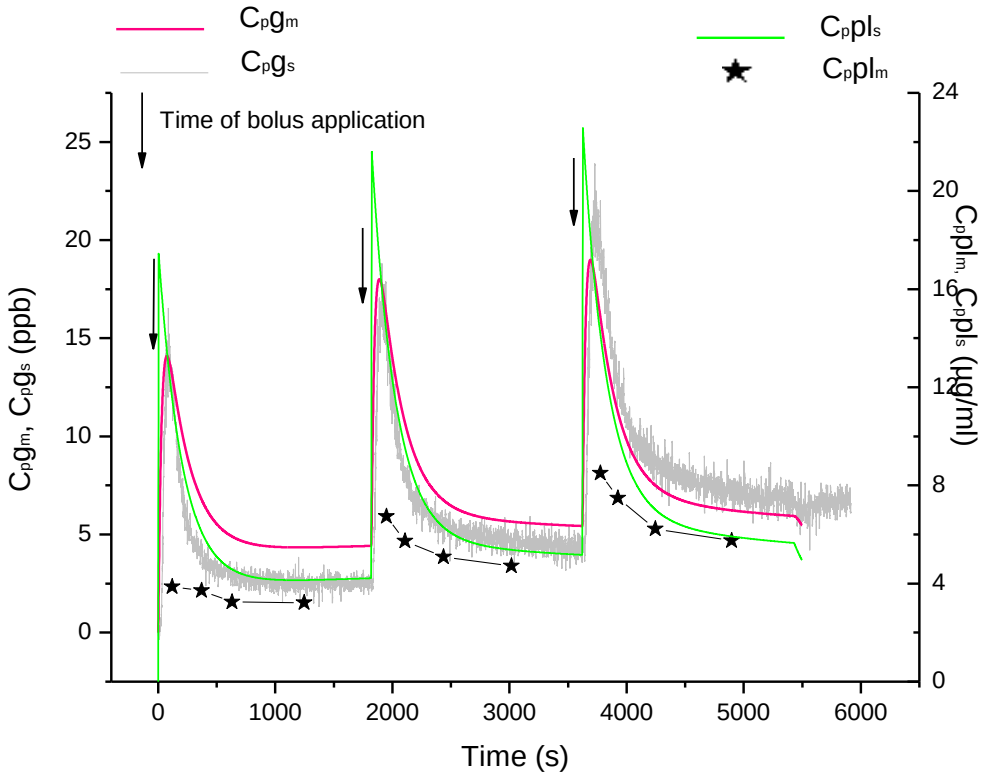

Figure 6.6 The changes in measured plasma propofol concentrations (C_pl_m), simulated plasma propofol concentrations (C_pl_s), measured expired propofol gas concentration (C_pg_m), and simulated expired gas propofol concentration (C_pg_s) after application of three propofol boli at 0 mins (together with the start of infusion), at 30 min and at 60 min is shown with light and dark

grey lines, respectively (for one pig). The black stars indicate arterial plasma concentrations at 2, 5, 10, and 20 minutes after bolus application obtained by HPLC analysis. The time at which the propofol bolus was applied is shown with arrow marks. The delay between the plasma and expired gas propofol concentrations seen after bolus application can be observed.

The time delays between predicted peak plasma and predicted peak expired gas concentrations are shown in figure 6.2 (149 ± 9 s for three boluses). Predicted propofol concentrations showed a time to peak concentration [C_pg_s] which ranged from 124 s – 212 s.

6.5 Performance analysis of the breath based pk model

The correlation r of C_pg_m and C_pg_s was between 0.81 to 0.98 ($p < 0.01$). Predictive performance (C_pg_m vs C_pg_s) of the model was evaluated by deriving the four indicators MDPE, MDAPE, wobble and divergence (refer section 3.7) (Table 6.1).

Table 6.1. Predictive accuracy indices derived from simulated expired gas concentrations (C_pg_s) and measured expired gas propofol concentrations (C_pg_m).

Parameter	Value (mean ± SD)
Median performance error (MDPE) [%]	-9.1 ± 7.8
Median absolute performance error (MDAPE) [%]	13.4 ± 6.2
Wobble [%]	17.2 ± 8.7
Divergence [ppb/s]	-0.1 ± 0.2

The graphical plot over time (figure 6.7) of the ratio of measured to simulated expired gas propofol values allows a visual assessment of the progression of error (increases from 0.6 ± 0.1 ppb to 1.1 ± 0.1 ppb) with time from the time point of anesthesia induction.

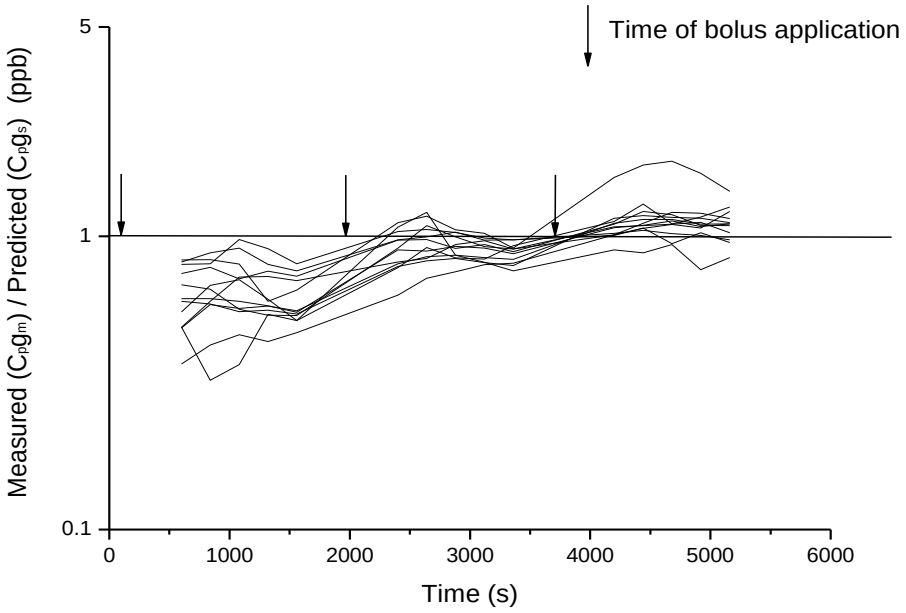

Figure 6.7 Ratio of measured to simulated expired gas propofol concentrations on a semi-logarithmic scale plotted for each pig over time. Equality between measured (C_pg_m) and simulated propofol concentrations (C_pg_s) is reflected by a ratio equal to 1 (central line).

6.6 Discussion

The feasibility of describing propofol exhalation on the basis of a three compartment pk (Marsh) model modified with a breath compartment was evaluated by comparing the measured data with predicted data incurred from the model. The inter-individual variability between the pigs was very high (see figure 5.3), so we did not develop a common model for all the pigs. Instead, we fitted simulated expired gas propofol concentrations for each individual pig The simulated TTPCs values determined from C_pg_s (149 ± 22 s) were close to the $TTPC_m$ values calculated from C_pg_m (113 ± 24 s). The simulated model performance can be evaluated by analysing the four performance indices (Table 6.1). Since no data was available from a prospective study to compare our breath-based pk-model, we decided to compare the performance characteristics of our pk-model to the data from a study based on a pk-model predicting plasma propofol concentrations. In comparison to the results reported by Pandin et al. [Pandin PC et al., 2000], the expired gas propofol concentrations revealed lower bias (MDPE - -9.1% vs -12.1%), lower inaccuracy (MDPE – 13.4% vs 22.1%) and a similar divergence (-0.1 ppb/s vs - 2.9 ppb/s). We obtained results similar to Pandin et al. [Pandin PC et al., 2000] except for the wobble which was

of a higher magnitude (17.2 % in comparison to 11.6 %). As such, our model may effectively predict expired gas propofol concentrations similarly to an already existing model which predicts plasma propofol concentrations. The predicted plasma levels and the simulated plasma concentrations appear different only under non-steady-state conditions, but it can be easily seen that they correlate significantly under steady-state conditions due to the pulmonary uptake of propofol which increases immediately after bolus injection and decreases with time.

During non-steady-state conditions, the technology may work well because the model fit considers both steady-state and non-steady-state conditions (C_pg_m vs C_pg_s - r value : 0.81 – 0.98; $p < 0.01$) (refer section 5.2.2). An online model could be used in future to validate the expired propofol after propofol infusion. For example, the model presented here could be used to activate alarms while an inverse model may be used to predict plasma concentrations from the expired propofol. One limitation of our study was that we used the human-based three compartment Marsh model to build the breath-based pk-model. However, when we compared the simulated plasma concentrations derived from Johnson et al. [Johnson KB et al., 2004] (a three compartment pharmacokinetic model for propofol used in pigs) with those from Marsh et al., no significant statistical difference was found between them in a two-sided t-test ($p > 0.05$).

References

Caruso A. Personalised drug dosing through modeling and feedback. Ph.D thesis 2009,ETH Zurich.

Charnick S.B et al.Perspectives in Pharmacokinetics. Physiologically Based Pharmacokinetic Modeling as a Tool for Drug Development. Journal of Pharmacokinetics and Biopharmaceutics, 1995, 23(2), 217–29.

Dhillion S and Kostrzewski A. Clinical pharmacokinetics, London, Pharamaceutical press 2006.

Gepts et al. Disposition of propofol administered as constant rate infusions in humans. Anesthesia and Analgesia 1987, 66, 1256-1263.

Gibaldi M, Presscott L . Handbook of clinical pharmacokinetics. Newyork ADIS Health Science press 1983.

Grossherr M et al.Blood gas partition coefficient and pulmonary extraction ratio for propofol in goats and pigs. Xenobiotica. 2009, 39(10),782-7.

Hetrick D.M et al.Sensitivity analysis for physiologically based pharmacokinetic models. Journal of Pharmacokinetics and Biopharmaceutics, 1991 , 19(1),1–20.

Johnson KB et al. Influence of hemorrhagic shock followed by crystalloid resuscitation on propofol: a pharmacokinetic and pharmacodynamic analysis. Anesthesiology 2004 , 101(3), 647-59.

Kenny GNC, White M. A portable computerised control system for propofol infusion. Anesthesia 1990; 45: 692-693.

Ludden T. M et al. Commentary on Physiologically Based Pharmacokinetic Modeling as a Tool for Drug Development.Journal of Pharmacokinetics and Biopharamceutics, 1995, 23(2):231–235.

Marsh B et al. Pharmacokinetic model driven infusion of propofol in children. Br J Anesth, 1991, 67,41 – 48.

Nestorov et al. Lumping of Whole-Body Physiologically Based Pharmacokinetic Models. Journal of Pharmacokinetics and Biopharmaceutics, 1998, 26(1),21–46.

Pandin PC et al. Predictive accuracy of target-controlled propofol and sufentanil coinfusion in long-lasting surgery. Anesthesiology 2000, 93, 653-61.

Schnider TW et al.The influence of age on propofol pharmacodynamics.Anesthesiology. 1999 , 90(6), 1502-16.

Sheiner L.B et al. Simultaneous modeling of pharmacokinetics and pharmacodynamics: Application of d-tubocurarine. Clin. Pharmacol. Ther. 1979, 25,358-371.

Stadler, K. S.: *Modeling and Control in Anesthesia from Design to Validation*.Dr. Tech. Sc. Thesis, Swiss Federal Institue of Technology (ETH),Zurich, Switzerland, 2003.

7

Anesthesia control

7.1 Introduction

Anesthesiologists often compare themselves to pilots who use automated flight control. Autopilot systems are routinely used in the airline industry to reduce the workload during busy periods and certain types of human error during takeoff, cruising, and landing. Two methods for controlling drug administration are commonly known: open- and closed-loop control. When the anesthetist makes a decision to maintain or change a desired target drug dose, concentration or clinical effect (e.g. the depth of the hypnotic or analgesic component of anesthesia), this is called ‘open-loop control’. ‘Closed-loop controllers’ are systems designed to maintain a target value by adapting the administered amounts of drug. In closed-loop control, the anesthetist enters only the desired variable to be maintained [I.J.Nagarath and M.Gopal, 2007]. One proposed benefit of automated, closed-loop anesthesia delivery systems is that a continuous, responsive control of anesthesia may improve quality of care compared with intermittent control (i.e. standard practice) [Struys MM et al., 1998]. The complexity of the human body makes it difficult to optimise all the basic components required for developing such a system figure 7.1:

1. An adequate control variable to measure the drug effect is obligatory.
2. An accurate set-point for this variable, which is the chosen target value specified by the user, should be defined.
3. A stable controller for the actuator is required.
4. The control actuator, which is in this case the infusion pump driving the drug, should be accurate.
5. A system, in this case a patient, must fit the described system model [Struys MM et al., 1998].

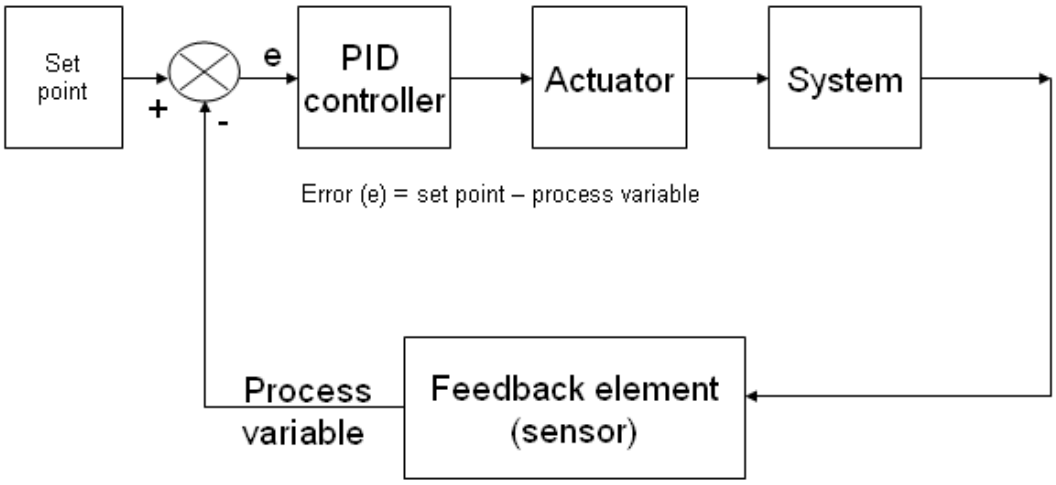

Figure 7.1 Basic components of a control system. The error is calculated from the difference of set point and process variable. The process variable is the parameter taken from the sensor or the feedback element.

7.2 Proportional-integral-derivative (PID) control for propofol sedation

The control design process begins by defining the performance requirements. Control system performance is often measured by applying a step function as the set point command variable, and then measuring the response of the process variable. Commonly, the response is quantified by measuring defined waveform characteristics.

Rise Time is the amount of time the system takes to go from 10% to 90% of the steady-state, or final value.

Percent Overshoot is the amount that the process variable overshoots the final value, expressed as a percentage of the final value.

Settling time is the time required for the process variable to settle to within a certain percentage (commonly 5%) of the final value. [IJ.Nagarath and M.Gopal, 2007]

Steady-State Error is the final difference between the process variable and set point. Note that the exact definition of these quantities will vary in industry and academia. After using one or all of these quantities to define the performance requirements for a control system, it is useful to define the worst case conditions in which the control system will be expected to meet these design

requirements. Often times, there is a disturbance in the system that affects the process variable or the measurement of the process variable. It is important to design a control system that performs satisfactorily during worst case conditions. The measure of how well the control system is able to overcome the effects of disturbances is referred to as the disturbance rejection of the control system.

Some systems exhibit an undesirable behavior called deadtime. Deadtime is a delay between when a process variable changes, and when that change can be observed. For instance, if a temperature sensor is placed far away from a cold water fluid inlet valve, it will not measure a change in temperature immediately if the valve is opened or closed. Deadtime can also be caused by a system or output actuator that is slow to respond to the control command, for instance, a valve that is slow to open or close. A common source of deadtime in chemical plants is the delay caused by the flow of fluid through pipes. Loop cycle is also an important parameter of a closed loop system. The interval of time between calls to a control algorithm is the loop cycle time. Systems that change quickly or have complex behavior require faster control loop rates.

The classical PID algorithm consists of three basic modes, the Proportional mode, the Integral and the Derivative modes. When utilising this algorithm it is necessary to decide which modes are to be used and then specify the parameters (or settings) for each mode used. The basic components included in a control system are shown in the figure 7.1a.

All three of these PID controller components create output based on measured error of the process being regulated.

Error (e) = set-point (SP) – process variable (PV)

In our study the process variable is expired gas propofol concentration.

If a control loop functions properly, any changes in error caused by setpoint changes or process disturbances are quickly eliminated by the combination of the three factors P, I, and D [IJ Nagarath and M Gopal, 2007]. Detailed explanations on these P, I and D parameters are given below.

Proportional response

The proportional component depends only on the difference between the set point and the process variable. This difference is referred to as the Error term. The proportional gain (Kc) determines the ratio of output response to the error signal. For instance, if the error term has a magnitude of 10, a proportional gain of 5 would produce a proportional response of 50. In general, increasing the proportional gain will increase the speed of the control system response. However, if the proportional gain is too large, the process variable will begin to oscillate. If K_c is increased further, the oscillations will become larger and the system will become unstable and may even oscillate out of control.

Integral response

The integral component sums the error term over time. The result is that even a small error term will cause the integral component to increase slowly. The integral response will continually increase over time unless the error is zero, so the effect is to drive the Steady-State error to zero. Steady-State error is the final difference between the process variable and set point. A phenomenon called integral windup results when integral action saturates a controller without the controller driving the error signal toward zero.

Derivative response

The derivative component causes the output to decrease if the process variable is increasing rapidly. The derivative response is proportional to the rate of change of the process variable. Increasing the derivative time (T_d) parameter will cause the control system to react more strongly to changes in the error term and will increase the speed of the overall control system response. Most practical control systems use very small derivative time (T_d), because the Derivative Response is highly sensitive to noise in the process variable signal. If the sensor feedback signal is noisy or if the control loop rate is too slow, the derivative response can make the control system unstable.

$$u(t) = K_c\left(e + \frac{1}{T_i}\int_0^t e\,dt + T_d\frac{de}{dt} \right) \qquad (7.1)$$

The PID controller calculates the controller action, u(t),where Kc is controller proportional gain.

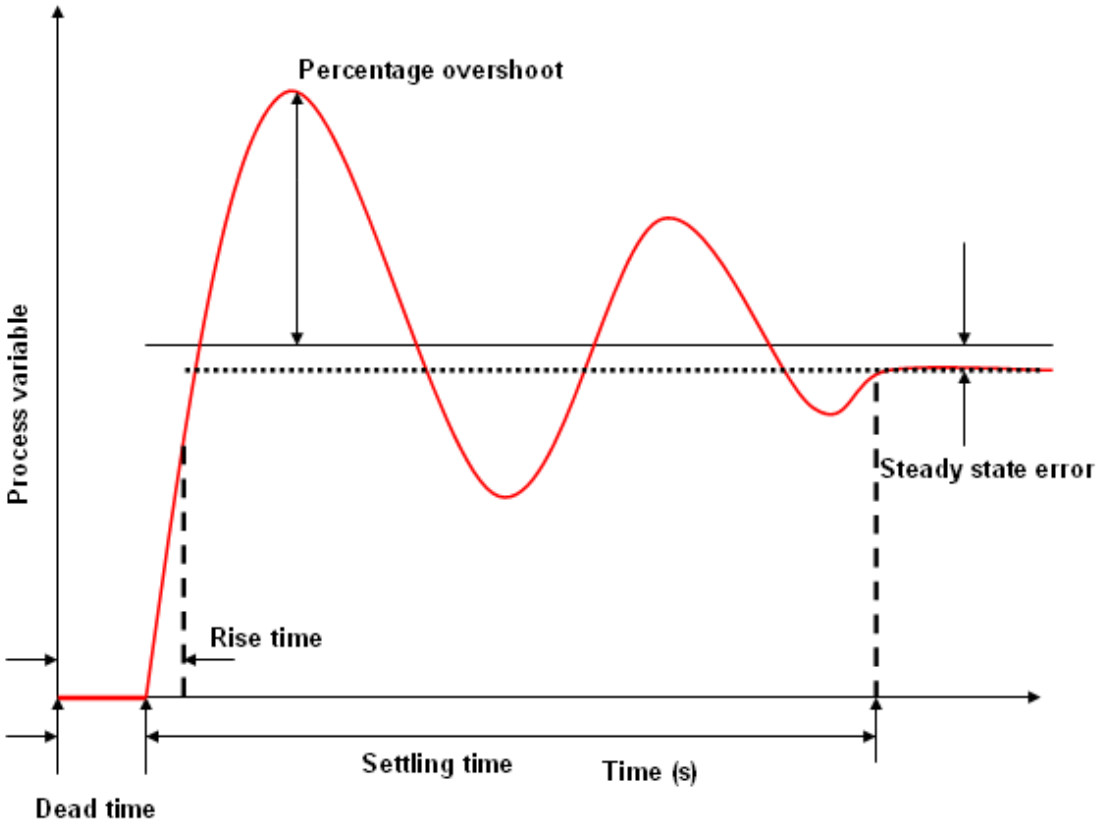

Figure 7.2 Response of a typical PID (Proportional Integral Derivative) closed loop system. The rise time, steady state error, settling time, dead time and percentage overshoot are displayed.

7.2.1 Controlled variable

The effectiveness of the control systems depends strongly on the reliability of the physiological signal to be controlled [Mortier E et al., 1998] and on the optimisation of control algorithms. The controlled variable or variables must be measured reliably. An ideal sensor for control must reflect the dose-response relation of the drug, the anesthetist's observations, and should not introduce non-linearities (especially discontinuities) and additional delay. These can be achieved

by detecting breath propofol using IMR-MS or electrochemical sensor (section 2.4.1). The breath propofol is a direct measure of the plasma propofol concentrations.

Some measured variables (e.g. blood pressure, muscle activity, ventilatory parameters, inhaled drug concentration) are direct indicators of the controlled variable and have been applied to developing closed-loop systems.[Hoeksel SA et al., 2001] Other drug effects are not directly measurable. 'Depth of hypnosis' or 'level of analgesia' is not measurable, so surrogate measures have to be applied as the controlled variable.

In the field of anesthesia control, Bispectral index (BIS) derived from electroencephalogram have been tested and validated as a promising measure of the hypnotic component of anesthesia. BIS® is a dimensionless number scaled from 100 to 0, with 90-100 representing an awake patient where as values around 60–70 and 40–60 indicate a light and moderate hypnotic state, respectively. If lower than 40, the BIS indicates too excessive a level of hypnosis [Morley A et al., 2000].Because it is a single composite measure monitored continuously, it has been used to control depth of hypnosis automatically [Absolam AR et al., 2002 ; Johansen JW and Sebel PS , 2000]. Bispectral Index (BIS) monitoring has emerged as a convenient and versatile tool to titrate hypnotic agents and to reduce drug consumption, therefore allowing faster recovery while avoiding side effects such as hemodynamic instability or awareness [Johansen JW et al., 2000; Bannister CF et al., 2001]. Closed-loop systems are not subject to fatigue, thus maintaining the same efficiency throughout a surgical procedure while freeing the physician for more demanding human tasks [Linkens DA and Hacisalihzade SS., 1990; Locher S et al., 2004].

Closed-loop control has the potential to improve the quality of anesthesia; we have created a system that controls a computer controlled infusion pump which delivers propofol and that is titrated to the expired gas propofol concentrations (C_pg_m). The system maintains general anesthesia using a proportional-integral-differential algorithm after a equilibrium in blood-breath concentration was reached. The current clinical study was designed to evaluate our breath propofol based closed-loop system during maintenance in anesthesia and to compare it with the performance of other closed loop systems using BIS as the control variable (using the performance indices).

7.2.2 Set-point

The set-point is the value of the controlled variable that the controller uses as its target. This target is specified by the anesthetist and will be approached as closely as possible during the maintenance of anesthesia; therefore, an adequate individual set-point for each controlled variable is very important for the accuracy of the closed-loop system. Two types of set-point can be used: set-points based on population mean data, and individual data measured at the start of or just before the control period. These setpoints can be changed according to clinical need during the course of the surgical procedure [Struys MM et al., 2002].

In our study for the initial one hour we used the $C_p g_m$ at blood-gas equilibrium (steady state or state of equilibrium) as the set-point. Then in the second hour (phase II-one hour) the setpoint was reduced to half of the initial value and in the third hour again increased back to initial set-point.

7.2.3 Actuator

The power supply base Fresenius Base A (Data Concentrator and power supply) attached with a DPS module (computer controlled infusion pump) was taken as the actuator for our control system. The pump was connected to the labtop via a RS 232 cable.

7.2.4 Proportional-integral-derivative controller applications

Various control strategies exist to guide closed-loop drug administration. Classically, proportional–integral–differential (PID) controllers have been used in several automated control systems in other professional areas (electronic engineering) and require some explicit understanding of the input–output relationship in terms of some mathematical solution [Schuettler J et al., 1999]. Proportional gain-Larger values typically mean faster response. An excessively large proportional gain will lead to process instability and oscillation. Integral gain-Larger values imply steady state errors are eliminated more quickly. Derivative gain-Larger values decrease overshoot, but slow down transient response and may lead to instability due to signal noise amplification in the differentiation of the error.

Closed-loop control to manage directly measurable physiological parameters has been stablished in anesthesia. Recently, a new anesthesia machine (Zeus; Dräger, Luebeck, Germany) became

commercially available that uses a newly designed, blower-driven ventilator and a servo-controlled valve system to control various ventilation modes. Anesthetic and fresh gas delivery is controlled by closed-loop feedback using direct injection into the breathing circle, making it possible to achieve closed-circuit ventilation.[Struys MM et al., 2004] Closed-loop mechanical ventilation has the potential to provide more effective ventilatory support to patients with less complexity than conventional ventilation.

Recently, Tehrani et al developed a dual closed-loop control system for mechanical ventilation. In one of the control systems, several physiological data are used to adjust the patient's frequency and tidal volume of breathing automatically. This system is combined with another closed-loop control system for automatic adjustment of the patient's inspired fraction of oxygen. This controller uses the feedback of the patient's arterial oxygen saturation and combines a rapid stepwise control procedure with a PID control algorithm to automatically adjust the oxygen concentration of the patient's inspired gas. The dual closed-loop control system has been examined using mechanical lung studies, computer simulations and animal experiments. It has been found that the controller maintained arterial blood gas concentrations within normal limits under steady-state conditions and the transient response of the system was robust in the face of various disturbances.[Tehrani F et al., 2004]

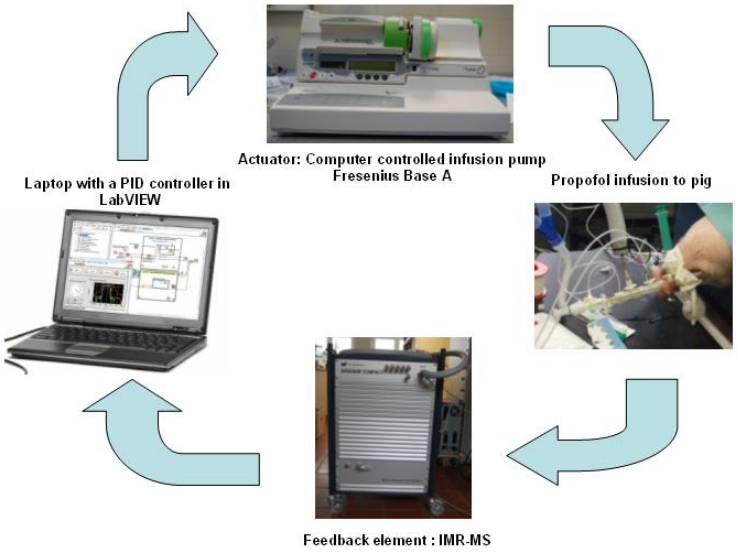

Figure 7.3 Closed loop control system with the breath propofol detected by IMR-MS as the controlled variable. A propotional-integral-derivative controller built in LabVIEW and Fresenius Base A was used the actuator to deliver propofol to pig.

PID control methods are implemented when direct measures are used, for example in closed-loop control systems for mechanical ventilation [Tehrani F et al., 2002; Liu N et al., 2006] PID algorithm being a simple and also breath propofol being a direct measure which reflects the plasma propofol concentration; the PID algorithm was selected. We opted for the manual control and selected three set of PID values (one set for each set-point change) for our experiments.

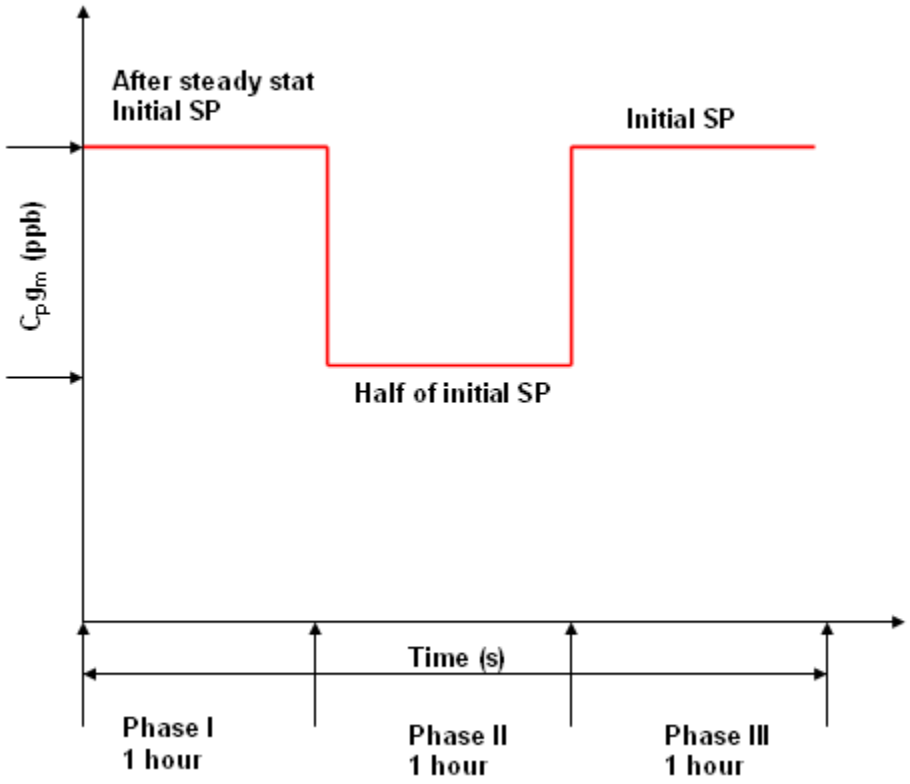

Figure 7.4 The protocol implemented in the preclinical study is shown. Phase I – Breath propofol concentrations at steady state (between the plasma and breath propofol conecntrations) was taken as the set point the phase was extended for one hour. Phase II – One hour , half of the initial set point was taken. Phase III – One hour, back to the initial setpoint.

In our preclinical study we conducted the experiment for three hours which was divided into three parts figure 7.4. Initial one hour with the set-point set as the expired gas propofol concentration at steady state phase [after the equilibrium between plasma and breath propofol

concentrations was reached] (first phase) after which the set-point was reduced to half (second phase-one hour) and then increased back to the initial full value (third phase-one hour) (section 3.2.2). Before the start of real time experiments, the PID control system was simulated considering the pharmacokinetic model (chapter 6) as a virtual patient. The prototype of our control system is shown in figure 7.3.

The table 7.1 display the values used in the study. The reason behind the value selection is discussed in the section 7.4.

The front panel display of the program used in real time is shown in figure 7.2

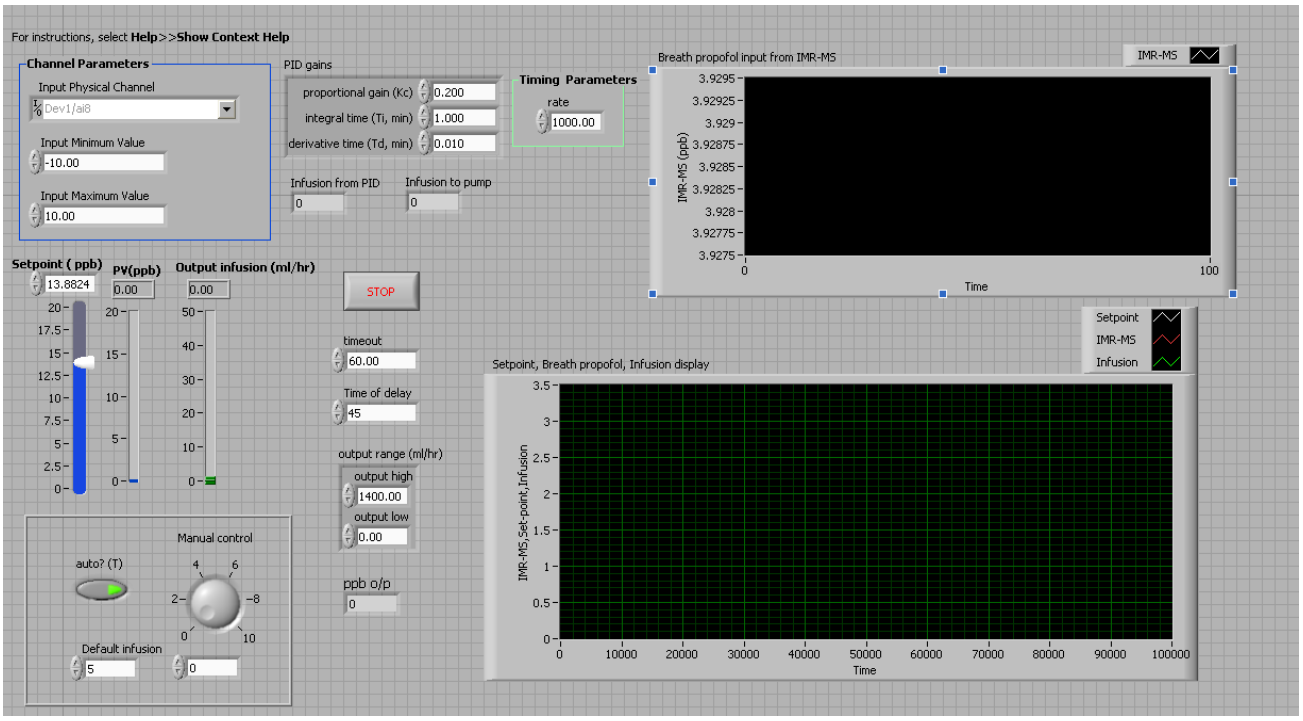

Figure 7.5 The front panel display of the developed breath based PID control system in LabVIEW.

Table 7.1 The Proportional-Integral-Derivative gain values at the three set-points.

Setpoint (ppb)	Proportional (P) gain values	Integral (I) gain values	Derivative (D) gain values
Initial value at state of equilibrium	0.2	1	
Half of initial value	0.3	1	0.01
Initial value at state Of equilibrium	0.25	1	0.01

The PID controller was built in LabVIEW software and the communications with the program was carried out using the DAQ (data acquisition board) installed in the laptop. The PID controller acquired signal from IMR-MS (digital data) and after error correction using the control algorithm, the corrected signal was sent to the infusion pump (Fresenius Base A module).

7.3 Control system performance

Perfomance of the control system during the entire study period is shown in figure 7.6. The control system performs well during the initial maintenance phase (figure 7.6) compared to the next two phases. The control system performance was analyses by calculating the four performance indices (section 3.7).Table 7.2 display the predictive accuracy indices at different set-points.

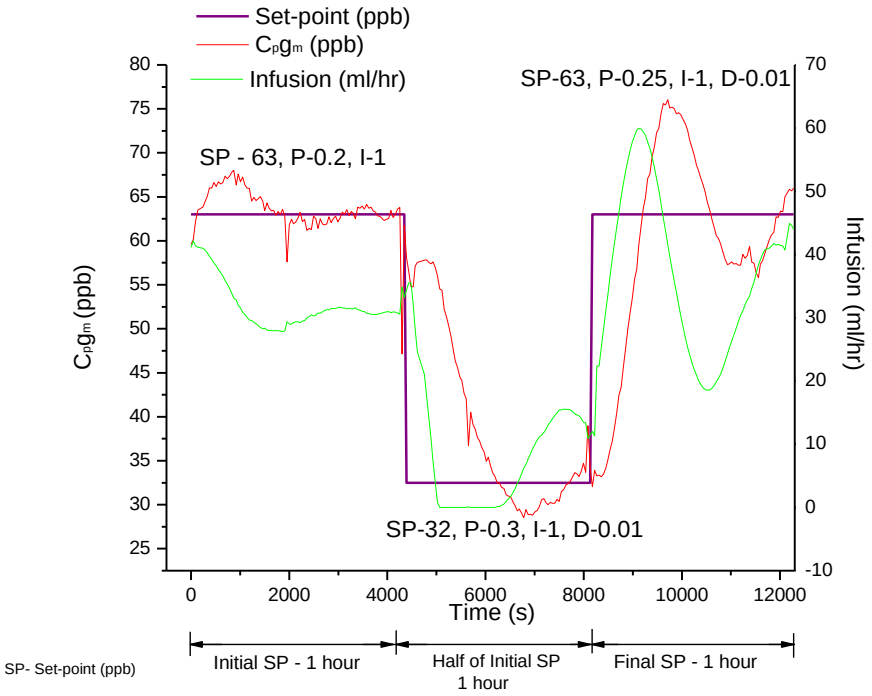

Figure 7.6 Performance of the control system from an individual pig for the total time course of three hours is shown. The initial one hour showing set-point after the steady state have been reached. The setpoint was reduced to half of initial value in the next one hour, again increased back to the initial value in the third hour. A better control is noticed in initial one hour compared to next two phases.

7.3.1 Goodness of fit

The graphical plot over time (figure 7.7 a, b, c) of the ratio of $C_p g_m$ to set-point values allows a visual assessment of the progression of error. The goodness of fit plots are given for initial set-point, the next half set-point concentration and the final set-point also.

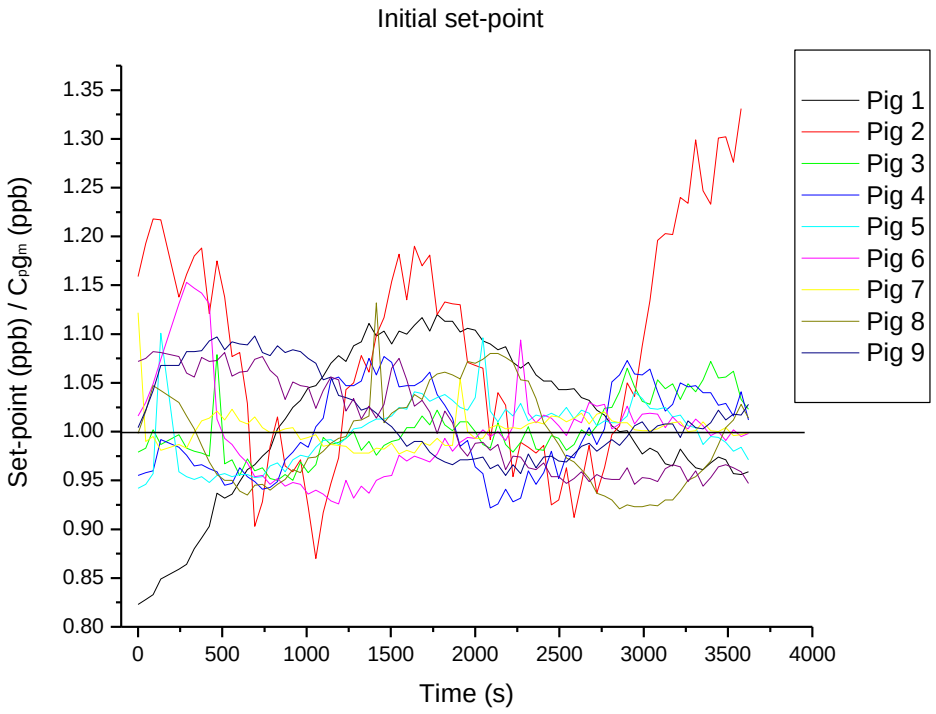

Figure 7.7a Goodness of fit plots calculated for the control system performance at the initial set-point.

Table 7.2 Predictive accuracy indices derived from measured expired gas concentrations (C_pg_m) and set-point concentration.

	Initial Set-point (SP) Phase I	Half of initial SP Phase II	Initial SP Phase III
MDPE (%)	0.95 ± 2.57	-6.64±12.16	2.67±5.57
MDAPE (%)	3.43±2.18	16.45±8.58	9.87±5.38
Wobble (%)	3.43±2.55	12.93±5.74	9.95±5.71
Divergence (%/s)	1E-4±0.001	-0.009±0.003	-0.01±0.005

(MDPE- Median percentage error, MDAPE- Median absolute percentage error)

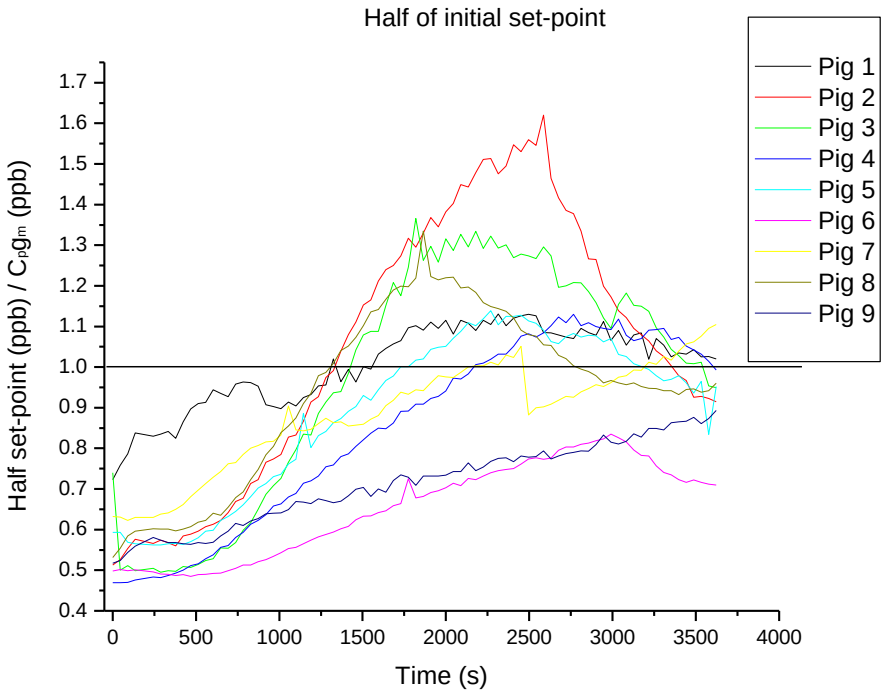

Figure 7.7b Goodness of fit plots calculated for the control system performance at half of initial set-point value.

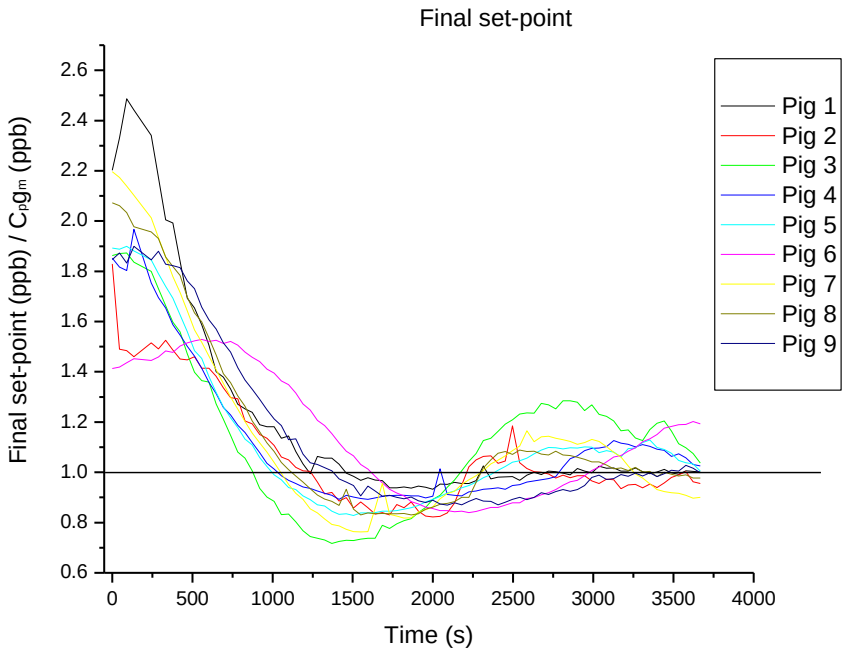

Figure 7.7c Goodness of fit plots calculated for the control system performance at final set-point value.

7.4 Discussion

In the current study, we have demonstrated that our closed-loop system guided by breath propofol allowed the titration of propofol during maintenance of anesthesia and automatic control of propofol sedation using breath propofol is feasible in pigs. The PID values used in the study were chosen according to the set-point changes. During the initial phase where the set-point is just steady state value of the breath propofol, only P and I values are needed as the D value may introduce oscillations inside the system hence the D value is not included. In the next phase where the set point was decreased to half of initial set-point value a disturbance is introduced in the controller hence a small D (0.01) value is also given with a little increase in P value (0.2 to 0.3). Finally for the final set-point increase P value was decreased to 0.25 as we hypothesized that the lung responds faster (lung can uptake propofol faster then elimination, a better controller performance is noted in the third phase compared to second phase (table 7.2))

compared to the previous phase (where P value was 0.3). The high intra-individual variability found in the pig lungs can be well noted from the goodness of fit plots figure 7.4 a, b, c.

We compared our predictive accuracy indices to the values of Absolam et al. [Absolam AR et al., 2002], Smet TD et al. [De Smet T et al., 2008] and Liu N et al. [Liu N et al., 2006]. As they have used the controller in the maintenance phase (after there was a steady state in plasma concentrations with effect site), the values from the initial one hour (steady state phase where initial set-point was set) is taken for comparison. The performance of our control was better compared to other studies (table 7.3).

Table 7.3 Predictive accuracy indices compared to previous study performances using BIS as the control variable.

	MDPE (%)	MDAPE (%)	Wobble (%)	Divergence (%/s)
Absolam et al.	2.52±2.37	7.80±3.00	7.32±3.54	
Smet TD at al.	7.78 ± 3.46	11.51 ± 4.0	8.44 ± 2.84	0.009 ± 0.012
Liu N et al.	-9.75 ± 11.02	-15.32 ± 7.00	9.19 ± 4.32	
Our study	0.95 ± 2.57	3.43±2.18	3.43±2.55	1E-4±0.001

The major limitation of PID controllers are that when applied to the closed-loop control of drug administration, the problem that PID controllers are essentially ‘ignorant’, i.e. without any knowledge of drug metabolism and the resulting (potentially dangerous) concentration values, might result in stability problems. Without fine-tuning for the specific situation, these general controllers can be slow to establish control and can be dangerous to use because of possible oscillations. Fine-tuning of a PID controller is difficult in this particular setting because the human body is very complex and much variability exists. This may lead to several clinical difficulties owing to the complex pharmacological behavior of the products used, interindividual pharmacological variability and the patient’s reactions to external surgical stimuli [Struys MM et al., 2002].

The model-based controller may be a better alternative. With this, the administration of drugs in response to clinical effect (surgical manipulations) is based on a knowledge of the fate of the drug and its effect in the human body, concentrated in a mathematical model. The

challenging problem of intra-individual variability among the animals may also be solved by using a model predictive controller. Although our system was only a prototype, it demonstrated that the breath propofol based closed-loop anesthesia device is not only a research tool but also a preclinical tool.

References

Absolam AR et al. Closed-loop control of anesthesia using Bispectral Index: Performance assessment in patients undergoing major orthopedic surgery under combined general and regional anesthesia. Anesthesiology 2002, 96,67–73.

Bannister CF et al. The effect of bispectral index monitoring on anesthetic use and recovery in children anesthetized with sevoflurane in nitrous oxide. Anesth Analg 2001,92,877–81.

De Smet T et al. The accuracy and clinical feasibility of a new bayesian-based closed-loop control system for propofol administration using the bispectral index as a controlled variable. Anesth Analg. 2008 ,107 (4),1200-10.

Hoeksel SA, et al. Computer control versus manual control of systemic hypertension during cardiac surgery. Acta Anesthesiologica Scandinavica 2001, 45, 553–557.

I.J.Nagarath and M.Gopal. Control systems engineering: 5th ed 2007, New age international publishers, New delhi.

Johansen JW et al. Clinical impact of hypnotic-titration guidelines based on EEG bispectral index (BIS) monitoring during routine anesthetic care. J Clin Anesth 2000, 12,433–43.

Johansen JW, Sebel PS. Development and clinical application of electroencephalographic bispectrum monitoring. Anesthesiology 2000, 93, 1336–44.

Linkens DA, Hacisalihzade SS. Computer control systems and pharmacological drug administration: A survey. J Med Eng Technol 1990, 14,41–54.

Liu N et al . Titration of Propofol for Anesthetic Induction and Maintenance Guided by the Bispectral Index: Closed-loop versus Manual Control. Anesthesiology 2006, 104,686–95.

Locher S et al. A new closed-loop control system for isoflurane using Bispectral Index outperforms manual control. Anesthesiology 2004, 101,591–602.

Morley A et al. Closed loop control of anesthesia: An assessment of the bispectral index as the target of control. Anesthesia 2000, 55,953–9.

Mortier E et al. Closed-loop controlled administration of propofol using bispectral analysis. Anesthesia 1998, 53,749–54.

Schuettler J and Schwilden H. Present state of closed-loop drug delivery in anesthesia and intensive care. Acta Anesthesiologica Belgica 1999, 50, 187–191.

Struys MM et al. Comparison of closed-loop controlled administration of propofol using Bispectral Index as the controlled variable versus “standard practice” controlled administration. Anesthesiology 2001, 95,6–17.

Struys MM et al. Closed-loop control of anesthesia. Current Opinion in Anesthesiology , 2002, 421-425.

Struys MM et al. Performance evaluation of two published closed-loop control systems using bispectral index monitoring: a simulation study. Anesthesiology 2004,100, 640–647.

Struys MM et al. Time course of inhaled anesthetic drug delivery using a new multifunctional closed-circuit anesthesia ventilator. In vitro comparison with a classical anesthesia machine. British Journal of Anesthesia 2005, 94, 306–317.

Tehrani F et al. Closed-loop control if the inspired fraction of oxygen in mechanical ventilation. Journal of Clinical Monitoring and Computing 2002, 17, 367–376.

Tehrani F et al. A dual closed-loop control system for mechanical ventilation. Journal of Clinical Monitoring and Computing 2004, 18, 111–129.

Bibliography

Chapter 1

Apfel CC et al. A factorial trial of six interventions for the prevention of postoperative nausea and vomiting. N Engl J Med, 2004, 350,2441–51

Bland JM and Altman DG. Statistical methods for assessing agreement between two methods of clinical measurement. Lancet, 1986, 307-310

Charlton JE. (editor): Core Curriculum for Professional Education in Pain. IASP Press, Seattle,2005.

Durbin CG. Respiratory Therapists and Conscious Sedation. Respiratory Care, 44(8), 1999.

Dawidowicz A et al. The role of human lungs in the biotransformation of propofol. Anesthesiology, 2000, 93,992–7

Egan TD and Shafer SL. Target-controlled infusions of intravenous anesthetics: Surfing USA not! Anesthesiology, 2003, 99,1039–41

Gentilini A et al. Modeling and closed-loop control of hypnosis by means of bispectral index (BIS) with isoflurane. IEEE Transaction of Biomedical Engineering, 2001, 48, 874–889.

Gentilini AL. Feedback Control of Hypnosis and Analgesia in Humans. Dr. Tech. Sc. Thesis, Swiss Federal Institue of Technology (ETH), Zurich, Switzerland, 2001.

Ghisi D et al. Monitored anesthesia care. Minerva Anestesiology, 2005, 71(9),533–538.

Hoeksel SA et al. Computer control versus manual control of systemic hypertension during cardiac surgery. Acta Anesthesiologica Scandinavica, 2001, 45, 553–557.

Hoymork SC et al. Bispectral index, serum drug concentrations and emergence associated with individually adjusted target-controlled infusions of remifentanil and propofol for laparoscopic surgery. Br J Anaesth, 2003, 91,773–80

Iwakiri H et al, Individual effect-site concentrations of propofol are similar at loss of consciousness and at awakening. Anesth Analg, 2005, 100,107–10

Linkens DA and Hacisalihzade SS. Computer control systems and pharmacological drug administration: a survey. Journal of Medical Engineering & Technology, 1990, 14, 41-51.

Morgan GE, and Mikhail MS. Clinical Anesthesiology, second ed. PrenticHall International, Inc., 1996.

Novak LC. ASA Updates its Position on Monitored Anesthesia Care. American Society of Anesthesiologists Newsletter, 62(12), 1998.

Pandin PC et al. Predictive accuracy of target-controlled propofol and sufentanil coinfusion in long-lasting surgery. Anesthesiology 2000, 93,653–61

Struys MMRF et al. Cost-reduction analysis of propofol versus sevoflurane: Manitenance of anesthesia for gynaecological surgery using the bispectral index. European Journal of Anesthesiology, 2002a, 19, 727-34.

Struys MMRF et al. Closed-loop control of anesthesia. Current Opinion in Anesthesiology,2002b,15, 421-425.

Soliman HM et al. Sedative and analgesic practice in the intensive are unit: the results of a European survey. Br J Anaesth, 2001, 87, 186-92.

Sheiner L.B et al. Simultaneous modeling of pharmacokinetics and pharmacodynamics: Application of d-tubocurarine. Clin. Pharmacol. Ther. 1979, 25,358-371.

Tucker GT. Pharmacokinetic and pharmacodynamic models. Advances in Pain Research and Therapy,1990, 14, 181-201.

Chapter 2

Abbott SM et al. Quantification of acetonitrile in exhaled breath and urinary headspace using selected ion flow tube mass spectrometry. I Int J Mass Spect, 2003, 228(2-3), 655-665.

Amann G et al. Applications of breath gas analysis in medicine. Int J Mass Spect, 2004, 239(2-3, 227-233.

Bauer TM, et al. Diagnosis of small intestinal bacterial overgrowth in patients with cirrhosis of the liver: poor performance of the glucose breath hydrogen test J Hepatol, 2000, 33, 382–386.

Boschetti F et al. PTR-MS real time monitoring of the emission of volatile organic compounds during postharvest aging of berryfruit. Postharvest Biology And Technology, 1999, 17(3), 143-151

.

Cheng WH and Lee WJ. Technology development in breath microanalysis for clinical diagnosis. J Lab Clin Med, 1999,133: 218-228.

Giardina M and Olesik SV. Application of low-temperature glassy carbon-coated macrofibers for solid-phase microextraction analysis of simulated breath volatiles. Ana Chem, 2003, 75(7), 1604-1614.

Ghoos Y et al. open-tubular gas chromatography in combination with an ion trap detector to assess volatile metabolites in human breath Biomedical and Environmental Mass Spectrometry 1989, 18(8), 613- 616.

Grossherr M et al. Discontinuous monitoring of propofol concentrations in expired alveolar gas and in arterial and venous plasma during artificial ventilation. Anesthesiology, 2006, 104, 786-90.

Gouw JD et al. Sensitivity and specificity of atmospheric trace gas detection by \proton-transfer-reaction mass spectrometry. Int J Mass Spect, 2003, 223-224,365-382.

Harrison GR et al. Real-time breath monitoring of propofol and its volatile metabolites during surgery using a novel mass spectrometric technique: A feasibility study. Br J Anesth, 2003, 91,797-9.

Hansel A et al. Proton-transfer reaction mass spectrometry-Online trace gas analysis at the ppb level. J Mass Spect Ion Proc, 1995, 150, 609-619.

Haley LV and Romeskie JM. Development of an explosives detection system using fast GC-IMS technology. IEEE 32nd Annual 1998 International Carnahan Conference on Security Technology, 12-14 Oct, Alexandria, VA, USA 1998, 59-64.

Hansen TK et al. Intensive insulin therapy exerts antiinflammatory effects in critically ill patients and counteracts the adverse effect of low mannose-binding lectin levels. J Clin Endocrinol Metab, 2003, 88, 1082–1088.

Hornuss C et al. Real-time monitoring of propofol in expired air in humans undergoing total intravenous anesthesia. Anesthesiology, 2007, 106, 665-74

Izumi M et al. Superoxide dismutase mimetics with catalase activity reduce the organ injury in hemorrhagic shock. Shock, 2002, 18, 230–235

Joseph Wang. Analytical electrochemistry, 3rd ed; John Wiley and sons,2006

Karl T et al. Human breath isoprene and its relation to blood cholesterol levels: new measurements and modeling. J App Physiol, 2001a, 91(2), 762-770.

Karl T et al. High concentrations of reactive biogenic VOCs at a high altitude site in late autumn. Geophysical Research Letters, 2001b, 28(3), 507-510.

Kharitonov SA et al. The elevated level of exhaled nitric oxide in asthmatic patients is mainly derived from the lower respiratory tract. Am J Respir Crit Care Med, 1996, 153, 1773–1780

Kneepkens CME et al. The potential of the hydrocarbon breath test as a measure of lipid peroxidation. Free Radic Biol Med, 1994, 17, 127-160.

Lindinger and Hansel A. Analysis of trace gases at ppb levels by proton transfer reaction mass spectrometry (PTR-MS). Plasma Sources, Science and Technology 1997, 6(2), 111-117.

Lindinger A et al. Online monitoring of volatile organic compounds at pptv levels by means of proton- transfer-reaction mass spectrometry (PTR-MS) medical applications, food control and environmental research. J Mass Spect Ion Proc, 1998, 173(3), 191-241.

Lord H et al. Breath analysis and monitoring by membrane extraction with sorbent interface. J. Ana Chem, 2002, 74(21), 5650-5657.

Lundberg J et al. Nasally exhaled nitric oxide in humans originates mainly in the paranasal sinuses. Acta Physiol Scand, 1994, 152, 431-432.

Manolis A. The diagnostic potential of breath analysis. Clin Chem, 1983, 29, 5-15.

Mayr D et al. Applications of breath gas analysis in medicine. Int J Mass Spect, 2003, 223-224, 743-756.

Mazzone PJ et al. Diagnosis of lung cancer by the analysis of exhaled breath with a colorimetric sensor array. Thorax, 2007, 62, 565-568.

Miekisch W et al. Assessment of propofol concentrations in human breath and blood by means of HS-SPME-GC-MS. 2008, Clin Chim Acta, 395,32–3

Mukhopadhyay R. Don't waste your breath. Anal Chem, 2004, 76, 273-276.

Nieminen U et al. Lactose malabsorption: use of breath hydrogen test and serum glucose analyses in diagnostics. Gastroenterology, 2000,118, 1132.

Perman JA. Clinical application of breath hydrogen measurements. Can J Physiol Pharmacol 1991, 69, 111–115.

Perl T et al. Determination of serum propofol concentrations by breath analysis using ion mobility spectrometry. Br J Anesth, 2009, 103,822-7.

Pleil JD and Lindstrom AB. Exhaled human breath measurement method for assessing exposure to halogenated volatile organic compounds. Cli Chem, 1997, 43, 723-730

Phillips M et al. Variation in volatile organic compounds in the breath of normal humans. J Chromatogr B Biomed Appl, 1999, 729, 75–88

Phillips M. Breath tests in medicine. Sci Am, 1992, 267, 74-79

Phillips M et al. Increased breath biomarkers of oxidative stress in diabetes mellitus. J. Clin Chim Acta, 2004, 344, 189–194.

Phillips M and Greenberg J. Ion-trap detection of volatile organic compounds in alveolar breath J Chrom Biomed Appl, 1991, 564(1), 242-249.

Sankaran S et al. Microfabricated differential mobility spectrometers for breath analysis. Sensors, 2007, 28-31, 16 – 19.

Sanchez JM and Sacks RD. GC analysis of human breath with a series-coupled column ensemble and a multibed sorption trap. Ana Chem, 2003, 75, 2231-2236.

Scholpp J et al. Breath markers and soluble lipid peroxidation markers in critically ill patients. Clin Chem Lab Med, 2002, 40, 587–594.

Schubert JK et al. Breath analysis in critically ill patients: Potential and limitations. Expert Review of Molecular Diagnostics, 2004, 4, 619-629

Smith D and Spanel P. The novel selected ion flow tube approach trace gas analysis of air and breath. Rapid Comm Mass Spect, 1996,10, 1183-1198.

Smith D and Spanel P. Selected ion flow tube mass spectrometry (SIFT-MS) for online trace gas analysis. Mass Spectrometry Reviews, 2005, 24, 661- 700.

Spanel P et al. Quantification of breath isoprene using the selected ion flow tube mass spectrometric analytical method. Rapid Comm Mass Spect, 1999, 13(17), 1733-1738.

Spanel P, Smith D. Selected ion flow tube mass spectrometry (SIFT-MS) and flowing afterglow mass spectrometry (FA-MS) for the determination of the deuterium abundance in water vapour.in Pier A. de Groot (ed.) Handbook of Stable Isotope Analytical Techniques, Elsevier. 2004, 88-102 .

Taucher J et al. Analysis of compounds in human breath after ingestion of garlic using protontransfer-reaction mass spectrometry. J Agr Food Chemy, 1996, 44(12), 3778-3782.

Takita A et al. On-line monitoring of end-tidal propofol concentration in anesthetized patients. Anesthesiology, 2007, 106,659-64.

Tzanani N and Amirav A. Flame-Based Method and Apparatus for Analyzing a Sample. Ana Chem, 1997, 69, 1248-1255

Varadarajan B et al. Monitoring of propofol boli in blood and breath described with a pharmacokinetic model.2011 (Under review)

Wallace L, et al. A linear model relating breath concentrations to environmental exposures: application to a chamber study of four volunteers exposed to volatile organic chemicals. J Expo Anal Environ Epidemiol, 1993, 3, 75–102.

Williams J et al. An atmospheric chemistry interpretation of mass scans obtained from a proton transfer mass spectrometer flown over the tropical rainforest of Surinam. J Atm Chem, 2001, 38(2), 133-166.

Chapter 3

Bland JM and Altman DG. Statistical methods for assessing agreement between two methods of clinical measurement. Lancet, 1986, 307-310.

Coetzee JF et al. Pharmacokinetic model selection for target controlled infusions of propofol. Anesthesiology 1995; 82: 1328-45

Grossherr M et al. Discontinuous monitoring of propofol concentrations in expired alveolar gas and in arterial and venous plasma during artificial ventilation. Anesthesiology, 2006, 104, 786-90.

Kita F et al. Determination of propofol in blood by high performance liquid chromatography. Okayama Shigakkai Zasshi, 2002, 21, 191-4

Schubert JK et al. CO2-controlled sampling of alveolar gas in mechanically ventilated patients. J Appl Physiol, 2001, 90,486–92.

Varvel JR et al. Measuring the predictive performance of computer-controlled infusion pumps. J Pharmacokinet Biopharm, 1992, 20, 63-94

Chapter 4

Hengstenberg A et al. Continuous Real-Time Monitoring of Propofol in Breathing Gas during Anesthesia. Anesthesiology, 2006, 105, A557

Joseph Wang. Analytical electrochemistry, 3rd ed; John Wiley and sons.

Chapter 5

Grossherr M et al. Discontinuous monitoring of propofol concentrations in expired alveolar gas and in arterial and venous plasma during artificial ventilation. Anesthesiology, 2006, 104, 786-90

Hornuss C et al. Real-time monitoring of propofol in expired air in humans undergoing total intravenous anesthesia. Anesthesiology, 2007, 106, 665-74

Hornuss C et al. The Relationship between Expiratory Propofol Concentrations and Changes in the Bispectral Index, Annual Meeting of the American Society Anesthesiologists,2009, A461

Johnson KB et al.: The influence of haemorragic shock on propofol: a pharmacokinetic and pharmacodynamic analysis. Anesthesiology, 2003,99,409-20

Kuipers JA et al.First-pass lung uptake and pulmonary clearance of propofol. Anesthesiology, 1999, 91, 1780-7

Miekisch W et al. Assessment of propofol concentrations in human breath and blood by means of HS-SPME-GC-MS. Clin ChimActa, 2008, 395(1-2),32-37

Perl T et al. Determination of serum propofol concentrations by breath analysis using ion mobility spectrometry. Br J Anesth, 2009, 103,822-7

Takita A et al. On-line monitoring of end-tidal propofol concentration in anesthetized patients. Anesthesiology, 2007, 106,659-64

Chapter 6

Caruso A. Personalised drug dosing through modeling and feedback. Ph.D thesis 2009,ETH Zurich.

Charnick S.B et al.Perspectives in Pharmacokinetics. Physiologically Based Pharmacokinetic Modeling as a Tool for Drug Development. Journal of Pharmacokinetics and Biopharmaceutics, 1995, 23(2), 217–29.

Dhillion S and Kostrzewski A. Clinical pharmacokinetics, London, Pharamaceutical press 2006.

Gepts et al. Disposition of propofol administered as constant rate infusions in humans. Anesthesia and Analgesia 1987, 66, 1256-1263.

Gibaldi M, Presscott L . Handbook of clinical pharmacokinetics. Newyork ADIS Health Science press 1983.

Grossherr M et al.Blood gas partition coefficient and pulmonary extraction ratio for propofol in goats and pigs. Xenobiotica. 2009, 39(10),782-7.

Hetrick D.M et al.Sensitivity analysis for physiologically based pharmacokinetic models. Journal of Pharmacokinetics and Biopharmaceutics, 1991 , 19(1),1–20.

Johnson KB et al. Influence of hemorrhagic shock followed by crystalloid resuscitation on propofol: a pharmacokinetic and pharmacodynamic analysis. Anesthesiology 2004 , 101(3), 647-59.

Kenny GNC, White M. A portable computerised control system for propofol infusion. Anesthesia 1990; 45: 692-693.

Ludden T. M et al. Commentary on Physiologically Based Pharmacokinetic Modeling as a Tool for Drug Development.Journal of Pharmacokinetics and Biopharamceutics, 1995, 23(2):231–235.

Marsh B et al. Pharmacokinetic model driven infusion of propofol in children. Br J Anesth, 1991, 67,41 – 48.

Nestorov et al. Lumping of Whole-Body Physiologically Based Pharmacokinetic Models. Journal of Pharmacokinetics and Biopharmaceutics, 1998, 26(1),21–46.

Pandin PC et al. Predictive accuracy of target-controlled propofol and sufentanil coinfusion in long-lasting surgery. Anesthesiology 2000, 93, 653-61.

Schnider TW et al.The influence of age on propofol pharmacodynamics.Anesthesiology. 1999 , 90(6), 1502-16.

Sheiner L.B et al. Simultaneous modeling of pharmacokinetics and pharmacodynamics: Application of d-tubocurarine. Clin. Pharmacol. Ther. 1979, 25,358-371.

Stadler, K. S.: *Modeling and Control in Anesthesia from Design to Validation*.Dr. Tech. Sc. Thesis, Swiss Federal Institue of Technology (ETH),Zurich, Switzerland, 2003.

Chapter 7

Absolam AR et al. Closed-loop control of anesthesia using Bispectral Index: Performance assessment in patients undergoing major orthopedic surgery under combined general and regional anesthesia. Anesthesiology 2002, 96,67–73.

Bannister CF et al. The effect of bispectral index monitoring on anesthetic use and recovery in children anesthetized with sevoflurane in nitrous oxide. Anesth Analg 2001,92,877–81.

De Smet T et al. The accuracy and clinical feasibility of a new bayesian-based closed-loop control system for propofol administration using the bispectral index as a controlled variable. Anesth Analg. 2008 ,107 (4),1200-10.

Hoeksel SA, et al. Computer control versus manual control of systemic hypertension during cardiac surgery. Acta Anesthesiologica Scandinavica 2001, 45, 553–557.

I.J.Nagarath and M.Gopal. Control systems engineering: 5th ed 2007, New age international publishers, New delhi.

Johansen JW et al. Clinical impact of hypnotic-titration guidelines based on EEG bispectral index (BIS) monitoring during routine anesthetic care. J Clin Anesth 2000, 12,433–43.

Johansen JW, Sebel PS. Development and clinical application of electroencephalographic bispectrum monitoring. Anesthesiology 2000, 93, 1336–44.

Linkens DA, Hacisalihzade SS. Computer control systems and pharmacological drug administration: A survey. J Med Eng Technol 1990, 14,41–54.

Liu N et al . Titration of Propofol for Anesthetic Induction and Maintenance Guided by the Bispectral Index: Closed-loop versus Manual Control. Anesthesiology 2006, 104,686–95.

Locher S et al. A new closed-loop control system for isoflurane using Bispectral Index outperforms manual control. Anesthesiology 2004, 101,591–602.

Morley A et al. Closed loop control of anesthesia: An assessment of the bispectral index as the target of control. Anesthesia 2000, 55,953–9.

Mortier E et al. Closed-loop controlled administration of propofol using bispectral analysis. Anesthesia 1998, 53,749–54.

Schuettler J and Schwilden H. Present state of closed-loop drug delivery in anesthesia and intensive care. Acta Anesthesiologica Belgica 1999, 50, 187–191.

Struys MM et al. Comparison of closed-loop controlled administration of propofol using Bispectral Index as the controlled variable versus “standard practice” controlled administration. Anesthesiology 2001, 95,6–17.

Struys MM et al. Closed-loop control of anesthesia. Current Opinion in Anesthesiology , 2002, 421-425.

Struys MM et al. Performance evaluation of two published closed-loop control systems using bispectral index monitoring: a simulation study. Anesthesiology 2004,100, 640–647.

Struys MM et al. Time course of inhaled anesthetic drug delivery using a new multifunctional closed-circuit anesthesia ventilator. In vitro comparison with a classical anesthesia machine. British Journal of Anesthesia 2005, 94, 306–317.

Tehrani F et al. Closed-loop control if the inspired fraction of oxygen in mechanical ventilation. Journal of Clinical Monitoring and Computing 2002, 17, 367–376.

Tehrani F et al. A dual closed-loop control system for mechanical ventilation. Journal of Clinical Monitoring and Computing 2004, 18, 111–129.

Publications

- **B. Varadarajan** , M. Grossherr, J. -U. Meyer, P. Schmucker ,L. Dibbelt, K. Keller, H. Gehring and A. Hengstenberg. Monitoring of Propofol Boli in blood and breath described with a pharmacokinetic model. (Under review in *Anesthesia and Analgesia*)

- M. Grossherr, **B. Varadarajan,** P. Schmucker, L. Dibbelt, H. Gehring and A. Hengstenberg. Comparison of ethanol and propofol breath gas signal after bolus injection, Analytical and Bioanalytical Chemistry,2010 In Press

- **B. Varadarajan**, M. Grossherr, J. -U. Meyer, L. Dibbelt, H. Gehring and A. Hengstenberg. Monitoring of Propofol Boli in Breathing Gas using Ion Molecule Reaction Mass Spectrometry. IFMBE Proceedings,2009,427-430

- M. Grossherr, A. Hengstenberg, **B. Varadarajan**, P. Schmucker, L. Dibbelt, R. Noel and H. Gehring. Breath Gas Monitoring of Ventilation and Drug Application as a Basis for Respiratory Therapy and Automated Infusion Systems. IFMBE Proceedings,2009,563-566

- M. Grossherr, **B. Varadarajan**, L. Dibbelt, P. Schmucker, B. Sedemund-Adib, H. Gehring and A. Hengstenberg Measurement of propofol exhalation in pigs, humans and sheep during anesthesia - the impact of reference methods. IFMBE Proceedings,2009,678-680

Conferences:

2010

- **B. Varadarajan**, M. Grossherr, J. -U. Meyer, L. Dibbelt, H. Gehring and A. Hengstenberg. The effect of cardiac output variations on exhaled breath propofol concentrations. American society of anesthesiology annual meeting, San diego, USA, October 16-20, 2010.

- Grossherr M , **Varadarajan B** , Dibbelt L , Klapproth P , Schmucker P ,Gehring H. Zeitlicher Verlauf von Plasma- und Atemgaskonzentrationen, Blutdruck, BIS und Suppression Ratenach einem Propofolbolus (Time course of plasma and breath gas concentrations, blood pressure, BIS and suppression ratio after a propofol bolus). Deutscher Anesthesie kongress (*DAC*), Nuernberg, Germany, June 19 - 22, 2010.

2009

- **B. Varadarajan**, M. Grossherr, J. -U. Meyer, L. Dibbelt, H. Gehring and A. Hengstenberg. Monitoring of Propofol Boli in Breathing Gas using Ion Molecule Reaction Mass Spectrometry. World Congress on Medical Physics and Biomedical Engineering, Munich, Germany, September 7 - 12, 2009.

- M. Grossherr, A. Hengstenberg, **B. Varadarajan**, P. Schmucker, L. Dibbelt, and H. Gehring. Propofol and ethanol concentration in breath gas. 2nd World congress on total intravenous anesthesia, Berlin, Germany, April 23-25,2009.

2008

- M. Grossherr, A. Hengstenberg, **B. Varadarajan**, P. Schmucker, L. Dibbelt, and H. Gehring. Infusion monitoring of anesthetic drugs: propofol in respiratory gas. EHRLICH-II 2nd World congress on magic bullets, Nueremberg, Germany, October 3-5, 2008.

Curriculum Vitae

Balamurugan Varadarajan

Address for communication:
Fischstrasse 6b
Zimmer 1.00.4, 23552
Luebeck, Germany
Phone No: +4917663292418
E-mail: bala.eie1982@gmail.com

Personal Summary:

- Finished PhD in a collaborative project with **Dräger (** www.draeger.com **)** , Research Unit, Luebeck in **"Breath based monitoring, modeling and control of propofol anesthesia".**
- Registered an **Invention disclosure** in Draeger AG & Co KGaA.
- Elaborate research experience on different analytical techniques – **IMR-MS, ESI- TOF-MS, MALDI-TOF-MS, HPLC-MS and GC-MS.**
- Developed a **three compartment breath based pharmacokinetic model** which predicts breath propofol.
- Designed a **breath sensor based control system to control propofol sedation**.
- Hands on experience in working with novel continuous real time breath monitoring methods to sense breath analytes using **Electrochemical sensors** and **IMR-MS**.

Education:

2007-Present	**Ph.D Thesis: Breath based monitoring, modeling and control of propofol anesthesia**
	University of Luebeck, Germany
2005- 2007	International Masters in Biomedical engineering - (M.Sc),
	Thesis title: The contribution of Arginine and Lysine methylation to mass spectometric ionization behaviour of peptides
	University of Luebeck, Germany.
1999-2003	Bachelors of Engineering in Electronics and Instrumentation
	Thesis title: Virtual instrumentation assisted resonance identification system for aircraft structures.
	Madras University, India

Research Experience:

7/2007 – Present Research staff, Draegerwerk AG & KGaA, Luebeck, Germany.

7/2007 – Present Ph.D Student, University of Luebeck, Germany.

04/2004-09/2005 Research Intern, National Aerospace Laboratories (NAL), India

List of Publications:

- **B. Varadarajan** , M. Grossherr, J. -U. Meyer, P. Schmucker ,L. Dibbelt, K. Keller, H. Gehring and A. Hengstenberg. An inverse pharmacokinetic model to predict blood propofol concentrations from breath propofol. (Under preparation)

- **B. Varadarajan** , M. Grossherr, J. -U. Meyer, P. Schmucker ,L. Dibbelt, K. Keller, H. Gehring and A. Hengstenberg. Monitoring of Propofol Boli in blood and breath described with a pharmacokinetic model. (Under review in *Anesthesia and Analgesia*)

- M. Grossherr, **B. Varadarajan,** P. Schmucker, L. Dibbelt, H. Gehring and A. Hengstenberg. Comparison of ethanol and propofol breath gas signal after bolus injection, Analytical and Bioanalytical Chemistry,2010 In Press

- **B. Varadarajan**, M. Grossherr, J. -U. Meyer, L. Dibbelt, H. Gehring and A. Hengstenberg. Monitoring of Propofol Boli in Breathing Gas using Ion Molecule Reaction Mass Spectrometry. IFMBE Proceedings,2009,427-430

- M. Grossherr, A. Hengstenberg, **B. Varadarajan**, P. Schmucker, L. Dibbelt, R. Noel and H. Gehring. Breath Gas Monitoring of Ventilation and Drug Application as a Basis for Respiratory Therapy and Automated Infusion Systems. IFMBE Proceedings,2009,563-566

- M. Grossherr, **B. Varadarajan**, L. Dibbelt, P. Schmucker, B. Sedemund-Adib, H. Gehring and A. Hengstenberg Measurement of propofol exhalation in pigs, humans and sheep during anesthesia - the impact of reference methods. IFMBE Proceedings,2009,678-680

- Gropengiesser J, **Varadarajan BT**, Stephanowitz H, Krause E.The relative influence of phosphorylation and methylation on responsiveness of peptides to MALDI and ESI mass spectrometry. Journal of Mass spectrometry, 2009, 44(5), 821-31.

Conferences:

2010

- **B. Varadarajan**, M. Grossherr, J. -U. Meyer, L. Dibbelt, H. Gehring and A. Hengstenberg. The effect of cardiac output variations on exhaled breath propofol concentrations. American society of anesthesiology annual meeting, San diego, USA, October 16-20, 2010.

- Grossherr M , **Varadarajan B** , Dibbelt L , Klapproth P , Schmucker P ,Gehring H. Zeitlicher Verlauf von Plasma- und Atemgaskonzentrationen, Blutdruck, BIS und Suppression Ratenach einem Propofolbolus (Time course of plasma and breath gas concentrations, blood pressure, BIS and suppression ratio after a propofol bolus). Deutscher Anesthesie kongress (*DAC*), Nuernberg, Germany, June 19 - 22, 2010.

2009

- **B. Varadarajan**, M. Grossherr, J. -U. Meyer, L. Dibbelt, H. Gehring and A. Hengstenberg. Monitoring of Propofol Boli in Breathing Gas using Ion Molecule Reaction Mass Spectrometry. World Congress on Medical Physics and Biomedical Engineering, Munich, Germany, September 7 - 12, 2009.

- M. Grossherr, A. Hengstenberg, **B. Varadarajan**, P. Schmucker, L. Dibbelt, and H. Gehring. Propofol and ethanol concentration in breath gas. 2nd World congress on total intravenous anesthesia, Berlin, Germany, April 23-25,2009.

2008

- M. Grossherr, A. Hengstenberg, **B. Varadarajan**, P. Schmucker, L. Dibbelt, and H. Gehring. Infusion monitoring of anesthetic drugs: propofol in respiratory gas. EHRLICH-II 2nd World congress on magic bullets, Nueremberg, Germany, October 3-5, 2008.

2007

- **Balamurugan V**, Cirit S, Speikermann M, Weiler SM, Siegers CP. Benzene in the environment and food stuffs. 11th International Congress *of* Toxicology , Montreal, Canada, July 15–19, 2007.

*Computer Proficiency***:**

Languages	:	C, C++, LabVIEW 7.1
Packages	:	MS Office, Code Composer Studio, Origin 8.0
Operating system	:	Windows (all platforms), Linux
Assembly language	:	TMS320C6711
Scientific Computation	:	MATLAB, WEKA

Laboratory Skills Acquired : ELISA, Western Blot, 1D-PAGE, PCR

Key research interests:

Compartmental pharmacokinetic modeling, Intrapulmonary pharmacokinetics , Proteomics, Model based control, Analytical instrumentation, Biosensors, Breath biomarkers, Biosignal processing.

References:

1. Prof. Joerg Uwe Meyer
   Managing director
   Richard Wolf GmbH
   Pforzheimer Strasse 32
   75438 Knittlingen, Germany
   Tel.: +49 7043 351332
   E-mail: joerg-uwe.meyer@richard-wolf.com

2. Dr. Andreas Hengstenberg
   Head - Department of Chemical and Biochemical sensors
   Research Unit
   Draegerwerk AG & KGaA
   Luebeck, Germany
   Tel: +49 451 8821987
   E-mail: andreas.hengstenberg@draeger.com

3. Prof. Hartmut Gehring
   University of Luebeck,
   Ratzeburger alle 160,
   Tel: +49 451 5006200
   E-mail: gehring@uni-luebeck.de